Dissipative Preparation of Entanglement of two emitters coupled to a One-Dimensional Quantum Wire

August 28, 2014

Frederik C.A. Kerling Bsc.

Contents

1 Introduction

In 1935 Einstein, Podolsky and Rosen elaborated on their view of interpretation of the then existing quantum mechanical theory. Near the end of their article they arrive at the following conclusion which would fuel discussions for not just their lifetimes but those of many other to come:

"One could object to this conclusion[(1)] *on the grounds that our criterion of reality is not sufficiently restrictive. Indeed, one would not arrive at our conclusion if one insisted that two or more physical quantities can be regarded as simultaneous elements of reality only when they can be simultaneously measured or predicted. ... No reasonable definition of reality could be expected to permit this."*[1]

Here the statement implies that quantum theory's criterion of reality, does not allow physical quantities that cannot be measured simultaneously to exist with arbitrary accuracy in reality. The discussion was about the opinion that reality should exist, regardless of our observation. In other words, the order of measurement should for instance not matter on the information that one can gather.
It wouldn't be until 1957 when the new science had matured that Bohm and Aharanov presented a suggestion for an experimental proof[2] of the discussion. This is where the current field of quantum computation basically found its roots. It has since left the infantile shoes of interpretation and endless discussions about physical reality, and rose up to answer the question of 'what we can do with it?'. The basis of this thesis is the same as was the basis of the experiment of Bohm and Aharanov, two entangled particles. However instead of asking whether or not it should be part of physical reality, one can question how to prepare this entanglement of for instance a qubit, and keep it that way for periods well beyond their normal decay times. In this way it can be employed for useful work and form a contribution to every-day reality. Therefore this thesis will focus on preparation of an entangled state in a condensed matter system of two emitters on a plasmonic wave-guide by use of external optical drives and internal dissipative dynamics.

This thesis is organized in five sections: Section 1, contains a short description of the previous work that has lead up to this work, it motivates the approach chosen and elaborates on the relevance of the work in society. In Section 2, there is a presentation of the methods and concepts used to model the situations concerned. Section 3 contains the first of the two situations, a two 2-level atoms on a plasmonic wave-guide, where there will be looked for the relation between the emitter's coupling to the wire and the fidelity of an entangled state. In Section 4 the same will be done however in this section for a novel two 3-level Λ-emitters on a plasmonic wave-guide, where schemes will be discussed to acquire a relation between the fidelity of an entangled state and the coupling to the wire. The section will also show that this two 3-level set-up has advantages over a two 2-level set-up. Section 5 is devoted to the conclusion and discussions.

(1) *The incompleteness of the quantum-mechanical description of physical reality*

1.1 Current status of the field

The field of quantum computation has not seen its birth come about by the exclamation of an 'Eureka!'[3], a single great speech about a pinhead[4] nor a controversial article[5]. Instead it has come about slowly from the first quantum information packages[6] and the need of a quantum information theory[7] during the 1970s, That was a response to the proposition and theoretical realization of a quantum computer.[8] It wasn't until the advent of quantum cryptography[9] and the derivation of Shor's algorithm[10] that the field has gathered great interest from both the scientific community and the public.

This thesis will focus on the preparation of the desired entangled states, and will not elaborate on other subjects in the field like computation and cryptography. Entangled states are the building block for the majority of quantum information processes. Moreover they also offer a great possibility in understanding the quantum states of matter. The exact usage of the term entanglement with respect to superposition states is elaborated in Sec. 2.1.1. These maximally entangled states, in particular the bipartite states, are the core of entanglement theory which is the origin of the predicted improved processing power of quantum computation over classical computation.

In every attempt to create a desired quantum state, one has to deal with undesired noise. This noise stems from either the surroundings or the system itself, that causes decoherences. Frequent examples of external noise are uncontrolled external processes like natural radiation, the lab environment, vibrations of the set-up, temperature fluctuations. Frequent examples of internal noise to a system can be impurities, higher order effects, and spontaneous decay of states or 'dissipative' noise. At the turn of the century it was however suggested that dissipative noise can be used in favour of quantum information processing and assist in the preparation of entangled states. Several works[11–17] showed that dissipative dynamics of two atoms coupled to a mutual reservoir could lead to entanglement. These works were generalized to reveal a general class of states and quantum information tasks that could be realized by dissipation.[18–20] Since then, various quantum information processes have been considered inside a dissipative state engineering framework. Several of these works show that dissipation alone is enough to fulfill tasks like, universal quantum computation,[18] entanglement distillation and quantum repeaters,[21] quantum simulators,[22;23] quantum memories[24] and various kinds of entangled state preparation.[25–38] Several physical set-ups have so far been applied in dissipative state preparation, cavity quantum electrodynamics,[26–28;30;32;35;38] optical lattices,[19;29] atomic ensembles,[28;33;34] ion traps[12;22;23;25]and plasmonic wave-guides.[36;37] The latter will be the focus of this thesis.

In this thesis two atoms on or near a plasmonic metallic wave-guide will be considered. The coupling of the atoms of this wire will be the main factor in achieving high fidelities. Different mechanisms will be given depending on coherent driving by optical and Raman fields. Two kinds of atoms will be considered, two 2-level atoms on a single-mode wire and two Λ-atoms on a single-mode wire. It will be shown that an arbitrarily fidelity can be achieved in different qualitative set-ups, depending on the coupling of the atoms to the wire. Also the thesis strives to give a a more hands on elaboration of the complicated processes present in a three level system. So that the reader has less difficulty comprehending the experimental set-ups that overall have a relatively complicated theoretical framework.

1.2 Why dissipative state preparation on a wire?

The choice of a plasmonic wave-guide does not seem straightforward. It is experimentally not a simple set-up. Since it has great loses due to the fact that half the plasmons will go into directions away from both atoms, and the dipole interaction mediated by the wire is not as great as that of a cavity. But the advantages outweigh these disadvantages. It will show that a good coupling between wire and atom presents a reasonably high dipole-dipole coupling. It will also show that the added channel of decay other then into the vacuum is a gift in dissipative state preparation. Foremost the plasmonic set-up is a viable technique for future mass production due to the relative simplicity and size of the system. It also offers a large set of physical advantages which, as shown below, is due to the decay of the atoms into the wire or wave-guide. It suffices to even say that this strong source of decoherence can be used to achieve great coherences.

In order to entangle two atoms, one needs to increase the interaction between them. This is generally done via electromagnetic or light-matter interactions. This increase in light-matter interactions has many structures to do so, among these but not limited to are for instance photonic crystal cavities[39;40] and wave-guides,[41] photonic nanowires,[42] and dielectric slot wave-guides.[43] All of these structures rely on an enhancement of the coupling to an electromagnetic (EM) field, which in turn causes a large Purcell factor, which is defined as the decay rate in the structure in comparison to the decay rate in vacuum. This EM field intensification is favoured by a confinement of the allowed EM modes. This strong field concentration is displayed in metallic structures that are known to support surface plasmon modes propagating at the metal interface.[44] This modal confinement can even be reached at a sub-wavelength level.[45;46] Surface plasmons have already been used to control certain properties of quantum emitters, including the decay rate,[47] energy transfer[48] and angular directionality.[49] The experimental realization of single plasmon generation,[50;51] detection,[52;53] the results on plasmon transport switching[54] and plasmon-assisted qubit-qubit interaction[36;55] show that the use of plasmonic wave-guides are just a few steps away from on-chip implementation.

1.3 Possible applications in industry, science and daily-life.

The application of wire mediated dissipative state preparation are mostly in the computing industry. A plasmonic wave-guide is simply not suitable for long distance cryptography. In computational structures the application in the computer is rather crucial for the eventual choice of structure and method of the computational device. If for instance the goal is to simulate quantum states in a universal quantum computer it would be preferred to have a computer with a quantum processor that can handle a large variety of set-ups. This would lead to a computer that can simulate a broad range of solid state models and efficiently model many problems in condensed matter and nanophysics. Such a machine would however not be the same as a computer designed to crunch numbers. Even though a quantum Turing machine is theoretically capable to do both,[56] the existence of separate markets will for the near future provide different specific needs in quantum computation and different advances. It is worth noting that current day applications alike D-wave[57] do not use such entangled states as such, and are most certainly not universal quantum computers.

For the number crunching market, the possibilities are great and promising. A quantum computer could with Shor's algorithm[10] easily factorize large numbers whereas this is impractical in normal

computers.[58] This impracticality is so far exploited in public-key cryptography, and would break a lot of coding as it is used today in web pages, email and many other types of data including monetary transactions. However there are no quantum algorithm's for all forms of encryption[59] and some forms of encrypted messages could of course become quantum encrypted and hence become intrinsically safer by construction. However most quantum algorithms are still in their infant years and have yet to prove their theoretical possibilities in order to live up to the expectancies of society. It is therefore that most of the finance is coming from industry whereas its application is more promising in scientific research and security.

2 Formalism and methods

In order to get to grips with the goal, this section will first discuss the principles of the applied theory, and attempts to elaborate on the choice of the approach used. Second to this, the modeling of the plasmonic wave-guide will be justified. Subsequently it is shown how the chosen formalism, the master equation, is to be calculated, used and interpreted for its physical meaning. Then, the approaches on solving the model will be discussed which is done in both an analytical way and a numerical way, and how these are applied to their best extend. Lastly a clear synopsis about the model in its most complicated application will be given by a novel but relatively simple diagrammatic model.

2.1 The principle of dissipative entangled state preparation

As an introduction to dissipative state preparation it is good to contemplate what the actual goal of such a venture is. Therefore an elaboration is made about some of the physical processes discussed in this work. It is here assumed that the reader has some knowledge about quantum mechanics, and is familiar with the concept of quantum states, their superpostions and Dirac's bra-ket notation. The focus here will be only on the most relevant concepts used in this work.

2.1.1 Entanglement

Entanglement was a term coined by Erwin Schrödinger[60] to describe the effect Einstein, Podolsky and Rosen had discussed previously.[(2)] It is considered to be one of the most baffling parts of quantum physics. It is meant to describe a feature of quantum mechanics that has no classical analogue. If a quantum state exists, that cannot be described by two separated parts, then this state is said to be entangled. This is not quantum superposition in general, however entanglement is a subgroup of quantum superpositions. A superposition is where a particle is said to be expressible as a complex sum of its pure states. This can be separable and non-separable in pure states, where the latter is entanglement.

Entanglement is a state that occurs only between two indistinguishable entities. This can vary from elementary particles to atoms, molecules or even increasingly larger entities. Theoretically there are no limits to the size of these entities, as long as the entangled state cannot be separated into 2 different states, either by observation or decoherence, it remains entangled. In practice however the concept of indistinguishability is very limiting to the concept of entanglement. Once one can distinguish between 2 entities, number them, label them, spatially determine their position or even uniquely define each as separate, then they are no longer indistinguishable from one another. Once two entities become distinguished entanglement is lost as they are by definition already described as two separate states. It is however possible to make distinguishable entities, indistinguishable by construction. Hence entanglement is also possible between un-equal entities.

In this work, entanglement is used in its simple form; *The description of an entangled state cannot be reduced to separate states.* As an example of such a state, the symmetric and anti-symmetric states $|T\rangle$ and $|S\rangle$ are introduced here respectively. These are symmetric and anti-symmetric under a parity transformation. In other words, they transform differently when you change their respective indices:

[(2)] (See Introduction)

$$|T\rangle = 2^{-1/2}(|1\rangle_1 \otimes |0\rangle_2 + |0\rangle_1 \otimes |1\rangle_2)$$
$$|S\rangle = 2^{-1/2}(|1\rangle_1 \otimes |0\rangle_2 - |0\rangle_1 \otimes |1\rangle_2)$$

Here $\otimes$ is the direct product which signifies that the multiplication is between two different Hilbert spaces, or in physical terms, a multiplication of states not part of the same entity. If for state $|S\rangle$ the indices $1 \longleftrightarrow 2$ that represent the two different entities and their separate (super)positions are interchanged. Then $|S\rangle$ will become:

$$|S\rangle \rightarrow 2^{-1/2}(|1\rangle_2 |0\rangle_1 - |0\rangle_2 |1\rangle_1) = -|S\rangle \tag{1}$$

Such a property of state $|S\rangle$ cannot be found in the sum of its separate superpostions of the individual entities:

$$|S\rangle \neq 4^{-1/2}(|1\rangle_2 - |0\rangle_2) \otimes (|0\rangle_1 + |1\rangle_1)$$

This is clearly a different state and has a different normalization too. In many occasions in this work, the use of the direct product $\otimes$ in the equations will be neglected if different indices of the states are given. On occasion, it is included to prevent any possible confusion.
In general the state in Eq. (1) is called a Bell-state. These states are maximally entangled. It is the properties alike parity transformations described above that are what make entangled states unique and which are exploited in quantum computers. It is in fact the entanglement that makes a quantum computer an actual universal quantum-computer. Therefore preparing such a state is elemental for the field of quantum computation.

2.1.2 Elimination & Utilization of decoherence

A dominant issue in preparation of an entangled state is the process of decoherence. Decoherence is the loss of coherence in general. Among these loss of coherence processes, states can decay or change from their present state to a superposition of others by noise. It is the elemental process that destroys the hard-won entangled states.

In practice sources of decoherence are numerous. In a typical experiment decoherences of the outside lab environment and the set-up itself are to be considered. The most profound process ascribed to decoherence can however not be isolated from the experiment in any possible way. This is the interaction of any system with the vacuum. The vacuum in physics can be paraphrased as the 'nothing' from which with respect to energy is measured. How or why this has a non-zero value at all is far beyond the scope of this work, but what matters is that it does. This means that any entity always couples to at least the vacuum. After all, there will always at least be nothing. This coupling to the vacuum causes spontaneous emission.

Spontaneous emission is therefore a leading source of decoherence in any theoretical work, since it cannot be turned off at even a theoretical level. In practice however it is more a matter of how dominant such decoherences are. In principle all states have some sort of coupling to the vacuum. This vacuum or electromagnetic vacuum, can support all possible sorts of EM radiation, yet the most dominant is the dipole radiation. This is what causes most of spontaneous emission to manifest itself

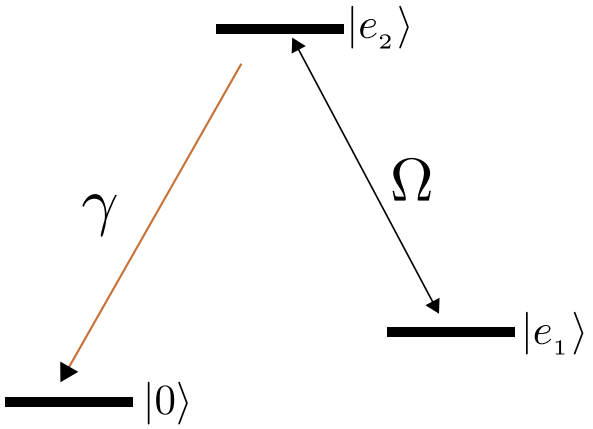

Figure 1: A simple three level system, where the ground state $|0\rangle$ is a dark state, as population does not leave the state. The other 2 exited states are driven and or decaying, and hence not dark. Of course this idealized set-up is isolated from the outside, otherwise even noise could make the ground state less dark.

as the emission of (dipole)-radiation into free space.

In the case of Eq. 1 it is not surprising that when a decay occurs $|1\rangle \rightarrow |0\rangle$, state $|S\rangle$ is no longer the same. However it is possible to reduce or utilize even this intrinsic process of decoherence. This is not done by isolating the set up from the vacuum itself. Instead the product of this coupling, a spontaneous emission, is utilized into a useful coherence. This can be done for instance by sending the lost photon back into the system. In such a case the only decoherence is then the inefficiency of the process that sends this light back into the system where it came from. A practical example of this would be an optical cavity, a system sandwiched between two highly reflective parabolic mirrors.

In an attempt to reduce the effects of decoherences, an added coupling to another electromagnetic field carrier will be used. This coupling can be much stronger then the coupling to the vacuum field, and can cause a useful coherence out of spontanteous emission. This process chosen for this work, the quantum wire, is described in Sec. 2.2

2.1.3 Dark states

The term 'Dark states' is often used in quantum optics. The darkness of a state represents basically how little energy is emitted by the state into an electromagnetic medium or to another state, as can be seen in Fig. (1). This means that the darker a state, the less likely it is for the state to lose population or occupation of the state to another state.

Resonant or off-resonant driving a state will make it brighter or less dark, and a strong spontaneous decay will also make it brighter. A perfect dark state would be a state that loses none of its occupation to another state. This means that a perfectly dark states cannot be driven.

In this work it is beneficial to make entangled states as dark as possible. This will increase their purity and their longevity. Since often processes cannot be eliminated it is attempted to reduces their brightness by making it comparatively small with respect to their gain of population. In short one

not-so-dark state surrounded by very bright states is effectively darker. The darkness of states should not be confused with subradiance or superradiance, which is a collective process for many particles which is not relevant in the case of only 2 emitters. Due to this possible confusion, more or less outward coupling of quantum states are expressed in terms of its *brightness* or *darkness*.

2.1.4 Steady states

A steady state, is a state whose population or occupation does not change over time. 'The steady state' in general is the distribution of population over all possible states, that is unchanging in time. This means in practice that the observable states, or the diagonal states of the density matrix, are unchanging in time. This also means that 2 equal systems both at their steady state will give the same distribution of states. As can be seen in Fig. (1) the states will eventually reach a steady state, since the ground state is dark, and the two exited states have a drive between them, the steady state of Fig. (1) is where all the population is in state $|0\rangle$.

It should be noted that the concept steady state, as will show in this work, can be a tricky one. First of all, for all experimental and perhaps even physical relevance, one only needs a systems observables to be unchanging in time. After all that is all one can know. This can be mathematically tricky, as the often used density matrix consists out of more then just these observables. A good reference for the use of density matrices can be found in Sakurai.[61]

Second one can argue when something is steady enough. Is something steady when it is unchanging on a time-span of a (quantum) computation? Or is something steady only when it is unchanging in large time spans like seconds, or even hours or days?

In this work, these problems are dealt with differently. At times an elaboration is given just what is found. In numerical calculations, the computer will decide where the cut-off of steady, and non-steady lies. In analytical considerations this is not always possible, and instead will show to sometimes be complicated, if for instance it is asymptotic with perfectly steady. In either way though, all results naming 'a steady state' will have at least the most dominantly populated state in a distribution to be unchanging in time. In this work this is always the desired prepared state. The actual complication in the analytical calculations can often be moved to the unobservable and does not affect the outcome of the steadiness of observable states.

2.1.5 Plasmons

Plasmons, which are the mediating mechanism of interaction through the quantum wire, is a quantization of (surface) plasma oscillations. Just like phonons are quantizations of lattice vibrations, plasmons are oscillations in the density of free charges. Plasmons exist in any matter which has enough free electrons, but play an important role in metals. In metals they are the dominant process of light effects like absorption and reflection. In the case of the quantum wire, plasmons only exist as oscillations in the otherwise confined uniform free one dimensional electron gas.

2.2 The plasmonic wave-guide

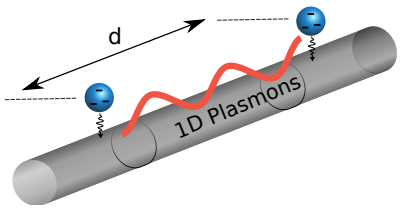

Figure 2: Two emitters separated by a horizontal distance d are positioned above a generic wave-guide. The plasmon modes supported by the structure constitute the electromagnetic interaction between the two emitters.

The two emitter system employed in this paper consists of two identical quantum emitters positioned on, or in close proximity to a metallic wave-guide. (see Fig. 2) The positioning is done in such a way that the emitters electromagnetic interaction can also revert into quasi one-dimensional plasmonic modes in the wave-guide instead of free-space decay alone. This coupling of the emitters to the wave-guide or wire can be affected by their distance to the wire, or to other factors depending on the sample's construction and geometry. This coupling has been shown to increase the spontaneous emission rate of the emitters with respect to their distance to the wire.[51] The emitters can be atoms, molecules quantum dots or some other solid state replacement of a level system, and will be modeled here only for two and three levels. Since the level systems are generally required to couple to plasmonic modes, these level structures will generally be that of an optical exited state and of a ground state. In the case of three levels there are two ground states and one optically excitable state.

The wave guide is generally a wire[62], a groove[63] or a confinement of a 2 dimensional electron gas.[64;65] These wires have been found to support plasmonic (surface) modes depending on the geometry used. And each has their own conduction effectiveness depending on the wavelength of the plasmons. The (spatial) confinement in the grooves, wires and electron gas make sure that in theory the wires only support certain modes. This in practice is also shown but are often still troubled by temperature broadening due to impurities and alike. All of these set-ups have metallic states which support plasmons on their surfaces or edges. Current advancement show great promise in qubits on a well-coupled and well defined single-mode plasmonic wires.

A predominately decay into the wire in the model is preferred, though it will show in Section 4 that we would rather tune the wire to be responsive to only one transition then to have a very strong coupling to the wire per se. The plasmonic wave-guide geometry can be very complicated[66] and the exact detailed physics of these wave-guides will be beyond the scope of this work.

Since there is a lot of possibilities and systems to chose from, here there will be worked with an effective result[36] from different geometries of systems that show that for reasonable energies plasmonic wave-guides exist that only excite a single mode. For simplicity from here on, the term wire will be used whenever a plasmonic wave-guide is inferred. All in all to correctly calculate the electromagnetic behavior the electric field operator is required:

$$\hat{\vec{E}}(\vec{r},\omega) = i\sqrt{\frac{\hbar\omega^2}{\pi\epsilon_0 c^2}}\int d^3\vec{r'}\sqrt{\varepsilon_i(\vec{r'},\omega)}\vec{G}(\vec{r},\vec{r'},\omega)\hat{\vec{f}}(\vec{r'},\omega) \tag{2}$$

In Eq. 2 $\hat{\vec{f}}$ is the bosonic lowering operator and $\vec{G}(\vec{r},\vec{r'},\omega)$ is the (retarded) Green's tensor which satisfies the Maxwell equations for an infinitesimal dipole source located at spatial position $\vec{r'}$. From a physical point of view, the Green's tensor describes how the electromagnetic interaction is carried from spatial point $\vec{r'}$ to $\vec{r}$. This Green's tensor is very complicated when expressed in modes, and far to general for the single mode use. Instead, only a single mode Green's tensor is considered. In Eqs. 3 & 4 are the expressions for the dipole-dipole interaction $g_{ij,kl}$ and the wire decay $\gamma_{ij,kl}$ which are the real and imaginary parts of the Green's tensor respectively.

$$g_{ij,kl} \backsimeq D_{ij,kl} e^{-d/2l} sin(k_r d) \tag{3}$$

$$\gamma_{ij,kl} \backsimeq W_{ij,kl} e^{-d/2l} cos(k_r d) \tag{4}$$

Here d is the distance between the two emitters and $k_r = 2\pi/\lambda_{pl}$ where λ_{pl} is the modal wavelength of the plasmon mode, typically in the order of $100's$ of nanometers. In doing so it is assumed that all the interaction between the emitters is mediated via the wire. The remainder of the decay is free-space decay and does not contribute to the interaction between the emitters. In Eqs. 3 & 4 , i and j are indices for the two emitters and in this case cannot be equal. Here $D_{ij,kl}$ & $W_{ij,kl}$ are constants, which can be expressed in terms of free-space or total decay and coupling to the wire. Due to the use of the formalism as expressed in section (2.3) these are not too straightforwardly defined. Constants k & l are indices for transitions between states within each emitter.

To further simplify Eqs. 3 & 4 it is assumed that the free-space decay does not contribute to the interaction between the emitters. This is a good approximation of the complete Green's tensor for distances exceeding half a modal wavelength in length.[36] In addition from here the plasmonic decay factor $e^{-d/2l}$ is neglected. This is a negligible change over the distance of a modal wavelength and is not of interest since Eqs. 3 & 4 are periodic over a modal wavelength. Whatever losses there might be due to plasmonic decay will not contribute to the interaction, and will therefore be incorporated within the constants $D_{ij,kl}$ & $W_{ij,kl}$ as free decay.

In an experimental set-up it is entirely seemingly that the dipole moment directions of each emitter coupling to the wire, do not align in the same direction. This can be a problem, but for simplicity it is assumed they are equal. The alignment of the dipoles does not influence the final results, as for these specific distances the dipole-dipole interaction is zero.

It is also possible that the distance of each emitter with respect to the wire is not necessarily equal, and therefore there would be a difference in the coupling strength to the wire for each emitter. It will show not to be a problem if the constants $D_{ij,kl}$ & $W_{ij,kl}$ are expressed in terms of wire and free decay, and since plasmons decay radiatively[67] these are incorporated in free decay which is easily measurable regardless of the geometrical set-up since the two emitters are observationally indistinguishable. Also, experimentally, wire decay is easily measurable. This is why the formulation of the constants $D_{ij,kl}$ & $W_{ij,kl}$ will prove to be very useful in preparation of the entangled state. The difference in coupling to the wire between two equal emitters has not been looked into in this work, and is assumed to be equal.

There are two different usages of the constants, one in terms of free, the other in terms of total decay as expressed before. When the state desired to be prepared couples to the wire, it is best to use

the constants $D_{ij,kl}$ & $W_{ij,kl}$ in their total-decay picture. This is because the parameters are expressed with respect to either free decay or total decay. And a good beta would mean low free decay, which is a problem for driving a fast decaying state if it needs to be prepared well, since it would be lower for better coupling. In the subsequent use in this work they will each be elaborated upon use.

It will show that, in simple physics terms, the wire can break or preserve symmetries. This will prove to be the most essential part of the dissipative preparation scheme, and also why the quantum wire is favourable over other set-ups.

2.3 The chosen formalism, the master equation

The formalism to model the time evolution of the system used here is that of the so called master equation. Many good derivations of this model exist[68–70]. However most of these only look into the simplified two-level case of the emitters. Agarwal (1975) however derives the master equation for density matrices starting from Liouville operators for an atomic system and radiation field. In doing so the Born approximation and a Markov approximation are applied. In addition to these approximation, the whole master equation is subject to a rotating wave approximation. This prevents complications from frequency shifts like the Lamb shift. The resulting master equation is expressed for N particles with M levels:

$$\frac{\partial \hat{\varrho}}{\partial t} = -\frac{i}{\hbar}\left[\hat{H}, \hat{\varrho}\right] - \frac{1}{2}\sum_{ij,kl}\gamma_{ij,kl}(\hat{\varrho}\cdot\hat{\sigma}_{lk,i}\otimes\hat{\sigma_{kl,j}} + \hat{\sigma}_{lk,i}\otimes\hat{\sigma_{kl,j}}\cdot\hat{\varrho} - 2\cdot\hat{\sigma}_{kl,j}\otimes\hat{\varrho}\otimes\hat{\sigma_{lk,i}}) \tag{5}$$

Where the sigma $\sigma_{lk,i} = |L\rangle_i \langle K|$ is an operator that changes a state $|k\rangle \rightarrow |l\rangle$ in the Hilbert space "i" and $\otimes$ is the direct product between Hilbert spaces. Formulations of Eq. 5 differ in literature greatly but all are mathematically identical. In this case, $\hat{H}$ is the Hamiltonian containing all interactions and energies:

$$\hat{H} = \hat{H}_0 + \hat{H}_d + \hat{H}_b + \hat{H}_g \tag{6}$$

Where $\hat{H}_0$ is the Hamiltonian containing the energies of the states under consideration. $\hat{H}_d$ contains the externally applied drives, their resonance specifications and the phase differences between the emitters determined by the geometry of the driving fields with respect to the emitters. $\hat{H}_b$ contains the magnetic fields between the two emitters. And $\hat{H}_g$ contains the interactions between the emitters are included, this is where the wire-mediated dipole-dipole interaction can be found. The presence or lack of these terms, and their varied respective strengths and symmetries determine the outcome the schemes which will follow in the coming chapters.

The summation in Eq. 5 implies that one has to sum over all possible decays. These decays include decays where an individual emitter decays. Or conversely in the wire mediated case where both emitters decay as a whole and have $i \neq j$, these two decays together can be symmetry conserving or breaking.

The density matrix $\hat{\varrho}$ in the case of the derivation by Agarwal[70] contains both the radiative density matrix as the atomic density matrix. On this point there are some differences with other work[71] in the expression of the master equation. These depend on the initial and final conditions of the radiation

field. Here the current derivation of Eq. (5) was chosen along the lines of previous work.[69;70;72] Since the coupling to the vacuum field does not contribute to mutual interaction, and the Born approximation allows to eliminate the possibility of an emitted photon to react back on its emitter, there is no need to include a radiation field. It should also be noted that in the case of set-ups where the emitted photon's in the vacuum field can react with other emitters inside the field, can result in a more complicated expression of the master equation. In that case, the density matrix needs to include states of the vacuum field as well, for instant excited modes of an optical cavity. In the cases that are described in this work, there is the relative luxury to not be bothered with this. Because the actual excitation of plasmons inside the wave-guide are not used, but instead their respective electron densities as expressed by Eqs. (2) , (3) & (4) . It is therefore noted that the master equation is mostly a formalism for atomic systems.

The master equation for this work is an ideal tool to model the time evolution of the system, since there are no vacuum exited states to be concerned. In other work there are plentiful of examples of the use of this master equation on an arbitrary amount of 2-level emitters, and it is a well known tool in the quantum optics community. This is in stark contrast with the application of three-level emitters. To the author's best knowledge, there is currently only one work mentioning the use this formalism in 3-level emitters[73] though the work by Bargatin *et al.* seems to apply a dipole interaction with optical pumping. This uncommonness could be attributed to the problem of non-Markovian noise in higher leveled emitters[74], which would render the master equation formalism inapt. The formalisms for non-Markovian systems is however beyond the scope of this work.

2.4 Clarification of parameters in the master equation

The physical interpretation of Eq. (5) is not straightforward. Constants $\gamma_{ij,kl}$ in Eq. (5) are defined for application of the joint system, and not for values of a single emitter alone. Different definition are used for these parameters in this work for different systems. Used parameters are clarified;

The parameter Γ, which signifies the total free decay, is all the decay that does not couple to the wire added to the total decay of the wire modes. In other words Γ is all the decay out of the system not via the wire.

The parameter β, which resembles the coupling of the emitters to the wire. The range of parameter β is 0 to 1, representing respectively no decay into the wire, and total decay into the wire.

The parameter γ, which is total decay, or all free decay plus all wire decay.

These parameters relate to each other via the logical formula:

$$\Gamma = \gamma(1-\beta)$$

Using these three parameters means that constants of decay in $\gamma_{ij,kl}$ of Eq. (5) can be described either by parameters $\beta\,\&\,\gamma$ or by $\beta\,\&\,\Gamma$. The choice which of the two lies in, whether or not one wants to scale all other parameters in the system by either the total decay, or the total free decay. All couplings to and from the wire will therefore scale accordingly:

$$g_{ji,lk} = g_{ij,lk} = g_{ij,kl} = g_{ji,kl} = c_{kl}\frac{\gamma\beta}{2}sin(k_{pl}d) = c'_{kl}\frac{\Gamma\beta}{2(1-\beta)}sin(k_{pl}d) \qquad for\ i \neq j \qquad (7)$$

$$\gamma_{ji,lk} = \gamma_{ij,lk} = \gamma_{ij,kl} = \gamma_{ji,kl} = c_{kl}\gamma\beta cos(k_{pl}d) = c'_{kl}\frac{\Gamma\beta}{(1-\beta)}cos(k_{pl}d) \qquad for\ i \neq j \tag{8}$$

Here constants c_{kl} & c'_{kl} specify how strongly the transition couples with respect to the other possible transitions, since these can be amplified they can vary greatly, but in this work there is only a single mode wire. For this reason in this work $c_{kl} = c'_{kl} = 1$, and the possible amplification is incorporated in the other parameters. $k_{pl} = 2\pi/\lambda_{pl}$ with λ_{pl} the modal wavelength of the plasmons. It can be seen that Eqs. (7) & (8) will become infinite for $\beta \to 1$. This corresponds to the unlikely case where there is no more decay into free-space as even plasmons decay. Furthermore as $\beta \to 1$ then $\Gamma \to 0$ since $\Gamma = \gamma(1-\beta)$, hence it cannot become infinitely large. And even if all free-space decay would be captured by a wire, parameter Γ would still include plasmonic decay, meaning it remains finite in the physical case. The fact that interaction from emitter i to j is equal from emitter j to i, lies in the indistinguishability of the two emitters.

Since there is no dipole moment in free-space, couplings of the individual dots and their decay become:

$$g_{ii,kl} = 0 \qquad \forall\, i,k,l$$

$$\gamma_{jj,kl} = \gamma_{ii,kl} = d_{kl}\gamma = d_{kl}\Gamma\left(1 + \frac{\beta}{(1-\beta)}\right) \tag{9}$$

Here the self decay of an emitter is described. Here d_{kl} is the constant of how strong transition from state $|k\rangle$ to state $|l\rangle$ is in respect to the whole, hence $\sum_{k,l} d_{kl} = 1$ at all times. In Eq. (9) on the far right, there is a term which represents the decay into the wire. This is present because an emitter, when decaying into the wire, will still decay by itself. The current formulation of parameter $\gamma_{jj,kl}$ in the master equation conserves the trace of the density matrix $Tr(\hat{\varrho}) = 1$.

2.5 Solution of the Master Equation

In an attempt to solve Eq. (5) various methods are employed, both analytical and numerical. Each with their benefits and drawbacks. For this reason each method will be examined before it will be applied in the coming two chapters. The results of these calculation will be compared in the conclusions per chapter.

2.5.1 Analytical methods

There are four different ways to find solutions for Eq. (5); Solving the differential equations that are produced per element of the density matrix in Eq. (5). Solving the steady state conditions for $\hat{\dot{\varrho}} = 0$ as a whole by use of an eigenvalue/eigenvector problem. Partially solving the differential equations, by demanding not all elements of the density matrix in Eq. (5) to be steady. And finally by the use of rate equations, as described below.

Differential equations Differential equation method attempts to solve the steady state of the system, by taking each equation per element of the density matrix in Eq. (5) and solve them as a set

of coupled differential equations. This is an exact solution, but not always possible. For N emitters of M levels, there will be $\frac{M^{2N}+M^2}{2}$ coupled time dependent differential equations. This number rises really quickly, being 9 in the case of two 2-level emitters, 45 in the case of two 3-level emitters, and 369 in the case of three 3-level emitters. Solving these can only be reasonably done for the simplest and least interesting set of parameters for the system, even if one is to use analytical software. It is sometimes possible to reduce the problem to an eigenvalue problem for the steady state which will greatly simplify the problem at hand.

Eigenvalue method The eigenvalue method with the density matrix in Eq. (5) is similar to solving the time dependent differential equations as a steady state. For this method a transformation to the Hamiltonian is applied to make it time independent, as the steady state cannot be time-dependent. This will prove to be possible for most cases. By looking at the general steady state of Eq. (5) $\dot{\hat{\varrho}} = 0$ one can then solve the system analytically with an eigenvalue problem of the matrix on the right-hand side of Eq. (5). One can then find the eigenvector of the density-vector below, that belongs to eigenvalue 0. Hence an effective matrix which works on this vectored density matrix needs to be constructed. Hence Eq. (5) would become:

$$\Big(\ M \ \Big)_{effective} \cdot (\hat{\varrho})_{vector} = (\dot{\hat{\varrho}})_{vector}$$

Here $M_{effective}$ is a matrix that has such a shape that each element inside the density vector has an identically matching element inside the density matrix of Eq. (5). Then the eigenvalue problem for eigenvalue zero exists that has the steady state solution as an eigenvector:

$$\Big(\ M \ \Big)_{effective} \cdot (\hat{\varrho})_{steady} = 0 \cdot (\dot{\hat{\varrho}})_{vector}$$

In the analytical case the determinant of $M_{effective}$ is zero for non-trivial solution. However the determinant has $M^{2N}!$ elements for N emitters of M levels, or in the two 2-level case $2.0 \cdot 10^{10}$ elements approximately. Even in the realistic physical case where the amount of elements can be reduced to $\frac{M^{2N}+M^2}{2}!$ elements, this is still a formidable number. But can in some rare cases be solved quite quickly by analytical software. Since most of these elements will be zero. Depending on the complexity of the Hamiltonian in Eq. (5) these density-vector and effective matrix can be made.

Limitations of eigenvalue equations Setting the general steady state $\dot{\hat{\varrho}} = 0$ implies the demand that all elements of the density matrix are constant in time. This isn't a strange demand, since the decay of the system will always stabilize the diagonal real elements of the density matrix. However in the case of 3 level or higher there is a problem. Coherences also decay, and though in a 2 level system coherences do not decay to another coherence, in a 3-level or higher system they do:

$$\dot{\varrho_{ie}} \sim -\gamma_{decay}\varrho_{ie} \quad \rightarrow \dot{\varrho_{if}} \sim +\gamma_{decay}\varrho_{ie} \tag{10}$$

In Eq. (10) a coherence between state $|i\rangle \longleftrightarrow |e\rangle$ exists and state $|e\rangle \rightarrow |f\rangle$ decays into a final state. A non-zero coherence $\varrho_{ie} \neq 0$ can form, due to decay, a non zero $\dot{\varrho_{if}} \neq 0$ time dependent coherence. In this case and of that of Rabi oscillations the general steady state $\dot{\hat{\varrho}} \neq 0$. Though this particular

solution might be very beneficial to prepare entangled states.
It is not particularly advantageous to exclude such a broad regime of physically stable steady state solutions.
As mentioned before the difference between 'a stead state' and 'the steady state' can make it difficult. In the case where $\hat{\dot{\varrho}} \neq 0$, where 'the steady state' does not exist, it is often more difficult to view the entire effective matrix, and the eigenvalue/eigenvector problem cannot be used.
It makes it necessary decompose the elements of the density matrix of Eq. (5) into separate coupled differential equations, and only solve some(most) of these equations as steady, as explained in the next method. The effective matrix will however prove numerically to be very beneficial as numerically it can be easily solved. As though they cannot be perfectly zero, numerically seen, a null vector can exist either way. This method therefore forms numerically the most reliable solving of the system.

It is worth noting in what numeric time dependent trial runs that where made of the evolution of the system over time, the $\hat{\dot{\varrho}_{if}} \neq 0$ time dependent coherences were seen. These generally simply kept growing in their absolute value, even when the seeming steady state of the diagonal elements were long reached. These results are not incorporated in this thesis, as they seemed to have no effect on the distribution of the population of the diagonal states in the density matrix.

Selective differential equation solving Solving the differential equations discussed above is also possible by selecting which elements from Eq. (5) need to be time independent. Though this is not a very aesthetic mathematical solution, it does allow to find steady on-diagonal steady states even when the general steady state $\hat{\dot{\varrho}} = 0$ is not attainable.

Even for time independent Hamiltonians oscillations can still occur in the more complicated systems from 3 levels or higher. This however needn't be a difficulty, as in the end only the desired state needs to have a time-independent population. Hence as long as $Tr(\hat{\varrho}) = 1$ and $\hat{\dot{\varrho}}_{desired\,state} = 0$ a steady state solution for the desired state is found. In general it will prove in Sec. 4 that there are solutions with only time dependencies present in coherences, and not in the population of diagonal states. This method means that the choice of demanding which off-diagonal elements of density matrix $\hat{\dot{\varrho}}$ to be zero dominates the shape of the resulting solution.

This method is called partially or selectively solved because the solution is only valid in the case where the choice of steady states and steady coherences applies in the physical case. Not surprisingly, choosing coherences to non-decaying heavily driven off-diagonal states to be time independent, is a less well approximation then coherences to a highly decaying weakly driven state to become a time independent steady state. For this reason this analytical method requires comparison with numerical simulations to verify its applicability. It does however prove to make very complicated systems analytically solvable for the regime of interest by simple means of step by step solving.

It should be noted that it is perhaps possible to solve the set of differential equations as described above, with different choice of which coherences should be steady and which do not need to be. Physically of course this should give the exact same answer for the diagonal elements of the density matrix. It is however not always possible, as was in this case, to find an analytical solution with other steady coherences that is doable with present day computers.

Rate Equations Rate equations employ a very different approach. In this method Eq. 5 is essentially deconstructed and reconstructed for the specific set of parameters, or scheme, which one is looking at. Firstly one transforms the specific scheme to a time independent representation due to a unitary transformation, which is possible in almost all practical cases. In this unitary transformation one can then also include the (time-independent) dipole couplings as level shifts. Then one only views the diagonal terms and the coherence terms with an optical coherence. As a final step one solves all equations with optical coherences, as being steady:[75]

$$\hat{\dot{\varrho}}_{ij,optical} = 0 \qquad for\, i \neq j$$

This is a reasonable demand as the desired steady state, is only attained when the decoherences have stabilized. Unlike the normal steady state solution this is a less heavy demand. The so derived equations give rates of how much goes into a state, and how much goes out of a state, depending on the populations of other states. In conjunction with a specified scheme, reasonable assumptions can be made, and one can calculate a fidelity of a state for the certain parameters analytically. Though these can be complicated, it will prove relatively simple to approximate these rate-equations for high beta factors and gain very useful predictions of a scheme whilst only looking at a part of the whole quantum system. Since this method is only used in the case of two 3-level emitters, the full derivation can be found in Sec. (4.3.1).

The methods described above have all been applied for this work, but are not as easily applicable on each model. The steady state and time dependent differential equations method can be tried by the use of computer analytics, yet even for the simple two 2-level case this becomes problematic due to the sheer size and duration of the calculations. In the two and three level cases the eigenvalue method will simplify numerical methods. In the 3-level case the selective differential equation solving method was used for the full analytical derivation, this is however not always as transparent and the method is incorporated in the appendix. In some specific parameter cases even the analytical software using the partial differential equation method is unable to find an analytical solution via this way. As it is limited to a single processor's speed.

In general using the analytical methods and their results are not a good option in the case at hand, as the expressions are often several pages long and highly complicated. Hence analytical results given here are only the lowest order Taylor approximations around $\beta = 1$ for simplification. In figures however the full analytical solutions were used where possible. Numerical methods are faster, easier, less complicated and more reliable, and are hence advised at any time.

2.5.2 Numerical Methods

Of the methods mentioned in Sec. (4.3.1) only the direct solving of the (time dependent) differential equations, and effective matrix eigenvalue problems are used in numerical calculations. The solutions are obtained with MATLAB. This can be done with a time-independent Hamiltonian, and with time dependent Hamiltonians. The two differ little in computation time in the case of the direct solving method, but the time dependent version isn't available for the eigenvalue method. This is because Eq. (5) which contains the decay dynamics and Hamiltonian is required to be recalculated for each

time step due to the time dependence of the Hamiltonian. For this reason, if any of the parameters is not in the same order of size as the others, computation time becomes drastically increased. This is mostly unbeneficial for $\beta \approx 1$ where Eqs. (8) & (7) grow, whereas parameter scaling lowers due to the choice of parameter expression. This is however the region which is of interest in this work. Even with a computer with many parallel processors calculating a simple fidelity versus β-factor curve using the differential equation solver can take up to a day, pending errors.

Instead, the numeric solving of the effective matrix eigenvalue problem as mentioned above was employed in most cases in this thesis. This works much faster but the here used method is only applicable if the effective matrix is diagonalizable. This method is therefore not usable for all possible 3-level schemes in general, but in this work these have not occurred at all. A good rule of thumb is, that any system where decay from a high state can reach the lowest state via other states, are always solvable by the effective matrix eigenvalue method. In many other cases the effective matrix might still be diagonalizable, and in this work this is the case for all numerics, but it cannot be made as a general statement.

Effective matrix numerical analysis This method was developed at the end of the work done for this research. It enables very fast calculation for complicated systems. If the right-hand-side of Eq. (5) can be made time independent. Then, and only then, it is possible to make a time-independent effective matrix. This matrix has dimension $M^2 \times M^2$ where $M \times M$ are the dimensions of the original density matrix. It is possible to numerically write this by defining a vector from $\hat{\varrho} \rightarrow \vec{\varrho}$ that has M^2 elements. Then Eq. 5 reduces to its numerical equivalent:

$$\frac{\partial \vec{\varrho}}{\partial t} = M_{eff} \cdot \vec{\varrho} \tag{11}$$

This implies that an effective matrix exists alike in Sec. 4.3.1 , with as one difference that solving the steady state of this system isn't the only option. Instead, if M_{eff} from Eq. 11 is diagonalizable, then a set of unique eigenvalues exist for the evolution of each term in the density-vector. This means that the density-vector from Eq. 11 can be expressed as:

$$\vec{\varrho}(t) = exp(M_{eff} \cdot t) \cdot \vec{\varrho_0} \tag{12}$$

Where $\vec{\varrho_0}$ are the initial conditions $\vec{\varrho}(t = 0)$. This equation allows for very fast calculations of the dynamics of the master equation. Analytically there are many sets of parameters that make M_{eff} not diagonalizable. In the case of numerics however it is nearly always possible to find a set parameters that are within the calculation tolerances that results in an M_{eff} which is diagonalizable. This enables the numerical computation time, in the most complicated cases, to be reduced from days to seconds. In the case where there are no interactions that isolate two states from the rest, and hence no stable state with Rabi oscillations occur, there is one solution with eigenvalue zero, that represents the steady-state case. This can be calculated very quickly numerically.

One drawback of using just the eigenvalue zero is that this is the long-term steady-state case. It is entirely possible for certain sets of parameters to have, even in the numerical case, an eigenvalue which is finite but still close to zero. These states could be semi-steady where they will live a long time before they reach the steady state. However, in this work, such states were not encountered. At

routine checks these values have not shown and therefore have not been explicitly tested for in this work. It is however possible that for some set-ups and some scheme's semi-steady states are relevant entangled states, depending on the scope of the work.

It should be stressed that the method also works in case of oscillations in time of elements $\hat{\varrho}$. The solution found in this case is simply for a moment $\hat{\varrho}\left(t_{knot}\right)$ where t_{knot} is the time where all the periods of each separate oscillations coincide. Hence $\hat{\varrho}\left(t_{knot}\right) = 0$, however, this might not coincide with the most stable state. Checking whether this happens or not is however practically not doable. Instead analytical arguments can be given to check with the applicability of these solutions.

2.6 Diagrammatic notation

In representing Eqs. (5) & (6) there is the difficulty of size. A lot of terms contribute to relatively simple physical processes. There is no generally unified way of expressing the processes at hand in a simple and concise way. Thought this work does not mean to suggest such a unified way, it will suggest a diagrammatic description to equally compare the set-ups chosen for ease of comparison. This will allow the reader to quickly see the differences between schemes. A different description will be used for the two 2-level description which is comparable in different works.

In general the following diagrammatic conventions are used for both models:

- Double headed arrows, front and end, represent optical drives between states, open for symmetric drives, closed heads for symmetry breaking drives.
- Single headed arrows represent the directional decay from one state into another.
- Thick bold lines are used to represent states.
- Thick dashed bold lines are used to represent states with a level shift.
- Colour is used to exemplify which or what wire coupling transition the states are tuned or shifted to.

In general this covers most of the possible interactions in possible system set-ups. Decay arrows are sometimes dashed when they can be affected by the wire decay. And on occasion a dashed field is made around a section to denote a process of interest.

2.6.1 Two 2-level graphs

The two 2-level graphs will be familiar to most readers. It is known not only in the field but is a very practical way to describe the two 2-level system. In Fig. 3 one can see an example where the emitters on the wire have been placed a distance $d \neq n\lambda_{pl}/2$ with n an integer and λ_{pl} the modal wavelength of the plasmons. In Sec. 3 , the set-up will be discussed and will be elaborated on all the effective interactions of the model.

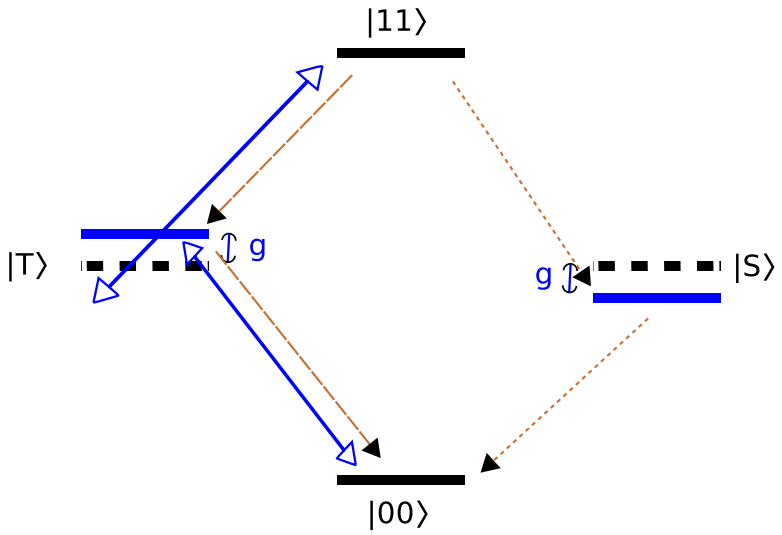

Figure 3: The two 2-level diagrammatic notation. In this case there is a dipole-dipole interaction between emitters which causes a level shift due to wire decay. The optical pumping drive has been detuned to be in resonance with the shifted transition $|00\rangle \longleftrightarrow |T\rangle$. Brown dashed arrows represent decay, long dashed arrows are decay increased by the dipole coupling and dotted brown arrows are decay decreased by the dipole coupling. In this example no one steady-state is prepared and Rabi oscillations occur between $|00\rangle \longleftrightarrow |T\rangle$.

The diagrammatic notation as in Fig. 3 is chosen such that all interactions can be placed without too much overlap. Symmetric states placed on the left and anti-symmetric on the right, and energy on the vertical axis. In this notation detuning alike in Fig. 3 the dashed lines can be incorporated to show level shifts when necessary. Colours can be used to emphasize why or why not and with respect to what the optical drives can detuned, as in the figure due to the dipole-dipole shift due to the distance. Decay can also be incorporated.

2.6.2 Two 3-level graphs

In Fig. 4 There is been given an example of how a diagrammatic notation of a three level scheme might look like. The clover shape is based upon the way two 2-level graphs are expressed. The basis and other details can be found in Sec. 4. A level shift due to a dipole-dipole interaction has only been shown in one of the two affected states. This is done, because in relevant schemes a drive detuning is used to put the the level shift on resonance for one transition and not the other. Drives which are affected due to this detuning, and are no longer resonant with the two states they drive between, are denoted by an apostrophe.

The example in Fig. 4 shows all three dipole couplings between the transitions "MW" $|0\rangle \longleftrightarrow |1\rangle$ (blue), "L" $|0\rangle \longleftrightarrow |e\rangle$ (green) and "Λ" $|1\rangle \longleftrightarrow |e\rangle$ (red). Where the dipole coupling of transition "L" has caused a dipole-dipole level shift in addition to wire decay, whereas transitions "MW" and "Λ" do not. The attentive reader will see that this example set-up is in fact only possible for a two-mode wire, as the distance of the two dots cannot vary per mode, in this example however it serves merely an

illustrative role. Due to the absence of any dipole-dipole interaction via the wire of the "Λ" transition there is a maximal decay via the wire, and always some free decay. In this case transition "MW" does not decay at all due to the emitters characteristics, and is displayed here only for completeness. For the full physical interpretation of example Fig. 4 one should continue to Sec. 4.4 where there is an elaborate description of the possibilities. In this Example case state $|00\rangle \,\&\, |11\rangle$ are essentially dark, and any steady state will end up in a linear superposition of these two.

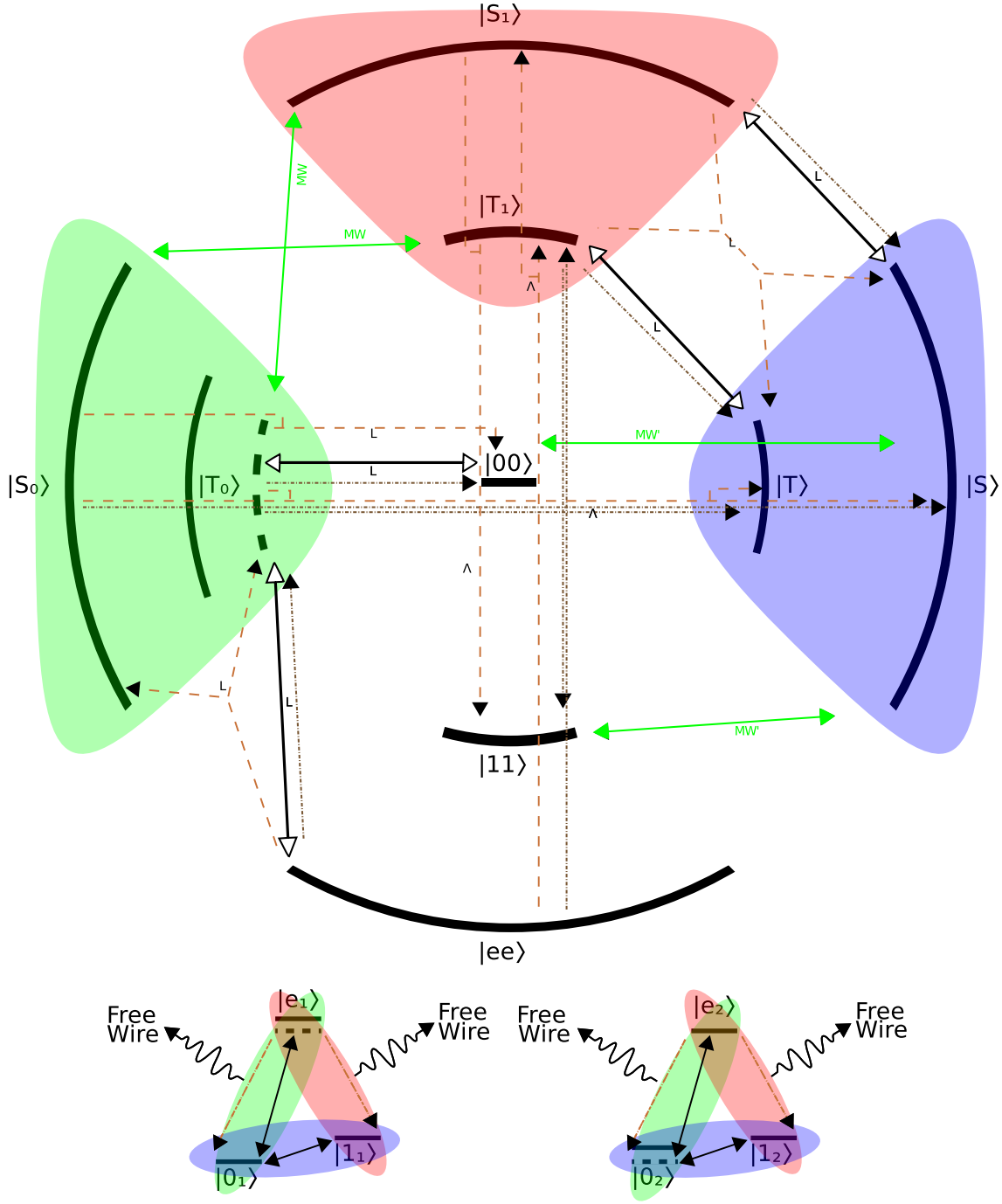

Figure 4: In this example all possible interactions are shown of each kind once. Open double-headed arrows are symmetric drives and closed arrows are anti-symmetric drives. Brown single headed arrows are non spontaneous decay, where dotted arrows are wire decays, and the long stripped arrows are free decay. The three colours represent the three possible dipole interactions. Blue is a dipole coupling between transition "MW" $|0\rangle \longleftrightarrow |1\rangle$, green is a dipole coupling between transition "L" $|0\rangle \longleftrightarrow |e\rangle$ and red is a dipole coupling between transition "Λ" $|1\rangle \longleftrightarrow |e\rangle$. In some cases a drive is coloured, this implies that the drive is detuned with respect to an associated level shift due to dipole interaction.

Generally 4 will not be seen as a 'simple' representation of the possible effects. However it is the authors opinion that the alternative, constantly changing locations of states to fit a readable figure, will only make it more difficult to compare schemes. For this reason each 3-level figure has the interactions upon each emitter written below. So that simple information of decay of emitters and drives to emitters separately is easily viewable. In the end, the possible and relevant interactions of a 9 state system will most of the time be complicated to comprehend, hence Sec. 4.4 is devoted entirely to just that.

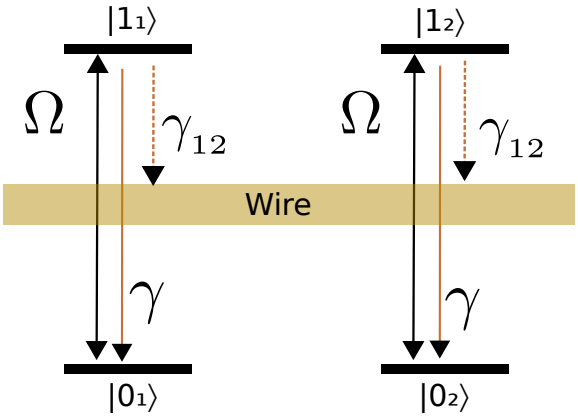

Figure 5: The two 2-level system coupled to a wire. This relatively simple set up has 2 equal emitters interacting with a single plasmon mode in a metallic wire. There is one drive Ω driving the ground state to the exited state. And there is a decay γ from the exited state to the ground state which can partially be mediated by the wire γ_{12}.

3 Two-level section

In this section the two 2-level emitter set-up will be discussed. The formalism used will be derived and several methods of solving the model will be employed. A new process of symmetry breaking will be uncovered and an elaboration of its use will be made. Subsequently, the results of all methods will be discussed, and an outlook will be given why a continuation of use of this set-up is unfavourable.

3.1 Derivation of the formalism

For derivation of the two 2-level scheme Eq. (6) is constructed for the two 2-level case:

$$\hat{H}_0 = \hbar \sum_{i=1}^{2} (\omega_0 |0_i\rangle \langle 0_i| + (\omega_1 + (-b)^i) |1_i\rangle \langle 1_i|) \tag{13}$$

$$\hat{H}_g = \hbar \sum_{i \neq j} (g_{ij} |1_i\rangle \langle 0_i| \otimes |0_j\rangle \langle 1_j|) \tag{14}$$

$$\hat{H}_d = 2^{-1}\hbar\Omega e^{i\omega_L t} (|1_1\rangle \langle 0_1| + e^{i\phi} |1_2\rangle \langle 0_2|) + H.c. \tag{15}$$

Here g_{ij} is alike in Eq. (7), Ω is the driving, ω_L is the frequency of the drive, ϕ the phase difference between two emitters, and b the magnetic field applied over the two emitters. In other sections a unitary transformation will reduce H_0 to Eq. (22). Any effect this magnetic field might have on the plasmon modes is neglected. Denote the absence of the magnetic parameter at the ground state as this isn't shifted by the Zeeman effect. From hereon ω_0 is defined as being zero, since the mechanics of the quantum system are not depended on absolute energies.

With the above the master equation Eq. (5) will become:

$$\frac{\partial\hat{\varrho}}{\partial t} = -\frac{i}{\hbar}\left[\hat{H},\hat{\varrho}\right] \quad - \quad \tfrac{1}{2}\textstyle\sum_{ij}\gamma_{ij} \quad [\quad \hat{\varrho}\cdot(|1_i\rangle\langle 0_i|\otimes|0_j\rangle\langle 1_j|) \quad +(|1_i\rangle\langle 0_i|\otimes|0_j\rangle\langle 1_j|)\cdot\hat{\varrho} \\ -2\cdot(|0_j\rangle\langle 1_j|\otimes\hat{\varrho}\otimes|1_i\rangle\langle 0_i|) \quad] \tag{16}$$

Where $\gamma_{12}=\gamma_{21}\ and\ \gamma_{11}=\gamma_{22}=\gamma$. Wire decay γ_{12} is now related to $\sim\beta\gamma cos(k_{pl}d)$ as is depicted in earlier work.[36] This could give the false impression that wire decay can in fact be turned off for the right distance, whereas the dipole term would be preserved. This is in reality of course not possible, as the only interaction is via the wire, it will always have plasmons in it, which in turn decay. In this section the total decay representation of Eqs. 8 & 9 are employed.

3.1.1 Unitary transformation

Following here will be a unitary transformation applied to the Hamiltonian in Eqs. (13), (14) & (15) , to make it time-independent:

$$\hat{\bar{H}} = i\hbar\dot{U}U^{\dagger} + UHU^{\dagger} \tag{17}$$

Where the bar over the Hamiltonian implies that $\hat{\bar{H}}$ satisfies the Schrödinger equation, if the wave functions transforms as $|\bar{\psi}\rangle = U|\psi\rangle$. The unitary transformation is:

$$U = exp(it\omega_L\sum_{i=1}^{2}|1\rangle_i\langle 1|_i) = e^{itH_U/\hbar} \tag{18}$$

Then the time independent parts of Eq. (17) transform as follows:

$$UH_0U^{\dagger} = H_0 \quad , UH_gU^{\dagger} = H_g \quad and \quad i\hbar\dot{U}U^{\dagger} = -H_U$$

The driving Hamiltonian transforms as:

$$\hat{H}_d \quad = \quad 2^{-1}\hbar\Omega \quad (|1_1\rangle\langle 0_1| \quad + \quad e^{i\phi}|1_2\rangle\langle 0_2|) \quad + H.c. \tag{19}$$

The resulting master equation is now time independent.

It is possible to further simplify the master equation by transforming the parameters into scalar parameters. Doing so means one needs to define an unique and characteristic decay time $\tau=\gamma^{-1}$ where γ is defined as the total decay. Then Eq. (16) will become:

$$\frac{\partial\hat{\varrho}}{\partial\tau} = -\frac{i}{\hbar}\left[\hat{H}(c'),\hat{\varrho}\right] \quad - \quad \tfrac{1}{2}\textstyle\sum_{ij}\gamma'_{ij} \quad [\ldots] \tag{20}$$

Where c' is a set of parameters. Here the apostrophe implies that all parameters are scaled by the total decay. In this section from hereon a parameter is implied to always be scaled with respect to the total decay and the apostrophe is neglected. In final results it will however be shown for completeness.

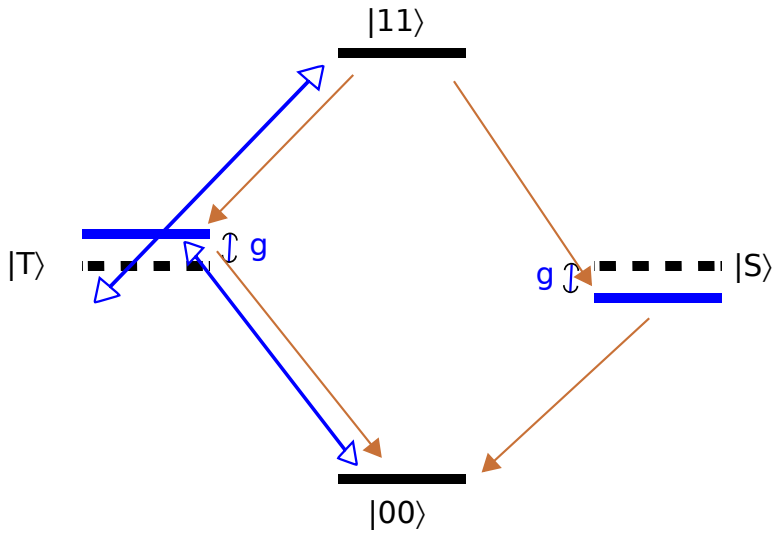

Figure 6: The two 2-level emitters under a symmetric driving tuned to be on resonance with the transition$|00\rangle \longleftrightarrow |T\rangle$. Normal brown decay arrows have unaltered total decay since for a detuning distance only dipole-dipole interactions exist on the wire. Denote that state $|S\rangle$ will therefore always decay.

3.2 Solutions to the two 2-level system

In the case if the two 2-level emitter it is theoretically possible to find an exact solution for the general case as described by the formalism in Sec. (3.1) . The method is discussed in paragraph 2.5.1 and would ask for an eigenvalue problem of the effective matrix for the two 2-level system. Since by construction all elements are decaying, there are no arguments against employing the eigenvalue method. However that practical limitations here are simple, by hand the amount of equations are too many, and the current computer analytical programs cannot handle these large symbolical equations. However by exploiting symmetry conditions, it is possible to have an analytical solution by the differential equation method for certain distances.

An attempt is made to prepare the system in a good entangled state to keep or get the preferred state as dark as possible. As previously discussed in paragraph 2.1.3 by eliminating as much interactions that move the system out of the desired state as possible. Alternatively a different basis is used which is dark with respect to certain interactions alike the magnetic field, to find a simpler solution.

Here, a first analysis of the preparation of the singlet and the problems that accompany it will be shown. Then in the following sections it will be shown that the method of symmetry breaking as proposed by Wang and Schirmer is theoretically sound, but is here not solely achieved by symmetry breaking through a magnetic gradient alone. And finally a scheme which makes steady state $|S\rangle$ dark and dominantly populated as $\beta \to 1$ is presented.

3.2.1 The two 2-level emitters under symmetric driving

To start the analysis of the system there will be looked at the system in the case of a coupling to the

wire and only a drive which has the same phase over both emitters. The basis chosen to do so is:

$$\begin{aligned} |00\rangle &= |0\rangle_1 |0\rangle_2 \\ |11\rangle &= |1\rangle_1 |1\rangle_2 \\ |T\rangle &= 2^{-1/2}(|1\rangle_1 |0\rangle_2 + |0\rangle_1 |1\rangle_2) \\ |S\rangle &= 2^{-1/2}(|1\rangle_1 |0\rangle_2 - |0\rangle_1 |1\rangle_2) \end{aligned}$$

The symmetric driving causes a coherence between the symmetric states $|00\rangle$,$|T\rangle$ & $|11\rangle$ as found in Fig. 6. From this figure there are 2 things to realize first. First there is always free space decay of all exited states $|S\rangle$,$|T\rangle$ and $|11\rangle$. Second that the coupling to the wire can have various effects, it can detune states $|S\rangle$ & $|T\rangle$, and it can affect the decay in a symmetry breaking or symmetry conserving way.

This shows the first problem, in order to make state $|S\rangle$ dark it needs to be made sure that it is the darkest of all states. However by using the detuning of the states by dipole-dipole interaction one can prefer transition from say $|T\rangle \leftrightarrow |11\rangle$ with respect to the transition $|T\rangle \leftrightarrow |00\rangle$. This is not as beneficial as it would seem as preferring one transition, means darkening the other. The lower the contrast between darkness of states, the less favourable the scheme will be.

Second as can be seen from Eq. (7) a larger detuning of the states, means a better beta-factor. Which as it will show in Sec. (3.4) is not in the benefit of state preparation by dipole-dipole interaction, as half of the plasmons disappear to the sides.

Finally it is obvious that under symmetric driving some mechanism is required to break symmetry. In the next sections Sec. (3.3 & 3.4) two of these will be discussed. First the widespread use of an externally applied magnetic field will be used. Then the intrinsic symmetry breaking due to the wire is shown to also do the symmetry breaking required to prepare the $|S\rangle$ state. In the final scheme both symmetry breaking mechanisms will prove to work most effectively when used simultaneously.

3.3 Symmetry breaking by magnetic field

As suggested before by Wang and Schirmer,[30] a breaking of symmetry is required. One way is by breaking the symmetry by an externally controlled applied magnetic field, which is opposite in strength for each emitter. Such a field will shift the energy levels up or down between emitters by the Zeeman effect, which effectively creates an asymmetry between the emitters. Below it will be introduced, put into a dark basis and shown to be not generally effective in the case of strong coupling to quantum wires.

3.3.1 Inclusion of the magnetic field

In the case of applying a magnetic field, there is a coherence between state $|T\rangle$ and state $|S\rangle$. In the basis chosen in Sec. (3.2.1) the general symmetrically driven Hamiltonian as seen in Figs. (6 & 7) becomes $\hat{H} = \hat{H}_d + \hat{H}_b + \hat{H}_g$ where

$$\hat{H}_d = \frac{\hbar\Omega}{2}(|T\rangle \langle 00| + |11\rangle \langle T|) + \ H.c. \tag{21}$$

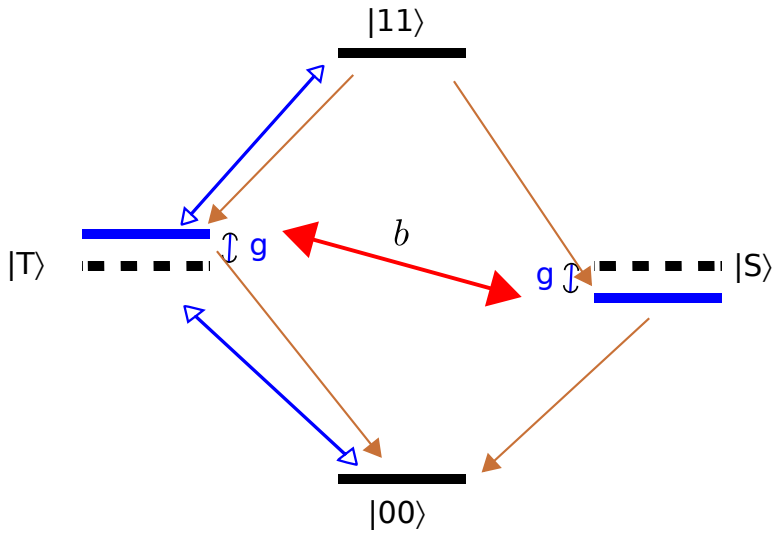

Figure 7: The two 2-level emitters under a symmetric driving tuned to be on resonance with the transition $|11\rangle \longleftrightarrow |T\rangle$. Normal brown decay arrows have unaltered total decay since for a detuning distance only dipole-dipole interactions exist on the wire. In this figure there is also a magnetic field applied which causes a coherence between states $|S\rangle \longleftrightarrow |T\rangle$.

$$\hat{H}_b = -\frac{\hbar b}{2}(|T\rangle\langle S| + |S\rangle\langle T|) \tag{22}$$

$$\hat{H}_g = \frac{\hbar g_{12}}{2}(|T\rangle\langle T| - |S\rangle\langle S|) \tag{23}$$

In a time independent rotating wave approximation with the ground state energy set to zero. It is worth noting that g_{12} is periodic over a modal plasmon wavelength in the wire and that it's maxima are at $d = \frac{1}{4}(1+2n)$ with n an integer.

This magnetic field introduces both a gain and a loss to state $|S\rangle$. There is a good reason to use this coupling, instead of, for instance, a drive to state $|S\rangle$. A drive between state $|00\rangle$ & $|11\rangle$ and state $|S\rangle$ would be anti-symmetric, and would mean a significant loss process as it drives population out of state $|S\rangle$.

In order to compensate for the losses created due to the coherent coupling by the magnetic field, the drive is made to be on resonance with transition $|11\rangle \longleftrightarrow |T\rangle$. As state $|11\rangle$ subsequently decays into state $|S\rangle$ again, as seen in Fig. (7). However good this process might be, there are still losses of states $|S\rangle$ & $|T\rangle$ as they decay into state $|00\rangle$. Even so, one can calculate the fidelity by the use of equations as found in appendix A which are the result of Eq. (16) for symmetric driving. This results in complicated function which has no maximum over a quarter of the total population in the system for state $|S\rangle$.

This result is not unsurprising. After all the decay out of the top three-state system $|11\rangle \overset{\Omega}{\leftrightarrow} |T\rangle \overset{b}{\leftrightarrow} |S\rangle$ is unaltered at dipole-dipole interaction distances. Though decay from state $|11\rangle$ stabilizes the top system, the system itself decays just as bad to the ground state. It is in fact with this basis very difficult to create a high fidelity of state $|S\rangle$. This is because any coherence that could cause any rate

into $|S\rangle$ is necessarily coupled to one of the other states, which each strongly decay into the ground state $|00\rangle$. In order to successfully engineer an entangled state, one needs to find a more simple basis with the magnetic field to do so.

This result seems to be in contrast to previous work[30] due to the lack of an optical cavity. In the paper by Wang and Schirmer the same set-up of two 2-level emitters are placed within an optical cavity. In that case the emitters are two Rubidium-87 atoms inside an optical lattice. One of the main differences between the here used approach and the approach expressed in the paper[30] is the driving of the cavity. In the paper the cavity modes are driven so that the cavity mode can be eliminated by adiabatic elimination. Then, a new basis is sought that is dark in the case of the elimination of the cavity mode. This has also been done for a two 3-level Λ system[38] and in the next paragraph a similar approach will be made.

3.3.2 A dark basis with the magnetic field

The basis as described in Sec. (3.2.1) is not generally arbitrarily preparable by dissipative state preparation with a plasmonic wire. It is therefore required to find a new basis, which is also an entangled basis, but expressed in parameters dependent on the system. The basis as expressed in Sec. (3.2.1) will transform as follows:

$$\begin{aligned} |00\rangle \rightarrow |\Psi_0\rangle &= \tfrac{1}{\sqrt{\Omega^2+b^2}}\left(-b\,|S\rangle + \Omega\,|00\rangle\right) \\ |11\rangle &\rightarrow |11\rangle \\ |T\rangle &\rightarrow |T\rangle \\ |S\rangle \rightarrow |\Psi_S\rangle &= \tfrac{1}{\sqrt{\Omega^2+b^2}}\left(\Omega\,|S\rangle + b\,|00\rangle\right) \end{aligned} \tag{24}$$

In these equations the new states are defined by the strength of the applied magnetic field b. As can be seen in Eq. (22) the opposing magnetic field does not cause a level shift but an effective interaction between the states $|T\rangle$ and $|S\rangle$. Even though these states can shift due to the dipole-dipole interaction the magnetic field will always be resonant with these shifted states.

An important note of this new basis is that it is no longer maximally entangled, as the state $|00\rangle$ is a separable and hence not maximally entangled state. Below the fidelity of the new state will be obtained. The choice of this basis is obvious, the losses from $|S\rangle$ go into $|00\rangle$, by combining these appropriately it can be seen later on that the fidelity with the new state $|\psi_S\rangle$ will be higher, and is analytically 1 for $\beta = 1$. This is not the case for the original basis with an applied magnetic field gradient.

3.3.3 Why a magnetic field alone will not work

As seen in this section, applying a magnetic field alone will not work. To find the reason why it is important to look back at Eqs. (7,8 & 9). There are basically two paths of steady state preparation to walk, first there is the use of level shifts and detunings. Basically this is state preparation by altering parameters within Eq. (13) and Eq. (14) and the unitary transformation to appropriately intermix these respective level shifts and dipole-dipole shifts. Then subsequently using the applied laser field frequency to make sure that a maximally entangled state is prepared. This is a very controllable process with a lot of room for adaptation, it also however does not work due to the coupling to the

wire. Which in this case is still very dissipative due to the use of the dipole-dipole detunings, where half of the plasmons are lost. This is not the case for optical cavities.

The second path one can walk is exploiting the inevitable path as seen in Eq. (9). The total decay is affected by the presence of the wire. As unlike an optical cavity, where even the most crude optical cavities have losses less then 50% per reflection at the mirror walls. In the wire, half of all plasmon excitations are lost because the wire has two ways. Surely this must mean that instead of using these level shifts, one must make more clever use of this decay? In the next section will be shown that the role of symmetry breaking can intrinsically be done by the wire itself. And at the right distance prove that losses outside the wire are negatively interfered for certain symmetric cases.

3.4 Symmetry breaking by the wire

Breaking symmetry is performed by tuning the plasmon wavelength or the distances between the emitters such that they differ a multitude of half modal plasmon wavelengths. This means that the electric field due to plasmons at each emitter is exactly zero. This in turn supports either enhanced decay for symmetric or anti-symmetric states or the exact opposite, due to the superposition of the plasmons in the wire. As can be seen in Fig. (8) different symmetries of state cancel each other out simply due to the distance. Either nullifying wire decay or nullifying constructive interaction.

As can be seen in Fig. (8), the symmetry breaking by the wire is strong. One either breaks symmetric states and enhances anti-symmetric, or the exact opposite. This however doesn't mean that one can only prepare the anti-symmetric state arbitrarily well. This is because Fig. (8) tells us that the state and how it decays is depended on where it came from. There is no physical reason why the separable state $|11\rangle$, can have its total decay interfered by the symmetries of the resulting decay. As can be seen in Eqs. (22) & (23), symmetrical rules or Hamiltonians depended on these only apply to states which have symmetrical preferences. Hence total decay from state $|11\rangle$, and total decay into $|00\rangle$ will be unaffected. And all symmetry breaking will be done between maximally entangled (anti)symmetrical states. In short, this is symmetry breaking by decoherence.

3.4.1 Decay dynamics of the two level case

As seen in Fig. (8) putting an anti-symmetric state on a single modal wavelength will conserve anti-symmetric states whilst enhancing decay on symmetric states. Looking at the right hand side of the master equation Eq. (16) and writing down its contribution to the $|S\rangle\langle S|$ component gives two terms. First there is the term for total decay

$$\begin{aligned}
&-\gamma\left[\tfrac{\hat{\theta}}{2}\left(2\left|11\right\rangle\left\langle 11\right|+\left|T\right\rangle\left\langle T\right|+\left|S\right\rangle\left\langle S\right|\right)+\left(2\left|11\right\rangle\left\langle 11\right|+\left|T\right\rangle\left\langle T\right|+\left|S\right\rangle\left\langle S\right|\right)\tfrac{\hat{\theta}}{2}\right]\\
&+\gamma\left[\left(\left|00\right\rangle\left\langle T\right|+\left|00\right\rangle\left\langle S\right|+\left|T\right\rangle\left\langle 11\right|-\left|S\right\rangle\left\langle 11\right|\right)\tfrac{\hat{\theta}}{2}\left(\left|00\right\rangle\left\langle T\right|+\left|00\right\rangle\left\langle S\right|+\left|T\right\rangle\left\langle 11\right|-\left|S\right\rangle\left\langle 11\right|\right)\right]\\
&+\gamma\left[\left(\left|00\right\rangle\left\langle T\right|-\left|00\right\rangle\left\langle S\right|+\left|T\right\rangle\left\langle 11\right|+\left|S\right\rangle\left\langle 11\right|\right)\tfrac{\hat{\theta}}{2}\left(\left|00\right\rangle\left\langle T\right|-\left|00\right\rangle\left\langle S\right|+\left|T\right\rangle\left\langle 11\right|+\left|S\right\rangle\left\langle 11\right|\right)\right]
\end{aligned} \tag{25}$$

And second there is a term for the fraction that is emitted in the wire

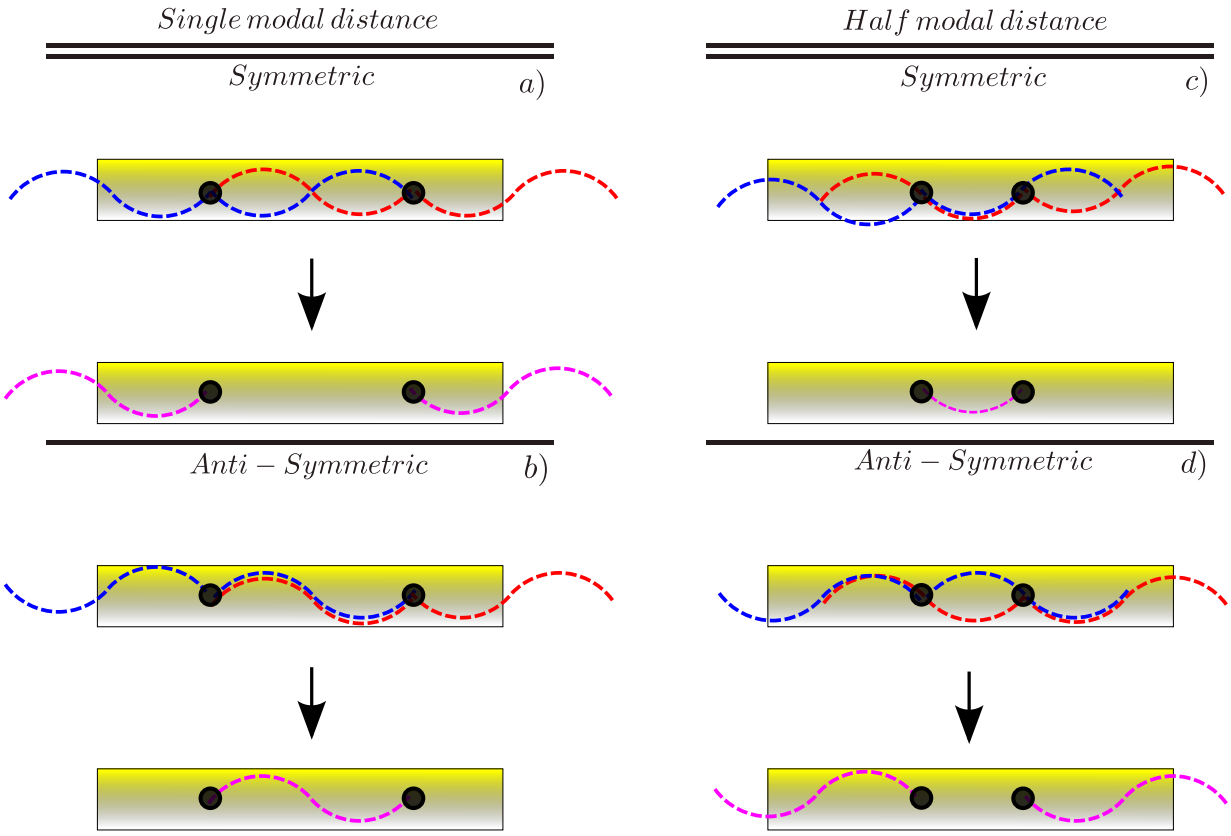

Figure 8: Two kind of states, at two kind of distances. Symmetric states are the same under parity transformations, whist anti-symmetric states change sign. **a)** At a single modal wavelength symmetric states cancel each other out in between the emitters. **b)** At a single modal wavelength anti-symmetric states amplify each other between the emitters. **c)** At a half modal wavelength symmetric states amplify each other between the emitters. **d)** At a half modal wavelength anti-symmetric states cancel each other out in between the emitters.

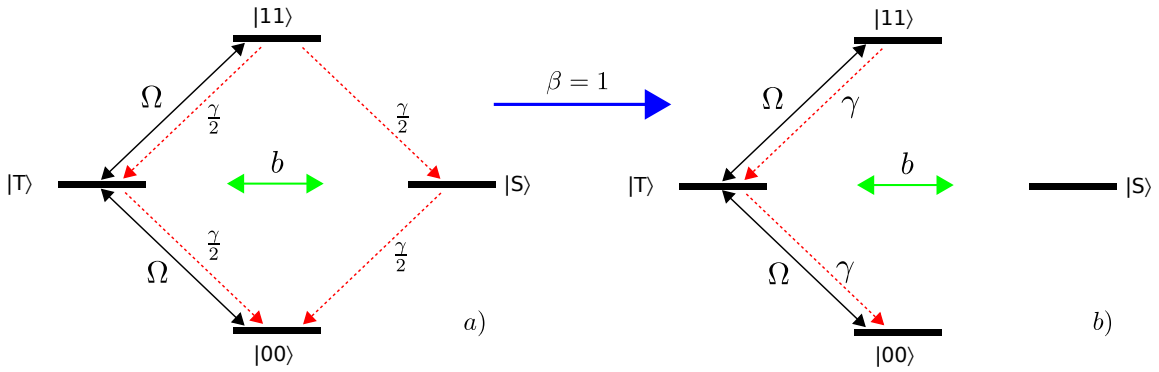

Figure 9: The two level scheme with wire decay. **a)** The drive Ω is symmetric and g_{12} could form a level shift at emitter distances of quarter and three-quarter modal wavelength between state $|S\rangle$,$|T\rangle$ and $|11\rangle$ (not shown) . The γ here represents the total decay from a state, hence it includes the contributions to the wire and the free decay. **b)** The same picture for $\beta = 1$ at integer modal wavelength emitter distance. The decay from and to the state $|S\rangle$ comes from the term right of the commutator in Eq. (5). The magnetic field b can be clearly seen to disturb the dark state $|S\rangle$ for $\beta = 1$, in earlier work this is compensated by fine tuning effective processes to make the state darker.[38]

$$\begin{aligned} &-\gamma_{12}\left[\tfrac{\hat{\varrho}}{2}\left(|T\rangle\langle T| - |S\rangle\langle S|\right) + \left[\left(|T\rangle\langle T| - |S\rangle\langle S|\right)\tfrac{\hat{\varrho}}{2}\right]\right. \\ &+\gamma_{12}\left[\left(|00\rangle\langle T| + |00\rangle\langle S| + |T\rangle\langle 11| - |S\rangle\langle 11|\right)\tfrac{\hat{\varrho}}{2}\left(|00\rangle\langle T| - |00\rangle\langle S| + |T\rangle\langle 11| + |S\rangle\langle 11|\right)\right] \\ &+\gamma_{12}\left[\left(|00\rangle\langle T| - |00\rangle\langle S| + |T\rangle\langle 11| + |S\rangle\langle 11|\right)\tfrac{\hat{\varrho}}{2}\left(|00\rangle\langle T| + |00\rangle\langle S| + |T\rangle\langle 11| - |S\rangle\langle 11|\right)\right] \end{aligned} \tag{26}$$

From Eqs. (25) & (26) it can immediately be seen why for single modal wavelength, state $|S\rangle$ becomes dark with respect to decay. Filling in the $|S\rangle\langle S|$ component of Eq. (5) in case of symmetric driving gives for the singlet state

$$|S\rangle\langle\dot{S}| = -{}^{ib}/_{2}\left(|S\rangle\langle T| - |T\rangle\langle S|\right) - \left(\gamma - \gamma_{12}\right)\left(|S\rangle\langle S| - |11\rangle\langle 11|\right)$$

In the single modal case where the wire decay parameter will become $\gamma_{12} = +\beta\gamma$. This means that the state $|S\rangle$ will be perfectly dark for $\beta = 1$ as depicted in Fig. (9 b). This set of parameters allows to analytically calculate the singlet state around $\beta = 1$ in the case of a single modal wavelength as can be seen below in Eq. (27) . The full analytical solution was done by the differential equation method in Maple using the equations from the density matrix as found in Appendix (A).

In contrast to Wang-Schirmer's scheme, here the applied magnetic field is not working with the cavity detuning but instead forms a coupling to state $|S\rangle$. Here there are two symmetry breaking processes working. The first which is the breaking of symmetry by applied coherence, is due tot he applied magnetic gradient. The second which breaks the symmetry by spontaneous decay into a symmetry preferring wire, is due to the decoherences inside the wire. This is the inevitable process as the system couples to the wire.

In essence one optimizes the two processes of symmetry breaking in both terms in the master equation (5), and then sets the externally controllable parameters to be at values that maximizes the effectiveness of these two processes together. The solution for state $|S\rangle$ at zero magnetic field equals

$$\hat{\rho}_{|S\rangle\langle S|} = 64\,\frac{{}^{\Omega}/_{\gamma}{}^{4}}{32\,{}^{\Omega}/_{\gamma}{}^{2}\left(8\,{}^{\Omega}/_{\gamma}{}^{2}+1\right)+(\beta+1)^{2}} \tag{27}$$

Not surprisingly this is not a very desirable way of producing a good fidelity. As can be seen from Fig. (9b) the magnetic field is required to couple state $|S\rangle$ to the rest of the system. Since there are no other processes that can go into state $|S\rangle$, the two level system requires a magnetic field to populate state $|S\rangle$ at all.

3.4.2 Two symmetry breaking mechanisms

To more easily solve the system the basis from Sec. (3.3.2) is used for the case of both symmetry breaking processes. This case is similar to the same set up in an optical cavity, but without the use of detunings.[38] In contrast with that work there is a slightly different choice of basis here due to different choice of parameters and that in this system all states interact in some way with the wire. The basis is repeated here:

$$|\Psi_S\rangle = \frac{1}{\sqrt{\Omega^2+b^2}}\left(\Omega\,|S\rangle + b\,|00\rangle\right) \tag{28}$$

$$|\Psi_0\rangle = \frac{1}{\sqrt{\Omega^2+b^2}}\left(-b\,|S\rangle + \Omega\,|00\rangle\right) \tag{29}$$

The state in Eq. (28) is a steady state of Eq. (5). The states $|T\rangle$, $|11\rangle$ and Eqs. (28) & (29) form an orthogonal basis. This basis can be seen in Fig. (10b)

In contrast to Wang-Schirmer's scheme for optical cavities, here the applied magnetic field is not the only symmetry breaking factor. Instead the magnetic field breaks the darkness that was caused by the symmetry breaking due to coupling to the wire as seen in Fig. (9b). The gray line in this picture shows the loss process of state $|\Psi_0\rangle$ that scales directly with the population of state $|11\rangle$ and increases rapidly for even small values of the magnetic field strength and the driving. Whereas the same processes scaling with $\sim(1-\beta)$ that affect state $|\Psi_S\rangle$ are only constructive in its population gain.

3.4.3 Solving for the new basis

It is possible to analytically solve Eq. (5). This is done the differential equation method using Maple. This leads to the following equations for a low magnetic field and a high magnetic field, which are the highest order Taylor terms only. This shows that both regimes work, and an optimum must exist.

$$|\Psi_S\rangle\langle\Psi_S|_{low} = 1 + (\beta-1)\,\frac{\left(48\left({}^{\Omega}/_{\gamma}\right)^{4}+8\left({}^{\Omega}/_{\gamma}\right)^{2}+1\right)}{128\left(4\left({}^{\Omega}/_{\gamma}\right)^{2}+1\right)\left({}^{b}/_{\gamma}\right)^{2}} + O((1-\beta)^{2} \tag{30}$$

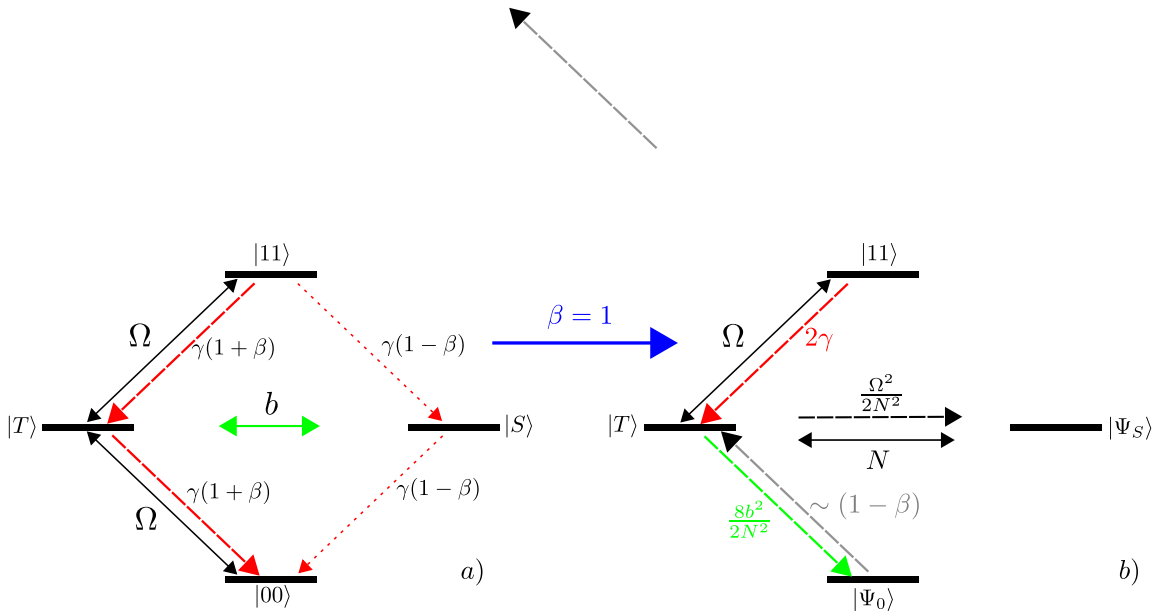

Figure 10: The two level scheme with wire decay. **a)** The drive Ω is symmetric and doesn't affect the anti-symmetric state $|S\rangle$. The dipole induced level shift g_{12} between state $|S\rangle$,$|T\rangle$ and $|11\rangle$ are zero due to the distance for $n = 2$. The γ here represents the total decay. **b)** The same picture in the new basis for $\beta = 1$, in this regime all but two coherences have disappeared. The state $|\Psi_S\rangle$ is dark with respect to decay. The grey arrow denotes the main loss process of state $|\Psi_S\rangle$ which scales linearly with the population of state $|11\rangle$.

$$|\Psi_S\rangle\langle\Psi_S|_{high} = 1 + \frac{(\beta-1)\left(\Omega/\gamma\right)^4}{256\left(b/\gamma\right)^4} + O((1-\beta)^2 \tag{31}$$

Here Eq. (30) is the case where the not maximally entangled state $|00\rangle$ is minimally present, whereas in Eq. (31) the maximally entangled state $|S\rangle$ is dominantly present. From this it can be seen that state $|\Psi_S\rangle$ can be prepared for different magnetic fields. In order to maximize the entanglement in state $|\Psi_S\rangle$ with respect to the ideal magnetic field strength it is required to add a correction for the presence of state $|00\rangle$. It should be worth noting that for $\beta = 1$, state $|\Psi_S\rangle$ is the only populated state regardless of the values of parameters Ω & b. This is in seeming contrast with Fig. (9b), but is caused by the exact contributions of the off-diagonal elements that make it so.

Maximizing the fidelity of state $|S\rangle$, which is maximally entangled, is done by applying a correction term

$$F_S = F_{\Psi_S} - \|\langle 11|\Psi_S\rangle\|^2 \tag{32}$$

Subsequently then one substitutes b in the expression for the fidelity with the state $|S\rangle$ in Eq. (32) with $b = \sqrt{2p}\Omega$ and take the limit of $\Omega \to \infty$. Where p is a parameter that expresses the ratio between driving and magnetic field strength. Then the limit for high driving is taken to find the optimal parameter conditions as discussed before, which are valid for all values of Ω. This results in the expression of the fidelity

$$F_{S,high\,\Omega} = \frac{1}{4}\,\frac{-8\beta p - 2\beta - \beta^2 - 2\beta^2 p + 26p + 3 + 16p^2}{14p + 20p^2 + 8p^3 + 3 - \beta^2 - 2\beta^2 p - 2\beta - 8\beta p - 8\beta p^2} \tag{33}$$

The expression found forms a near perfect approximation for driving over $\Omega > 2\gamma$, and is expressed here as 'high Ω' only for simplicity. Denote that for $p = 0$, or no magnetic field, the fidelity is only a quarter and hence *both symmetry breaking mechanisms are required.*

The Eq. (33) has a global maximum with respect to p. This maximum is the ideal ratio for between drive and magnetic field depending on β alone. This maximum scales with a square root near $\beta = 1$

$$p_{max} = \sqrt{\frac{3}{8}}\sqrt{1-\beta} - \frac{1}{4}\,(1-\beta) + O((1-\beta)^2 \tag{34}$$

Substituting the expression for the ideal case from Eq. (34) into a non limit version of Eq. (33) and expanding around $\beta = 1$ results in the following fidelity with state $|S\rangle$ in the strongly dissipative regime for all driving strengths

$$F_S = 1 - \frac{1}{24}\,\frac{\left(12\,{}^{\Omega}\!/_{\gamma}{}^2 + 1\right)\left(8\,{}^{\Omega}\!/_{\gamma}{}^2 + 1\right)}{{}^{\Omega}\!/_{\gamma}{}^2\left(4\,{}^{\Omega}\!/_{\gamma}{}^2 + 1\right)}\sqrt{6}\sqrt{1-\beta} + O((1-\beta)^1 \tag{35}$$

It is emphasized that this is not just for high driving alone. As can be seen from this expression the fidelity does however not benefit from a low driving. This was to be expected from Fig. (9 b), as for low driving the term out of state $|\Psi_0\rangle$ is reduced making the state the most populated in contrast to state $|\Psi_S\rangle$. Also in the original basis, a low driving will not favour the populations of the higher states and it simply reduces to the ground state $|00\rangle$. Expanding Eq. (35) for higher driving $\Omega \approx 2\gamma$ and higher, results in a simpler equation with the highest order Taylor terms only

$$F_{S,high\,\Omega} = 1 - \sqrt{6}\sqrt{1-\beta} + \frac{11}{2}\,(1-\beta) - \frac{13}{3}\sqrt{6}\,(1-\beta)^{3/2} + O((1-\beta)^2 \tag{36}$$

This scaling of the fidelity with the coupling to the wire is due to the fact that there are two symmetry breaking processes working conjunctively in the system. One symmetry breaking process is the same as was done in the work of Wang Schirmer with the magnetic field. This is the process we want and can easily control. Whereas the other is the symmetry breaking done by decay into the plasmonic wire. This is the inevitable process as the system couples to the wire and not an optical cavity. In essence one optimizes the two processes of symmetry breaking in both terms in the master equation (5), and then sets the externally controllable parameters to be at values that maximizes the effectiveness of these two processes together.

Optimizing here means that the distance between the emitters is chosen to be of a distance that is the lesser of two evils. As the distance that maximizes dipole-dipole coupling also maximizes decay out of states $|S\rangle$ and $|T\rangle$. Decay to a wire can, at certain distances, also be an elemental symmetrical mechanism that favours certain symmetric conditions, without the losses from the dipole-dipole distances.

It should be noted that even though Eq. (36) scales with the square root of $(1-\beta)$, it also means that for $\beta \approx {}^{9}\!/_{10}$ the fidelity is only $F_S \approx 0.56$, whereas for $\beta \approx {}^{99}\!/_{100}$ the fidelity is $F_S \approx 0.80$. This is experimentally seen not very favourable.

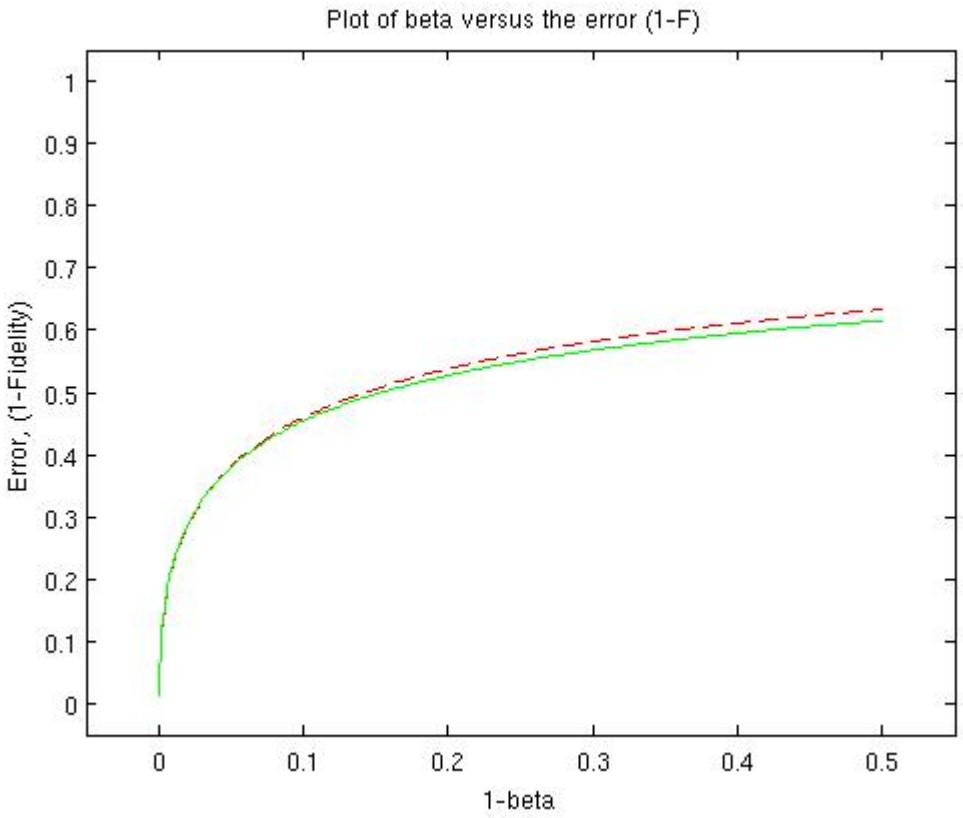

Figure 11: The numerical result (dashed red) versus the analytical result (green) for a high driving $\Omega/\gamma = 4$, at the ideal ratio of Ω/b for each β separately. The curves change little for all values of $\Omega/\gamma \geqslant 2$. For values of driving strength below this value, both the analytical and the numerical results will scale more steep near $\beta = 1$.

3.5 Numerical comparison

The results as found in Eqs. (35) & (36) have also been found in the numerical solving of Eq. (5) using the null-vector method from Sec. 2.5.2. This result can be seen in Fig. (11).

From Fig. (11). It can be seen that the numerical result matches well with the analytical result. This weak driving shows worse scaling with the error for both the analytical and the numerical result. There is a small difference between the two curves for lower β. The reasons for this is that the analytical answer is only computed for the first 5 terms of the Taylor approximation around $\beta = 1$. Unlike the case that will be seen for Sec. 4.5.1 here the analytical solution is unique and the steady state is found completely analytically without additional approximations. The scaling of Eq. (36) is numerically confirmed.

3.6 Results

In this chapter it was shown that dissipative state preparation on a wire can be achieved for two 2-level emitters. It was also shown that symmetry breaking by the wire alone is insufficient in producing good fidelities in two 2-level systems. It was also shown that by inclusion of a magnetic symmetry breaking it is possible to achieve arbitrarily good fidelities. This fidelity scales with the square root of the error $(1-\beta)$ for high β.

Furthermore the results suggest that the process of symmetry breaking by the wire, or by decoherence, could be a sufficient symmetry breaking process on itself in the case of coupling to higher exited states when a magnetic field is not required to couple to the desired state.

4 Three-level section

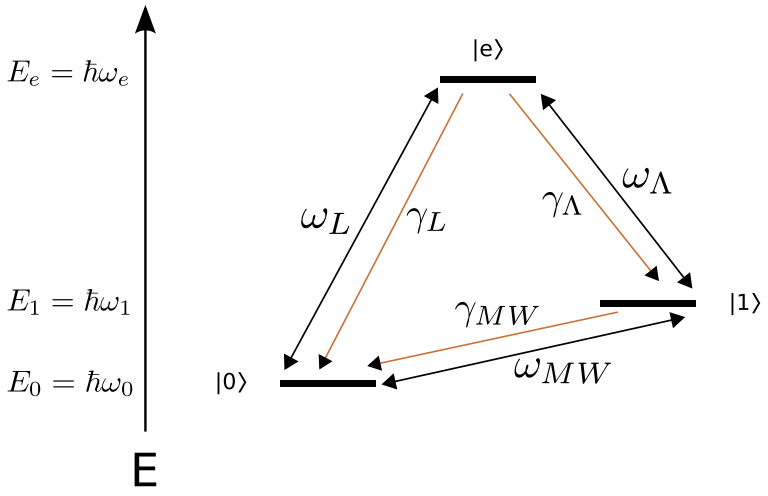

Figure 12: A single Λ-emitter. The three levels are labeled accordingly. Also shown are three possible interaction two by lasers $\omega_\Lambda \, and \, \omega_L$ and a microwave field or Raman transition of Rabi frequency Ω_{MW} and energy $\hbar\omega_{MW}$ in black arrows. The brown arrows represent the decay from each transition. Each transition has a unique label as can be seen in the figure.

In this section, we investigate why to take 3-level emitters instead of 2-level emitters. The formalism used will be derived. Methods used to find solutions and their advantages and drawbacks will be discussed. A road map will be given to more easily understand the results of Sec. (4.2) and to facilitate possible exploration to other scheme's of entanglement production. After this a scheme is given that result in dissipative state preparation of a maximally entangled state scaling linearly with the β-factor. Based on the principle of this scheme other schemes are suggested. Subsequently the results will be discussed, and a experimental set-up is suggested.

4.1 Why look at two 3-level Lambda emitters at all?

An interesting question is why to use a 3-level emitter in the first place. The two 2-level system works, is more easily solvable and is much simpler to understand. It doesn't however represent the average experimental set-up. In practice emitters are not as simple as they are described. They are either a set of atoms, or molecules up to relatively large quantum dots. And whatever emitter used interactions will be found are merely considered as-if it were a 2-level or 3-level emitter. Finding the right set-up in an experiment is therefore never easy. In practice superconducting qubits[76] are used for 3-level emitters, based upon Josephson junction since these have a lot of freedom and couple relatively well to optical cavities. Since here, the used level system needs to be coupled primarily to electronic states like plasmons, we can employ gate controlled quantum dots[77–80] instead.

An added difficulty of the 2-level emitters is that the different ways to make a state maximally entangled through dissipative state preparation is very limited. With only one drive, one phase difference, one decay and one dipole coupling to tune doing this is theoretically simple, but experimentally

troublesome. This is where 3-level Λ-emitter comes in use. As can already be seen in Fig. 4 were there is three drives, phase differences, decay channels and three dipole couplings. Alongside this with the 3-level Λ-emitters there is a relative luxury to have an exited and hence fast decaying state.

In contrast to the 2-level emitters where the highest energy state is part of the desired entangled state, the 3-level Λ-emitters have a highest state which is not only much higher, but also not part of the desired prepared state. Due to Fermi's golden rule one can quickly see that these exited states are fast decaying, meaning that undesired states are from the start physically unlikely to live long.

In conclusion, 3-level Λ-emitters are faster in dissipative state entanglement, are more easily to find and are more easy to engineer regardless of experimental shortcomings. It will also show that 3-level Λ-emitters have the unique possibility to optimize the wire usage in a system, where the best results are found in an imperfect set of parameters.

4.2 Derivation of the formalism

In order to view all the possibilities, here the derivation of the general solution will be given. Unlike the two 2-level case there will not be a magnetic field used. This is partially for simplicity and, it is not necessary due to the more varied possibilities of a three level system. In the derivation there will firstly be given a set of operators who act on each emitter and each emitter is part of its own Hilbert space. From thereon an unitary transformation is given for the Hamiltonian which can be different for different preparation schemes and conditions. Only the general transformation is fully derived by the selective differential equation method for the case of resonant drives.

To accommodate the large equations to follow, the lowering operators will be defined as earlier in comparison to Fig. 12 :

$$\begin{aligned}
\hat{\sigma}_{e1,i} &= |1\rangle_i \langle e|_i \qquad \hat{\sigma}_{1e,i} = |e\rangle_i \langle 1|_i \\
\hat{\sigma}_{e0,i} &= |0\rangle_i \langle e|_i \qquad \hat{\sigma}_{0e,i} = |e\rangle_i \langle 0|_i \\
\hat{\sigma}_{10,i} &= |0\rangle_i \langle 1|_i \qquad \hat{\sigma}_{01,i} = |1\rangle_i \langle 0|_i
\end{aligned}$$

The index $i = 1, 2$ represents the emitter the operator is working on. And the raising operators are their respective Hermitian conjugates. The terms in Eq. 6 then become:

$$\hat{H}_0 = \hbar \sum_{i=1}^{2} (\omega_0 \hat{\sigma}_{e0,i}\hat{\sigma}_{0e,i} + \omega_1 \hat{\sigma}_{e1,i}\hat{\sigma}_{1e,i} + \omega_e \hat{\sigma}_{1e,i}\hat{\sigma}_{e1,i}) \tag{37}$$

$$\hat{H}_g = \hbar \sum_{i \neq j} (g_{ij,e0}\hat{\sigma}_{0e,i} \otimes \hat{\sigma}_{e0,j} + g_{ij,e1}\hat{\sigma}_{1e,i} \otimes \hat{\sigma}_{e1,j} + g_{ij,10}\hat{\sigma}_{01,i} \otimes \hat{\sigma}_{10,j}) \tag{38}$$

$$\begin{aligned}
\hat{H}_d &= 2^{-1}\hbar\Omega_L e^{i\omega_L t} \quad (\hat{\sigma}_{0e,1} + e^{i\phi_L}\hat{\sigma}_{0e,2}) + H.c. \\
&+ 2^{-1}\hbar\Omega_\Lambda e^{i\omega_\Lambda t} \quad (\hat{\sigma}_{1e,1} + e^{i\phi_\Lambda}\hat{\sigma}_{1e,2}) + H.c. \\
&+ 2^{-1}\hbar\Omega_{MW} e^{i\omega_{MW} t} \quad (\hat{\sigma}_{01,1} + e^{i\phi_L}\hat{\sigma}_{01,2}) + H.c.
\end{aligned} \tag{39}$$

Filling in Eq. 6 the Eqs. (37),(38) & (39). The master equation Eq. (5) becomes:

$$\begin{array}{rcccl}
\frac{\partial\hat{\varrho}}{\partial t} = -\frac{i}{\hbar}\left[\hat{H},\hat{\varrho}\right] & - & \frac{1}{2}\sum_{ij}\gamma_{ij,e0} & [& \hat{\varrho}\cdot(\hat{\sigma}_{0e,i}\otimes\hat{\sigma}_{e0,j}) \quad +(\hat{\sigma}_{0e,i}\otimes\hat{\sigma}_{e0,j})\cdot\hat{\varrho} \\
 & & & & -2\cdot(\hat{\sigma}_{e0,j}\otimes\hat{\varrho}\otimes\hat{\sigma}_{0e,i}) \quad] \\
 & - & \frac{1}{2}\sum_{ij}\gamma_{ij,e1} & [& \hat{\varrho}\cdot(\hat{\sigma}_{1e,i}\otimes\hat{\sigma}_{e1,j}) \quad +(\hat{\sigma}_{1e,i}\otimes\hat{\sigma}_{e1,j})\cdot\hat{\varrho} \\
 & & & & -2\cdot(\hat{\sigma}_{e1,j}\otimes\hat{\varrho}\otimes\hat{\sigma}_{1e,i}) \quad] \\
 & - & \frac{1}{2}\sum_{ij}\gamma_{ij,10} & [& \hat{\varrho}\cdot(\hat{\sigma}_{01e,i}\otimes\hat{\sigma}_{10,j}) \quad +(\hat{\sigma}_{01,i}\otimes\hat{\sigma}_{10,j})\cdot\hat{\varrho} \\
 & & & & -2\cdot(\hat{\sigma}_{10,j}\otimes\hat{\varrho}\otimes\hat{\sigma}_{01,i}) \quad]
\end{array} \tag{40}$$

In the above equation all considered interactions of two Λ-emitters as in Fig. (12) have been taken into account.
To further accommodate simplicity and make a comparison with this figure the following relations are given:

$$\begin{array}{ccc}
\gamma_{ii,e0} = \gamma_L & \gamma_{ii,e1} = \gamma_\Lambda & \gamma_{ii,10} = \gamma_{MW} \\
\gamma_{12,e0} = \beta\gamma_L & \gamma_{12,e1} = \beta\gamma_\Lambda & \gamma_{12,10} = \beta\gamma_{MW}
\end{array} \tag{41}$$

$$with \qquad \gamma_{ji,kl} = \gamma_{ij,kl} \qquad \forall\, k,l$$

Where the the γ's are the total decay of a transition, and the beta is the fraction of decay into the wire. **Take note** that the total decay does not equal the free decay $\gamma \neq \Gamma$ unless there is no decay into the wire. The exact expressions of these γ_{12}'s are given in Eq. (8).

4.2.1 Unitary transformation

Following here will be an unitary transformation applied to the Hamiltonian above, in an attempt to make it time-independent:

$$\hat{\bar{H}} = i\hbar\dot{U}U^\dagger + UHU^\dagger \tag{42}$$

Where the bar over the Hamiltonian implies that $\hat{\bar{H}}$ satisfies the Schrödinger equation, if the wave functions transforms as $|\bar{\psi}\rangle = U|\psi\rangle$. The unitary transformation chosen for the general case is:

$$U = exp(it\sum_{i=1}^{2}(|0\rangle_i\langle 0|_i\,\omega_L + |1\rangle_i\langle 1|_i\,\omega_\Lambda)) = e^{itH_U/\hbar} \tag{43}$$

Then parts Eq. 42 transform as follows:

$$UH_0U^\dagger = H_0 \& \quad UH_gU^\dagger = H_g \quad \& \quad i\hbar\dot{U}U^\dagger = -H_U$$

And the desired change takes place in the H_d part of the Hamiltonian that contains the drives:

$$\begin{array}{rcccccc}
\hat{H}_d & = & 2^{-1}\hbar\Omega_L & (\hat{\sigma}_{0e,1} & + & e^{i\phi_L}\hat{\sigma}_{0e,2}) & + H.c. \\
 & + & 2^{-1}\hbar\Omega_\Lambda & (\hat{\sigma}_{1e,1} & + & e^{i\phi_\Lambda}\hat{\sigma}_{1e,2}) & + H.c. \\
 & + & 2^{-1}\hbar\Omega_{MW}e^{i(\omega_{MW}+\omega_\Lambda-\omega_L)t} & (\hat{\sigma}_{01,1} & + & e^{i\phi_L}\hat{\sigma}_{01,2}) & + H.c.
\end{array} \tag{44}$$

As can be seen in the equation above, the only case where the general solution is time-independent is

for the case where all three drives are on resonant, then $\omega_{MW} + \omega_\Lambda = \omega_L$ and the Hamiltonian becomes time independent.

An important note to make is that this is the only possible case where a system with three drives becomes time independent. However, in the case of two or one drive(s) applied there always exists an unitary transformation transforming alike Eq. (42) that will make the system time-independent. It will show that for all practical purposes this is the case. When so required the desired transformation and resulting change H_U will be given.

It is possible to further simplify the master equation by transforming the parameters into scalar parameters. Doing so means one needs to define an unique and characteristic decay time $\tau = \Gamma^{-1}$ where Γ is defined as the total free decay. Then Eq. (16) will become:

$$\frac{\partial \hat{\varrho}}{\partial \tau} = -\frac{i}{\hbar}\left[\hat{H}(c'), \hat{\varrho}\right] \quad - \quad \frac{1}{2}\sum_{ij}\gamma'_{ij} \quad [\ldots] \tag{45}$$

Where c' is a set of parameters. Here the apostrophe implies that all parameters are scaled by the total decay. In this section from hereon a parameter is implied to always be scaled with respect to the total free decay and the apostrophe is neglected. In final results it will however be shown for completeness.

4.2.2 Basis

So far the explicit basis as is used in Fig. 4 has not yet been expressed. The solving of Eq. 40 is of course not dependent on any basis whatsoever. It is however cognitively more pleasant to work in a basis where all the states are part of the joint Hilbert space $H_1 \otimes H_2$. In the end, any entangled state worth researching is part of this Hilbert space. Many bases are possible, in this work however the basis is used as used in other work[38] and that has the same anti-symmetric ground state as for the 2-level case:

$$\begin{aligned}
|00\rangle &= |0\rangle_1 |0\rangle_2 \\
|11\rangle &= |1\rangle_1 |1\rangle_2 \\
|T\rangle &= 2^{-1/2}(|1\rangle_1 |0\rangle_2 + |0\rangle_1 |1\rangle_2) \\
|S\rangle &= 2^{-1/2}(|1\rangle_1 |0\rangle_2 - |0\rangle_1 |1\rangle_2) \\
|T_0\rangle &= 2^{-1/2}(|e\rangle_1 |0\rangle_2 + |0\rangle_1 |e\rangle_2) \\
|S_0\rangle &= 2^{-1/2}(|e\rangle_1 |0\rangle_2 - |0\rangle_1 |e\rangle_2) \\
|T_1\rangle &= 2^{-1/2}(|e\rangle_1 |1\rangle_2 + |1\rangle_1 |e\rangle_2) \\
|S_1\rangle &= 2^{-1/2}(|e\rangle_1 |1\rangle_2 - |1\rangle_1 |e\rangle_2) \\
|ee\rangle &= |e\rangle_1 |e\rangle_2
\end{aligned}$$

Alike in the 2-level case, the entangled state that is to be prepared will be the $|S\rangle$ state in this section unless explicitly noted otherwise.

4.3 Solving methods for 3-level systems

As expressed in Sec. (2.5) there two methods of solving are employed. In this case there will be an elaboration of the two analytical methods and the numerical method used. These analytical methods

are used specifically for the 3-level case as they cannot or are not be applied to the 2-level case. The numerical method is the same.

4.3.1 Analytical methods

For the analytical methods rate equations will be used. The approximation is made that after the coherence is balanced out with respect to the decay of this coherence, the term in the density matrix is evolving very slowly. This approximation can be applied to nearly all optical coherences between higher exited states. This is popularly applied to solve the optical Bloch equations.[81] First there will be a derivation of this method for the general case which can be used to quickly analyze the dynamics between two states mediated by a higher exited state.

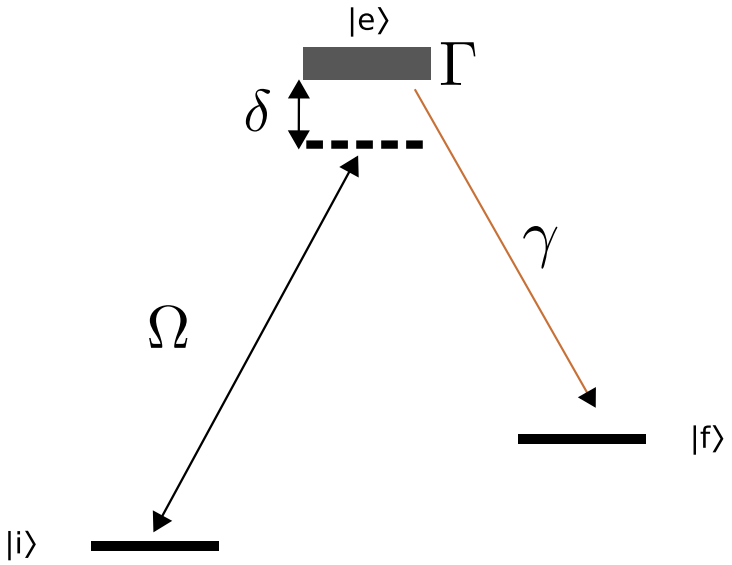

Figure 13: The general case for the effective rate between the initial state $|i\rangle$ and the final state $|f\rangle$ via the higher broadened and detuned state $|e\rangle$.

In Figure (13) one can see the system used in the effective rate derivation. Here Ω is the driving from the initial state to a higher exited state, δ is the detuning of the higher state, Γ is the width of the exited state which represents all its possible decay channels and γ is the decay[(3)] from the excited state to the final state specifically. Then the change of the density matrix elements over time becomes:

$$\dot{\varrho}_{ii} = i\Omega(\varrho_{ie} - \varrho_{ei}) \tag{46}$$

$$\dot{\varrho}_{ie} = i\Omega(\varrho_{ee} - \varrho_{ii}) - (\frac{\Gamma}{2} + i\delta)\varrho_{ie} \tag{47}$$

[(3)] Not to be mistaken with the total and total free decay

$$\dot{\varrho}_{ee} = -\Gamma\varrho_{ee} - i\Omega(\varrho_{ie} - \varrho_{ei}) \tag{48}$$

$$\dot{\varrho}_{ff} = \gamma\varrho_{ee} \tag{49}$$

Then solving the optical coherence Eq. (47) so that $\dot{\varrho}_{ie} = 0$ will give an expression for ϱ_{ie} :

$$\varrho_{ie} = \frac{-i\Omega}{\Gamma + i2\delta}(\varrho_{ee} - \varrho_{ii}) \tag{50}$$

Substituting Eq. 50 into Eq. 48 yields:

$$\dot{\varrho}_{ee} = -\Gamma\varrho_{ee} + \frac{\Omega^2\Gamma}{\Gamma^2 + 4\delta^2}(\varrho_{ii} - \varrho_{ee}) \tag{51}$$

Now approximating the higher states as fast decay so that there is no build up of population and the change of population over time is zero $\dot{\varrho}_{ee} = 0$, and subsequently substituting this result into Eq. 49 results in the effective rate expression:

$$\dot{\varrho}_{ff} = \frac{\gamma\Omega^2}{\Omega^2 + \Gamma^2 + 4\delta^2}\varrho_{ii} \tag{52}$$

This formula will allow a quick evaluation of the schemes as will be considered in Sec. 4.5. The system as expressed in Fig. 13 and calculated above is in fact analytically solvable within the assumptions taken. If one is to calculate with the selective differential equation method a similar technique is used, with just much more differential equations.

The second analytical method is therefore the selective differential equation method. Where the same approximations as named above are applied for all states. There is no general solution via this method. The general solution of Eq. (40) is not practically solvable. Such a solution is not mathematically impossible, however due to the limitations in computational power impossible to find.

4.3.2 Numerical methods

A time independent Hamiltonian , as was expressed in Sec. (4.2) , is not possible to make if one has three drives. However as also previously expressed in Sec. (2.5.2) the time dependence of the formalism is inherently there for some numerical methods, for these methods work independent of the time dependency of the Hamiltonian. If knowledge of the change of the system over time is desired. Therefore it is possible to numerically calculate inherently time-dependent systems, as discussed before. They are however not as fast as the eigenvalue method.

Codes were written with explicit time dependence and without time dependence with MATLAB. The first is a time differential equation solving method, and the latter the eigenvalue method as described in Sec. (2.5.2). A template of this method for MATLAB can be found in de Appendix.

It should be noted that the computation speed of the time dependent codes depend entirely on the size of the parameters used. This is only as relevant as the order of size differences between different parameters in the time dependent code. Due to Eqs. (7) & (8) this becomes problematic. As $\beta \to 1$ these parameters become arbitrarily large and computation time is increased dramatically or simply incomputable, since the the parameters scale with free decay and become smaller. For this reason

the time dependent method was abandoned in favor of a, though more complicated, time independent eigenvalue method. It can however be used to plot the evolution of the system for a specific set of parameters.

In this case it is possible to construct the time-independent effective matrix as discussed in Sec. (2.5.2).

4.4 How the system works.

In an attempt to understand how the system actually works a synopsis is given of all the terms that are expressed in Eq. (40). With use of these it is far simpler to theorize possible schemes. It can also be used in itself to understand the dynamics of a complicated system in a simpler way.

All the discussed sections below represent the system in their ideal case. In all realistic cases a superposition of the driving field with both driving symmetric and antisymmetric transitions are amongst things possible. Most notably is the wire decay and the dipole-dipole shift which cannot be taken in a simple superposition, for an increased strength of the one is automatically a loss of interaction strength of the other, as seen in Eqs. (8) & (7).

4.4.1 Total Decay

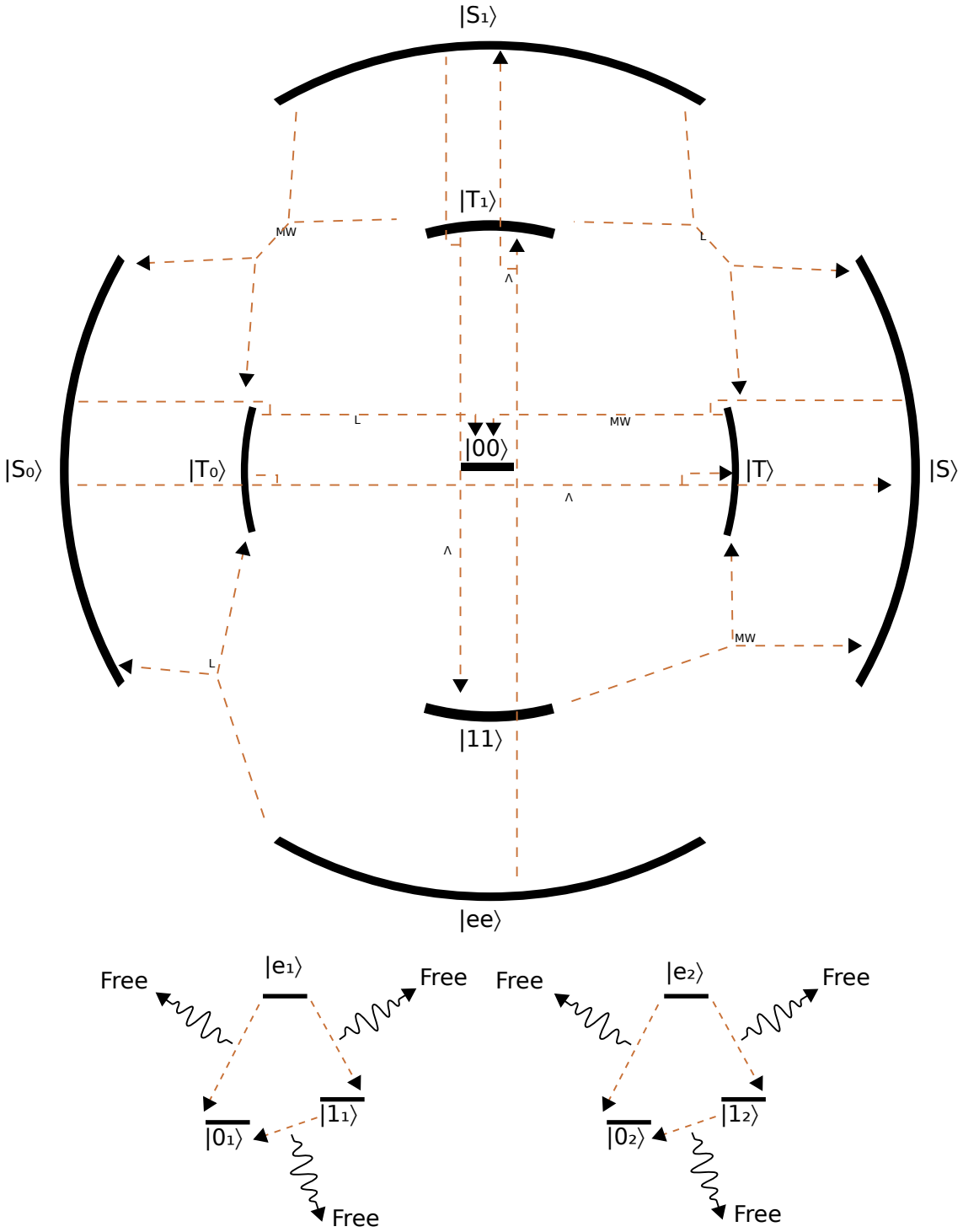

Figure 14: Here all the spontaneous total decay is shown between the states in the basis as chosen in Sec. 4.2.2. The split lines imply that a state equally decays into or from one or either states in the direction of the arrow.

In the Fig. 14 one sees all the possible total decay transitions. The values of the strengths can be found in table 1. Decay elements with respect to off-diagonal elements of the density matrix can be found in Appendix (C).

Initial state	Resulting states: 'L' $\|e\rangle \to \|0\rangle$	'Λ' $\|e\rangle \to \|1\rangle$	'MW' $\|1\rangle \to \|0\rangle$
$\|00\rangle$	■	■	■
$\|11\rangle$	■	■	$(\gamma_{MW}/4)$ $[\|T\rangle + \|S\rangle]$
$\|T\rangle$	■	■	$(\gamma_{MW}/4)$ $\|00\rangle$
$\|S\rangle$	■	■	$(\gamma_{MW}/4)$ $\|00\rangle$
$\|T_0\rangle$	$(\gamma_L/4)$ $\|00\rangle$	$(\gamma_\Lambda/32)$ $[\|T\rangle + \|S\rangle]$	■
$\|S_0\rangle$	$(\gamma_L/4)$ $\|00\rangle$	$(\gamma_\Lambda/32)$ $[\|T\rangle + \|S\rangle]$	■
$\|T_1\rangle$	$(\gamma_L/8)$ $[\|T\rangle + \|S\rangle]$	$(\gamma_\Lambda/4)$ $\|11\rangle$	$(\gamma_{MW}/32)$ $[\|T_0\rangle + \|S_0\rangle]$
$\|S_1\rangle$	$(\gamma_L/8)$ $[\|T\rangle + \|S\rangle]$	$(\gamma_\Lambda/4)$ $\|11\rangle$	$(\gamma_{MW}/32)$ $[\|T_0\rangle + \|S_0\rangle]$
$\|ee\rangle$	(γ_L) $[\|T_0\rangle + \|S_0\rangle]$	$(\gamma_\Lambda/4)$ $[\|T_1\rangle + \|S_1\rangle]$	■

Table 1: This table shows where a population from the initial state, or diagonal element of the density matrix, will decay into and with what strength due to free decay. The strength is noted within brackets. A ■ implies that the decay does not apply to this transition.

4.4.2 Wire Decay + Free Decay

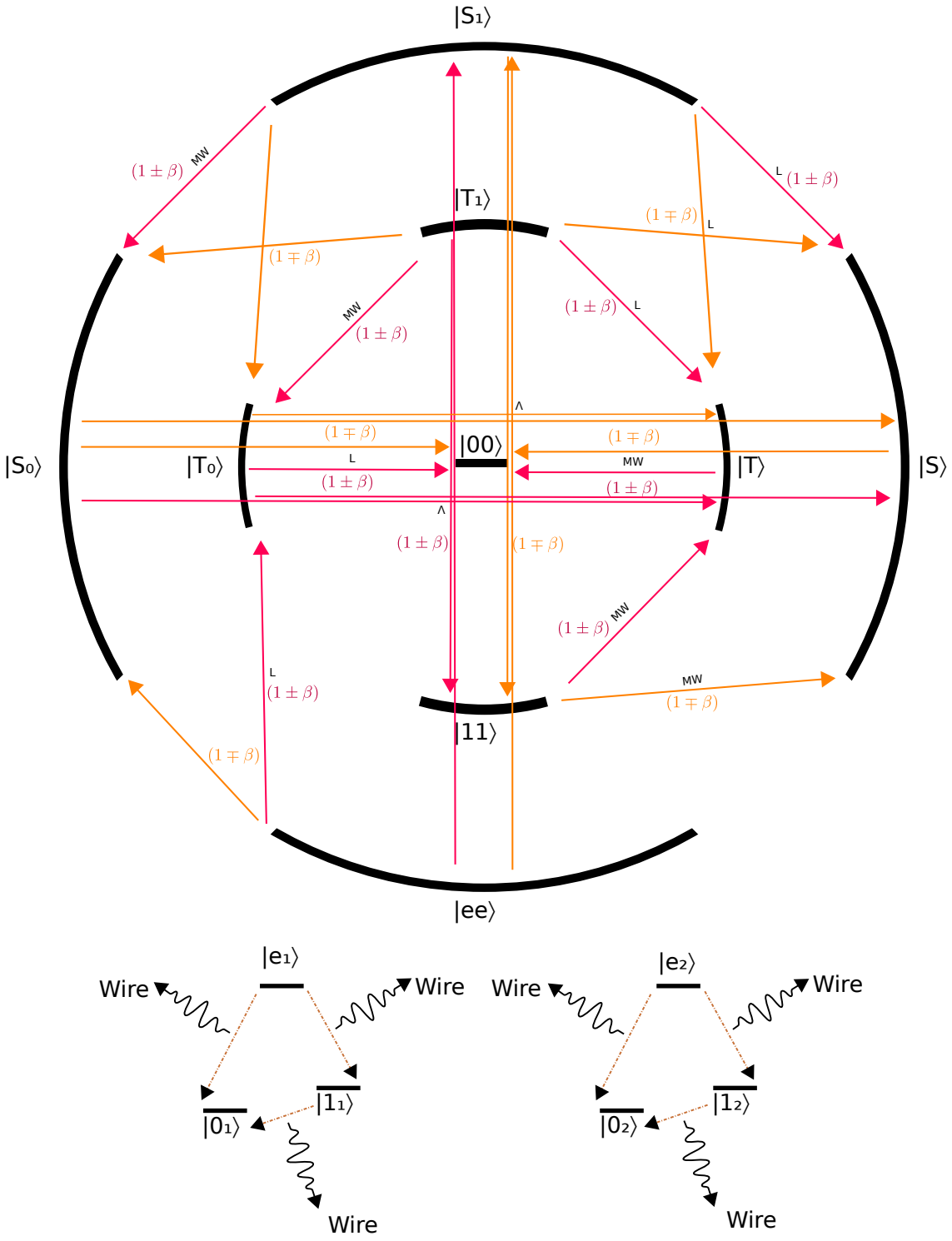

Figure 15: Here all the wire decay is shown between the states in the basis as chosen in Sec. (4.2.2). Orange arrows scale with $(1 \mp \beta)$ and purple arrows scale with $(1 \pm \beta)$. In future diagrams the spontaneous decay will be shown with the above arrows as if $\beta = 1$ for simplicity. For the right parameters decay will either become predominately symmetry breaking or symmetry preserving.

In the Fig. (15) one can see all the possible wire decay transitions. The values of the strengths can be found in table 2. The decay is at its maximum symmetry breaking, favouring either symmetric or anti-symmetric states, as seen in Fig. (8), and in strength dependent on the coupling to the wire. This kind of decay is a superposition of symmetry breaking and symmetry preserving, depending on the distance between the emitters with respect to the modal plasmon wavelength. Fig. (15) only shows the arrows for half-integer plasmon wave-lengths between emitters. At all other distances dipole-dipole interaction, discussed in Sec. (4.4.5), is also incorporated. It should be noted that Fig. (15) does not represent a very good experimental set-up as it would require three separate wires and various distances. Decay elements with respect to off-diagonal elements of the density matrix can be found in Appendix (D).

Initial state	Resulting states: 'L' $\|e\rangle \to \|0\rangle$	'Λ' $\|e\rangle \to \|1\rangle$	'MW' $\|1\rangle \to \|0\rangle$
$\|00\rangle$	■	■	■
$\|11\rangle$	■	■	$(\pm^{\beta\gamma_{MW}}/4) \quad [\|T\rangle - \|S\rangle]$
$\|T\rangle$	■	■	$(\pm^{\beta\gamma_{MW}}/4) \quad \|00\rangle$
$\|S\rangle$	■	■	$(\mp^{\beta\gamma_{MW}}/4) \quad \|00\rangle$
$\|T_0\rangle$	$(\pm^{\beta\gamma_L}/4) \quad \|00\rangle$	$(\pm^{\beta\gamma_\Lambda}/32) \quad [\|T\rangle - \|S\rangle]$	■
$\|S_0\rangle$	$(\mp^{\beta\gamma_L}/4) \quad \|00\rangle$	$(\mp^{\beta\gamma_\Lambda}/32) \quad [\|T\rangle - \|S\rangle]$	■
$\|T_1\rangle$	$(\pm^{\beta\gamma_L}/32) \quad [\|T\rangle - \|S\rangle]$	$(\pm^{\beta\gamma_\Lambda}/4) \quad \|11\rangle$	$(\pm^{\beta\gamma_{MW}}/32) \quad [\|T_0\rangle - \|S_0\rangle]$
$\|S_1\rangle$	$(\mp^{\beta\gamma_L}/32) \quad [\|T\rangle - \|S\rangle]$	$(\mp^{\beta\gamma_\Lambda}/4) \quad \|11\rangle$	$(\mp^{\beta\gamma_{MW}}/32) \quad [\|T_0\rangle - \|S_0\rangle]$
$\|ee\rangle$	$(\pm^{\beta\gamma_L}/4) \quad [\|T_0\rangle - \|S_0\rangle]$	$(\pm^{\beta\gamma_\Lambda}/4) \quad [\|T_1\rangle - \|S_1\rangle]$	■

Table 2: This table shows where a population from the initial state, or diagonal element of the density matrix, will decay into and with what strength due to wire decay. The strength is noted within brackets. A ■ implies that the interaction does not apply to this transition.

4.4.3 Symmetric Driving

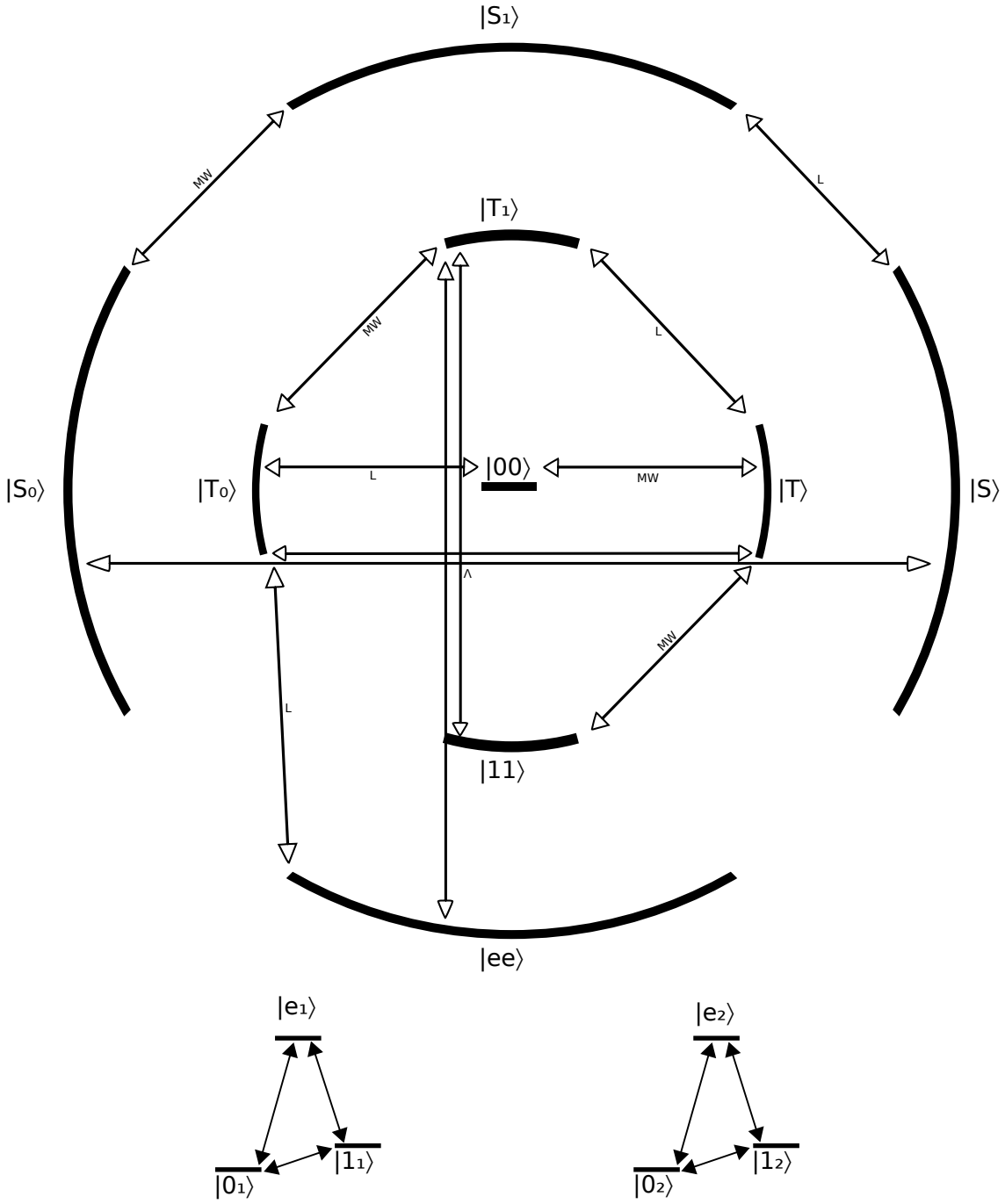

Figure 16: Here all the symmetric drives shown between the states in the basis as chosen in Sec. 4.2.2. This implies that the drive is symmetry conserving. In the physical case this means that both emitters are driven with the same phase of the driving field.

In the Fig. (16) one sees all the possible symmetry conserving driving transitions, in this case all on resonance. The values of the strengths can be found in table 3. Unlike dipole interaction and decay this interaction is completely externally applied and can be tuned in whatever way the experiment requires. An example of this can be seen if Fig. (4) , it should be noted that for detuned drives, the driving strength has a different form of term due to the detuning. This form is similar to the result from the effective rate formulation Eq. (52).

Initial state	Resulting states: 'L' $\|e\rangle \leftrightarrow \|0\rangle$	'Λ' $\|e\rangle \leftrightarrow \|1\rangle$	'MW' $\|1\rangle \leftrightarrow \|0\rangle$
$\|00\rangle$	$\left(\sqrt{2}\Omega_L\right)$ $\|T_0\rangle$	■	$\left(\sqrt{2}\Omega_{MW}\right)$ $\|T\rangle$
$\|11\rangle$	■	$\left(\sqrt{2}\Omega_\Lambda\right)$ $\|T_1\rangle$	$\left(\sqrt{2}\Omega_{MW}\right)$ $\|T\rangle$
$\|T\rangle$	(Ω_L) $\|T_1\rangle$	(Ω_Λ) $\|T_0\rangle$	$\left(\sqrt{2}\Omega_{MW}\right)$ $[\|00\rangle + \|11\rangle]$
$\|S\rangle$	(Ω_L) $\|S_1\rangle$	(Ω_Λ) $\|S_0\rangle$	■
$\|T_0\rangle$	(Ω_L) $[\|00\rangle - \|ee\rangle]$	(Ω_Λ) $\|T\rangle$	(Ω_{MW}) $\|T_1\rangle$
$\|S_0\rangle$	■	(Ω_Λ) $\|S\rangle$	(Ω_{MW}) $\|S_1\rangle$
$\|T_1\rangle$	(Ω_L) $\|T\rangle$	$\left(\sqrt{2}\Omega_\Lambda\right)$ $[\|ee\rangle - \|11\rangle]$	(Ω_{MW}) $\|T_0\rangle$
$\|S_1\rangle$	(Ω_L) $\|S\rangle$	■	(Ω_{MW}) $\|S_0\rangle$
$\|ee\rangle$	$\left(\sqrt{2}\Omega_L\right)$ $\|T_0\rangle$	$\left(\sqrt{2}\Omega_\Lambda\right)$ $\|T_1\rangle$	■

Table 3: This table shows where a population from the initial state to the resulting state and with what strength due to symmetric driving. The strength is noted within brackets. A ■ implies that the interaction does not apply to this transition.

4.4.4 Anti-Symmetric Driving

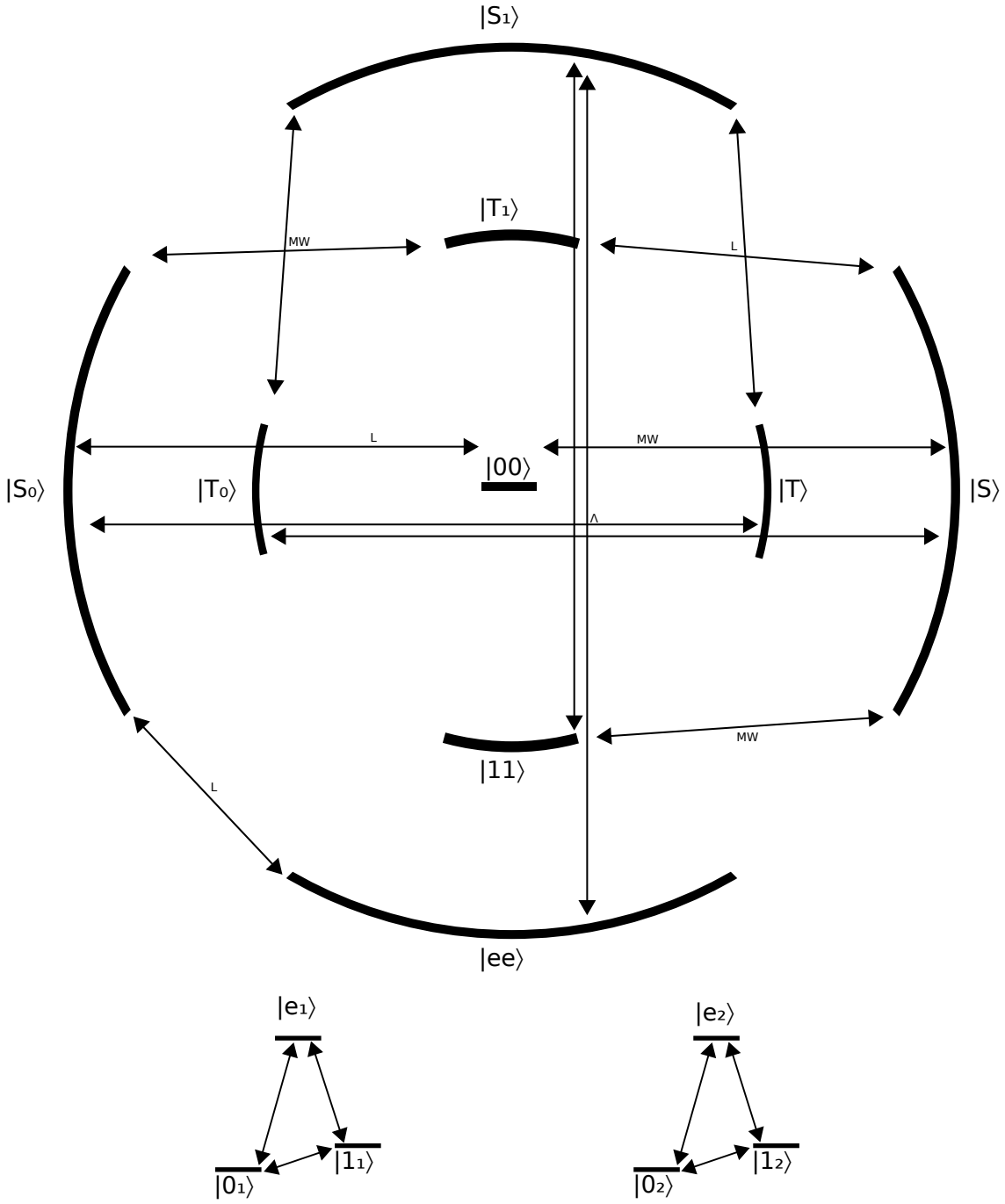

Figure 17: Here all the anti-symmetric drives are shown between the states in the basis as chosen in Sec. 4.2.2. In this case the driving does not preserve symmetry but instead completely inverts the symmetry. This corresponds to a physical case of two emitters being drive with opposite phase of the driving field.

In the Fig. (17) one sees all the possible anti-symmetry conserving driving transitions, in this case all on resonance. The values of the strengths can be found in table 4. As in Sec. (4.4.3) the drives can be detuned or super-positioned accordingly.

Initial state	Resulting states: 'L' $\|e\rangle \leftrightarrow \|0\rangle$	'Λ' $\|e\rangle \leftrightarrow \|1\rangle$	'MW' $\|1\rangle \leftrightarrow \|0\rangle$
$\|00\rangle$	$\left(\sqrt{2}\Omega_L\right)$ $\|S_0\rangle$	■	$\left(\sqrt{2}\Omega_{MW}\right)$ $\|S\rangle$
$\|11\rangle$	■	$\left(\sqrt{2}\Omega_\Lambda\right)$ $\|S_1\rangle$	$\left(\sqrt{2}\Omega_{MW}\right)$ $\|S\rangle$
$\|T\rangle$	(Ω_L) $\|S_1\rangle$	(Ω_Λ) $\|S_0\rangle$	■
$\|S\rangle$	(Ω_L) $\|T_1\rangle$	(Ω_Λ) $\|T_0\rangle$	$\left(\sqrt{2}\Omega_{MW}\right)$ $[\|00\rangle - \|11\rangle]$
$\|T_0\rangle$	■	(Ω_Λ) $\|S\rangle$	(Ω_{MW}) $\|S_1\rangle$
$\|S_0\rangle$	(Ω_L) $[\|00\rangle + \|ee\rangle]$	(Ω_Λ) $\|T\rangle$	(Ω_{MW}) $\|T_1\rangle$
$\|T_1\rangle$	(Ω_L) $\|S\rangle$	■	(Ω_{MW}) $\|S_0\rangle$
$\|S_1\rangle$	(Ω_L) $\|T\rangle$	$\left(\sqrt{2}\Omega_\Lambda\right)$ $[\|ee\rangle + \|11\rangle]$	(Ω_{MW}) $\|T_0\rangle$
$\|ee\rangle$	$\left(\sqrt{2}\Omega_L\right)$ $\|S_0\rangle$	$\left(\sqrt{2}\Omega_\Lambda\right)$ $\|S_1\rangle$	■

Table 4: This table shows where a population from the initial state will be going to and with what strength due to anti-symmetric driving. The strength is noted within brackets. A ■ implies that the interaction does not apply to this transition.

4.4.5 Dipole-Dipole level shifts

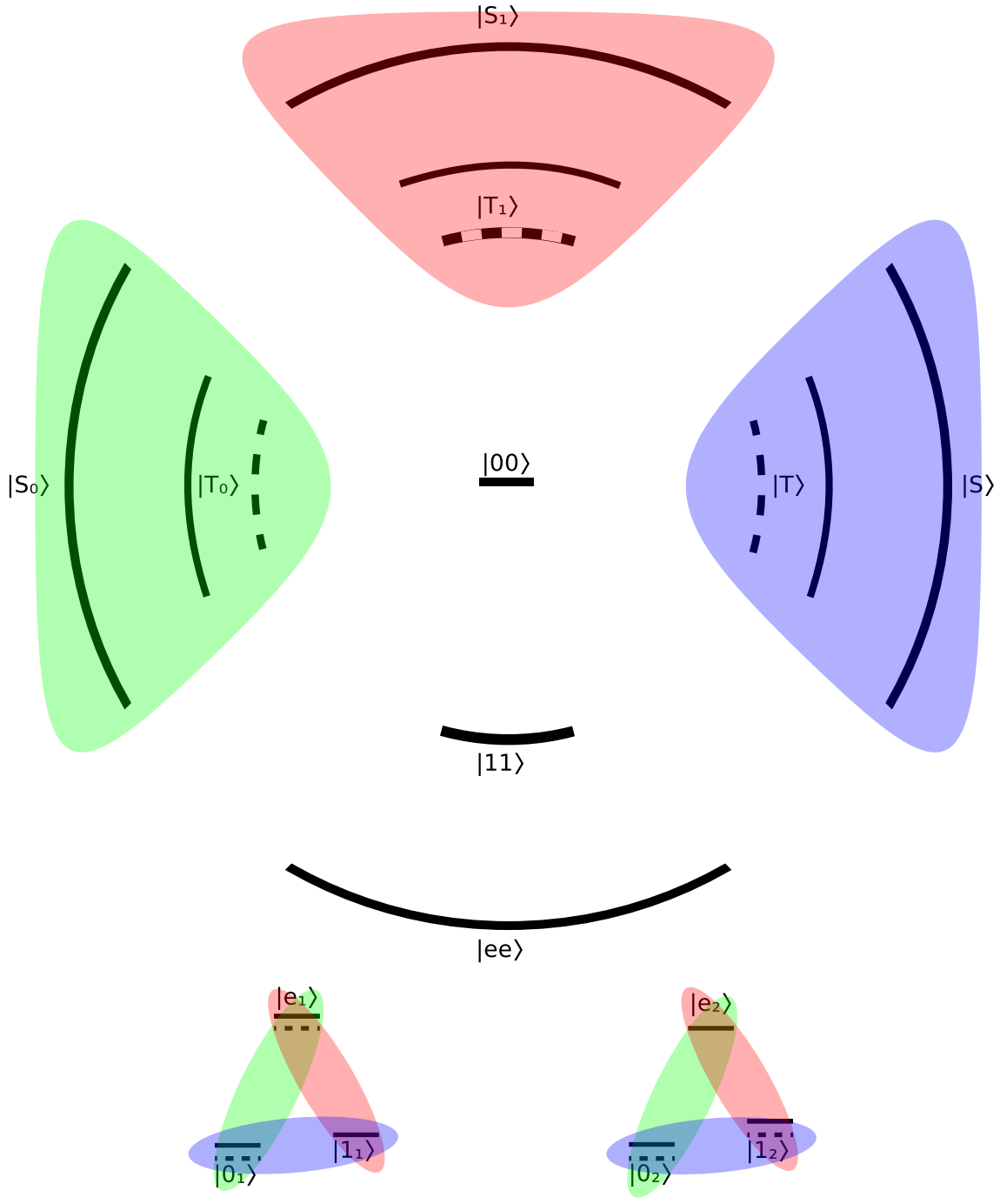

Figure 18: Here all the spontaneous free decay is shown between the states in the basis as chosen in Sec. 4.2.2. As in Fig. 15 there is a decay into the wire, however due to the separation of the emitters this only constitutes in a maximal dipole-dipole interaction there remains wire decay. In this figure a Unitary transformation is applied so that the detuning is only effectively manifesting itself upon the symmetric parts of the coloured regions. Without this the dipole interaction would be equal in size but opposite for states with different symmetry.

Unlike the other interactions the dipole-dipole interaction is different, it shifts energy levels. Alike in the case of wire decay, this kind of coupling will only be in the system, if the parameters have a distance $d \neq (n/2)$ where the distance is expressed in terms of the modal wavelength of the plasmons and n is an integer. In some cases, the distance can be tuned so that the maximal level shift is reached for a certain coupling between emitter and wire.

The shift caused by the dipole-dipole interactions with respect to Eq. 7 is:

$$\begin{array}{ccccc} g_L & \dashrightarrow & T_0 \rightarrow (1+g_L)T_0 & \& & S_0 \rightarrow (1-g_L)S_0 \\ g_\Lambda & \dashrightarrow & T_1 \rightarrow (1+g_\Lambda)T_1 & \& & S_1 \rightarrow (1-g_\Lambda)S_1 \\ g_{MW} & \dashrightarrow & T \rightarrow (1+g_{MW})T & \& & S \rightarrow (1-g_{Mw})S \end{array}$$

In most cases a unitary transformation will be applied so that the detuning is only on one level and leaves the other stable. In this transformation the dipole-dipole interactions look as follows:

$$\begin{array}{ccc} g_L & \rightarrow & T_0 \rightarrow (1+2g_L)T_0 \\ g_\Lambda & \rightarrow & T_1 \rightarrow (1+2g_\Lambda)T_1 \\ g_{MW} & \rightarrow & T \rightarrow (1+2g_{MW})T \end{array} \tag{53}$$

This is the level shift that is displayed in Fig. 18. Again the example figure does not represent a good physical set-up as it would require three wires at three different emitter distances.

The above discussed transitions in the above tables and figures are what work on the system. Combinations of these interactions are what make up the schemes that will be discussed below. However the contents of this section can also be used to give a hands on approach what other schemes can be made. Naturally not all possible schemes have been considered. And a focus has been made on a scheme that works really well. The results of this scheme can be found in the next section.

4.5 Schemes

4.5.1 S1 scheme

The first scheme to look at is the so called S1 scheme, as proposed in other work.[38] In this scheme only transitions L & Λ decay. A microwave drive and a drive on the L-transition are applied. Here, only the Λ ($|e\rangle \rightarrow |1\rangle$) transition couples to a mode in the single-mode wire. The diagrammatic representation can be seen in Fig. 19 . In contrast to previous work this S1 scheme works with coupling to a lossy wire instead an optical cavity, with emitters at a distance of a single modal plasmon wavelength.

For the S1 scheme both a solution via the selective differential equation method and a numerical solution are given because the general analytical solution $\dot{\hat{\rho}} = 0$ does not exist as was expressed in Sec. (4.3.1). It should be noted that for a different set of parameters the general analytical steady state solution $\dot{\hat{\rho}} = 0$ might exist. However if it exist, it must exist for all separate differential equations per element of the density matrix too. And here that is not the case for the S1 scheme.

The time dependent elements of the analytical solution are irrelevant for the population of state $|S\rangle$, this allows a comparison between numerical and analytical results for sets of parameters for which

this is relevant. This allows good analytical solution for a range of parameters, and good solution for all possible set of parameters near $\beta = 1$.

Other then for the two-level emitters, it is undesirable to express parameters in terms of total decay. Instead $\gamma_{ii,e0} = \gamma_L$,$\gamma_{ii,e1} = \gamma_\Lambda$and $\gamma_{ij,e1} = \frac{\Gamma\beta}{1-\beta}\, cos(k_{pl}d)$ for $i \neq j$. In this case $\gamma_L = \gamma_\Lambda = \frac{\Gamma}{2}$.

The S1 scheme relies on the same symmetry breaking principle as in the two-level case. This time however the symmetry breaking does not take place at the level of the ground states, but instead symmetry is broken between the excited states $|T_1\rangle$ and $|S_1\rangle$. This is simply because this time the ground states themselves do not decay. The effect is that the state $|S_1\rangle$ is predominantly less dissipative then state $|T_1\rangle$. This is opposite to the S1-scheme discussed by Reiter, Kastoryano and Sørensen.[38] In that case state$|S_1\rangle$ is rapidly decaying into state $|S\rangle$, whereas in this case state $|T_1\rangle$ is rapidly decaying in contrast to state $|S_1\rangle$. The main loss process from state $|S\rangle$ is the driving to state $|T_1\rangle$, since this is strongly decaying, coherences have a harder time to establish and will result to be weaker. This immediately also results in a problem, as an accumulation of population in states $|S_1\rangle$and $|S_0\rangle$ is reshuffled between them. This together with changed coherence due to the decay dynamics make the steady state solution $\dot{\hat{\rho}} = 0$ for this scheme non existent. It will however be shown to be possible to solve the system effectively.

Looking at Fig. 19 immediately reveals the effective processes at hand. The L-drive drives resonantly out of states $|T\rangle$,$|S\rangle$ and $|00\rangle$. This excites them to a state of different symmetry, $|S_1\rangle$, $|T_1\rangle$ and $|S_0\rangle$ respectively. This means that in contrast to the aforementioned scheme S1 scheme, the main gain process for state $|S\rangle$ is not state $|S_1\rangle$ but rather state $|S_0\rangle$. This however changes when $\beta \to 1$. When the state $|S_1\rangle$ becomes the predominant source of gain to state $|S\rangle$. This can be seen when combining Tables (1) & (2). Then decay between the following states is enhanced

$$\begin{aligned} |T_1\rangle &\to |11\rangle \\ |T_0\rangle &\to |T\rangle \\ |S_0\rangle &\to |S\rangle \\ |ee\rangle &\to |T_1\rangle \end{aligned} \tag{54}$$

And the decay between the following states is reduced

$$\begin{aligned} |S_1\rangle &\to |11\rangle \\ |S_0\rangle &\to |T\rangle \\ |T_0\rangle &\to |S\rangle \\ |ee\rangle &\to |S_1\rangle \end{aligned} \tag{55}$$

In other words, alike we saw in Sec. (3.4) the coupling to the wire breaks symmetry by preferring either symmetry breaking, or symmetry conserving decay channels. What should be noted is that though Eqs. (54) & (55) show which transitions have enhanced and reduced decay, the total decay of states $|T_0\rangle$,$|S_0\rangle$ and $|ee\rangle$ is unaffected. The increases in one channel is negating the loses due to decreases in the other decay channel. This is in contrast to decay from states states $|T_1\rangle$,$|S_1\rangle$, which are respectively increased and decreased. The total decay from state $|S_1\rangle$ scales down making it the second most populated. For this reason the scheme is named after the S1 scheme.

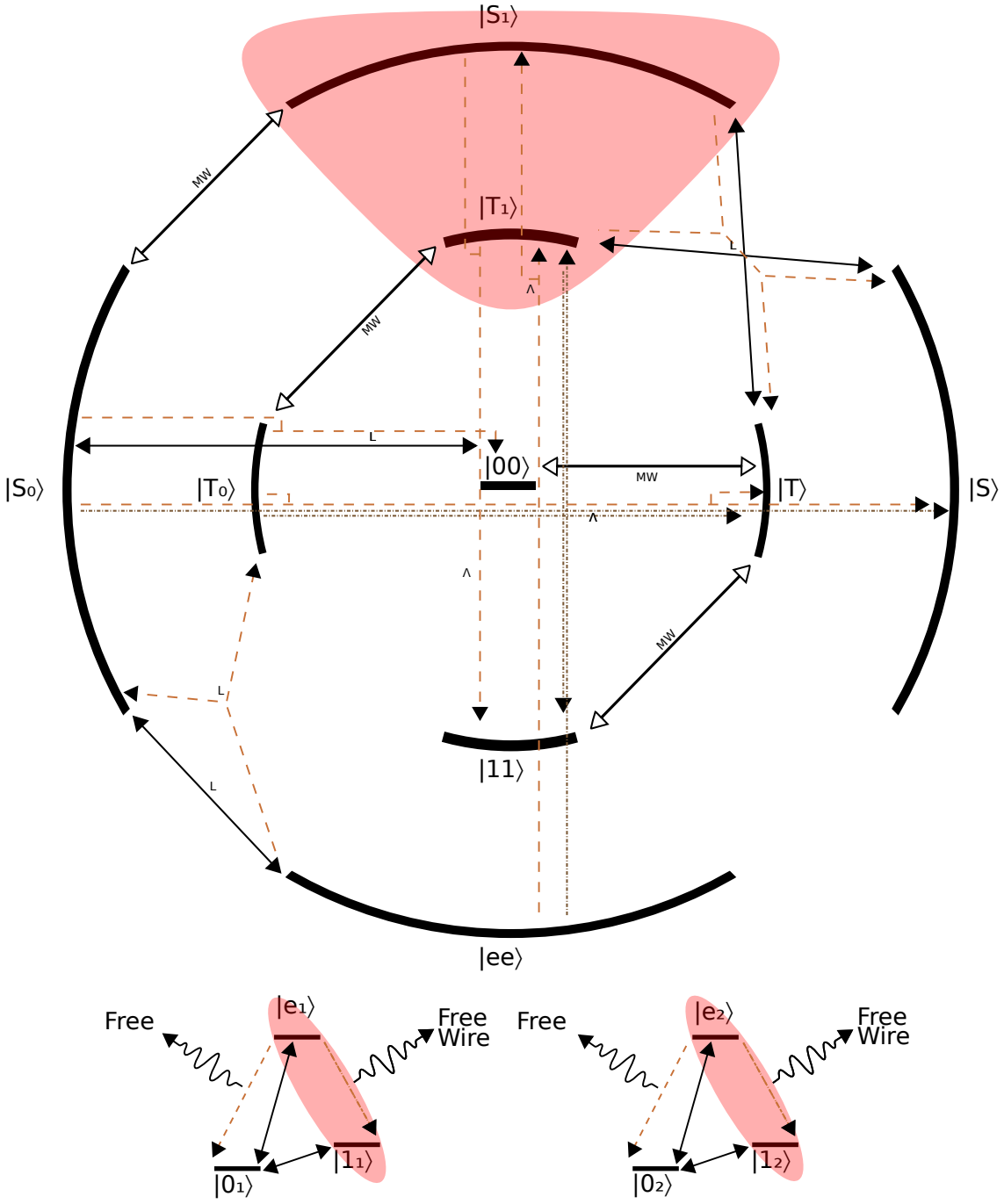

Figure 19: The S1 scheme. At integer distance decay is enhanced or subdued between various transitions favouring anti-symmetric states. A microwave field is applied to reshuffle the lower states with exception of the target state $|S\rangle$. A resonant driving of the L-transition is used which couples state $|T\rangle$ to state $|S_1\rangle$ and the target state $|S\rangle$ to state $|T_1\rangle$, where the latter has enhanced decay.

The main contributing factors off loss are the driving out of state $|S\rangle$. Since parts of this decays back into state $|S\rangle$ via natural free decay, only losses via state $|T_1\rangle$ into states $|T\rangle$ *and* $|11\rangle$ are suspected to be dominant.

Rate equations To exemplify the scheme the main loss and gain processes will be calculated by affective rates to result the main contribution of the fidelity with state $|S\rangle$. The main loss process is

$$|S\rangle \overset{\Omega_L}{\leftrightarrow} |T_1\rangle \overset{\left(\frac{\gamma}{2}+\gamma_{12}\right)}{\rightarrow} |11\rangle \tag{56}$$

Where the main gain processes are

$$\begin{array}{ccc} |T\rangle \overset{\Omega_L}{\leftrightarrow} |S_1\rangle \overset{\left(\frac{\gamma}{2}\right)}{\rightarrow} |S\rangle \\ \Omega_{MW} \updownarrow \\ |00\rangle \overset{\Omega_L}{\leftrightarrow} |S_0\rangle \overset{\left(\frac{\gamma}{4}+\frac{\gamma_{12}}{2}\right)}{\rightarrow} |S\rangle \end{array} \tag{57}$$

Since the microwave field strongly reshuffles the symmetric ground states, they can be assumed to be equally populated at all times in this rate equation consideration. The above three processes are the dominant processes in the scheme, but their reconciliation is everything but trivial. If one for instance only views the bottom gain and the only loss process, the two dominant processes, were to be taken into account the steady state can be found by solving

$$\frac{\left(\frac{\gamma}{4}+\frac{\gamma_{12}}{2}\right)\Omega^2}{\Omega^2+\gamma^2}\left(\frac{1-\rho_{SS}}{3}\right)-\frac{\left(\frac{\gamma}{2}+\gamma_{12}\right)\Omega^2}{\Omega^2+\left(\gamma+\gamma_{12}\right)^2}\rho_{SS}=0$$

This yields the following expression for the fidelity $F_{|S\rangle\langle S|}$ of state $|S\rangle$ that scales wrongly (quadratically) with the β-factor

$$F_{|S\rangle\langle S|}=1-6\left(\frac{\Omega}{\Gamma}^2+1\right)(\beta-1)^2$$

Whereas the process via state $|S_1\rangle$contributes a linear term to the scaling with the β-factor. We immediately see that for at least $\beta=1$ it is expected that state $|S\rangle$ is the most populated.

It is striking that these three main processes are *not sufficient enough* to produce a linear scaling as found by numerical considerations. The reason for this lies in the wire decay terms in the coherences between the Eqs. (56) & (57). The coherences with higher states scale only slightly different from lower processes as can be seen in Fig. (20). But as $\beta\rightarrow 1$, this minor difference is amplified until their contributions to the lower coherences exceed the decay loss. These are the transitions with the red arrows in Fig. (20), they change not only the coherence strengths, but also increase the decay into lower coherences. In other words, the off diagonal terms in the density matrix that describe the coherences in the ground states, have a increasingly growing term due to decay. This is not incorporated in the rate equations used, making the result incorrect.

Hence a general solution of the entire density matrix must be found in order to produce the linear scaling as is also found in the numerical calculations.

Selective Differential equation analysis

For the analytical analysis, it is required to express the equations of the complete system. These can be found in Appendix B . Here the matrix elements are expressed as $\varrho_{ij} = \varrho_{ij} |i\rangle \langle j|$ in other words all elements of the density matrix.

In order to calculate a fidelity the following approach is used. All equations of states with optical and decay terms are taken to be steady. This is the same approximation made in Sec. 4.3.1 . The problem as described in Sec. 2.5.1, is that the steady state in this case does not exist analytically. This problem is circumvented by choosing the states $|00\rangle$,$|T\rangle$ and $|11\rangle$ to be well reshuffled and hence equally populated at all times. Also it is assumed the higher states $|S_0\rangle$,$|T_0\rangle$,$|T_1\rangle$,$|S_1\rangle$,$|T\rangle$ and $|ee\rangle$ are essentially empty. After these assumptions a solution is obtained for the population of $\rho_{SS}(\Omega_L, \Omega_{MW}, \Gamma, \beta)$ in terms of the parameters $\Omega_L, \Omega_{MW}, \Gamma \,\&\, \beta$ where Γ is the total free decay. And β the parameter that represents coupling to the wire as expressed in Sec. (2.4).

The full solution is very complicated, but can be Taylored around $\beta = 1$. This yields the following expression for the fidelity F_S of state $|S\rangle$:

$$F_S = 1 - 6\left(1 + \frac{{\Omega_L}^2}{\Gamma^2}\right)(1-\beta) + \frac{3}{4}\left(77 + \left(157 + 32\frac{{\Omega_{MW}}^2}{\Gamma^2} + 80\frac{{\Omega_L}^2}{\Gamma^2}\right)\frac{{\Omega_L}^2}{\Gamma^2} + 24\frac{{\Omega_{MW}}^2}{\Gamma^2}\right)(1-\beta)^2 \tag{58}$$

Plus higher order terms.
Eq. (58is what was more or less expected based upon some of the rate equations. Surprisingly the first order term is not depended on Ω_{MW}. This is not entirely strange as our assumption of equal ground states already imposes the importance of the reshuffling of the ground states by Ω_{MW}. Since this isn't done explicitly in the analytical derivation it stands to reason it not being present in the first term. The full expression of Eq. (58) is plotted in Fig. 21.

Understanding the result From Fig. (20) it can be immediately seen why the scheme works. The red arrows direction is dependent on the distance between the emitters. When this is a single modal plasmon wavelength, it results in a reduced decay of the antisymmetric state $|S_1\rangle$ versus an increased decay to the symmetric state $|T_1\rangle$. Where the symmetric ground-state $|11\rangle$ can be seen as a transition state of this process as the chosen basis does not include a description for excitations inside the wire (not depicted in the figure).
If the symmetry of this decay process where to be reversed, when the distance of the emitters is half a modal plasmon wavelength, then all red arrows from Fig. (20) will invert direction. The arrow hence represents which of the two connected coherence becomes stronger than the other. At distances other then half-integer distances detunings need to be considered due to dipole-dipole coupling from Eq. (14).

Comparing the main terms in Eq. (58) with the Figure (20) we see an equation with the lowest order Taylor terms with the error, and a figure who is also at the lowest order Taylor terms. Looking only at the coherences and populations in Fig. (20) with the first and zeroth order terms from Eq.

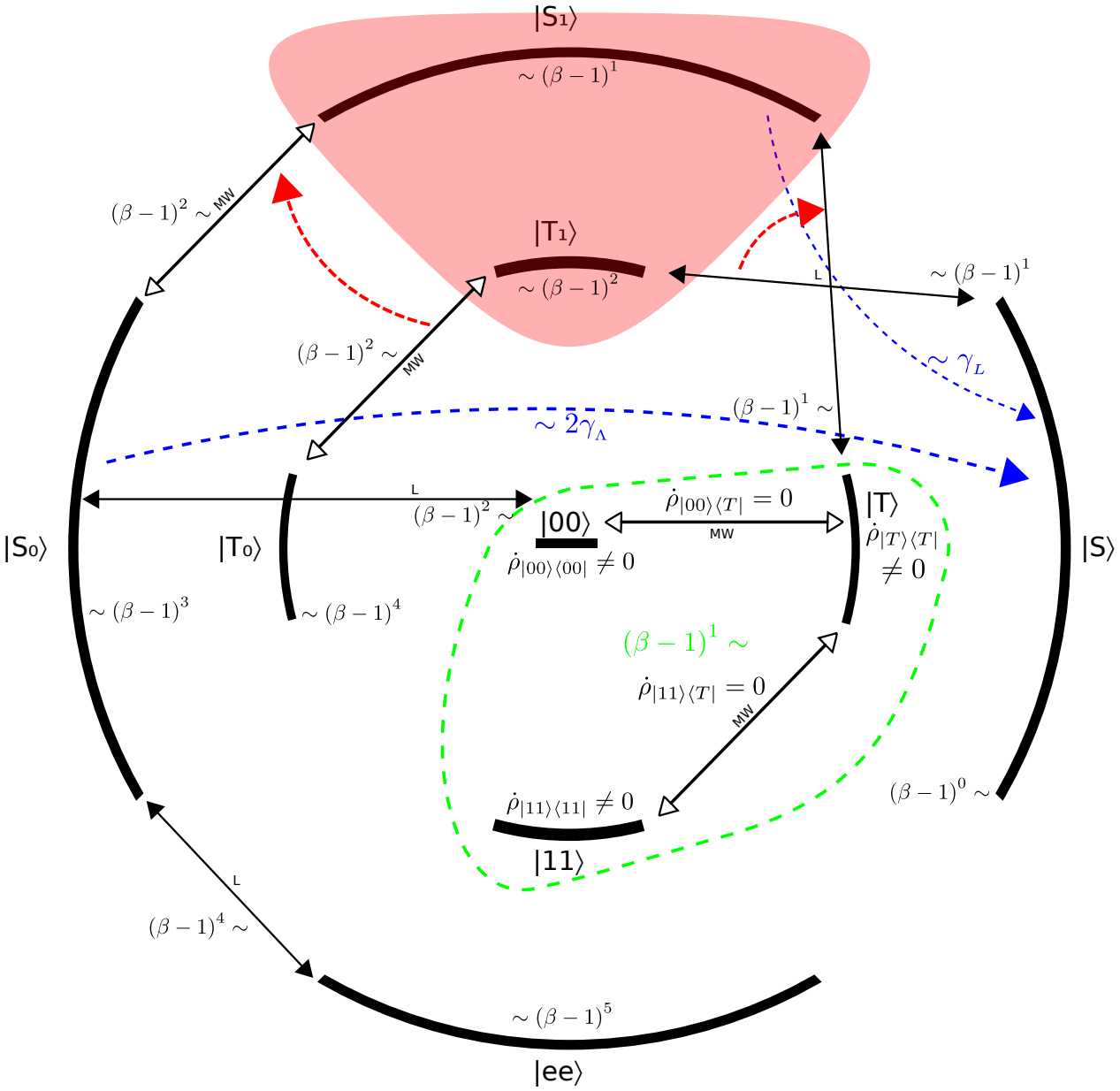

Figure 20: Lowest order Taylor approximation of all elements from the analytical solution. Here decay has stabilized the system in its current form. Near coherences and states can the scaling be found. **Blue** lines represent the two dominant gain process, where gain from $|S_1\rangle$ can only occur via free decay and gain from $|S_0\rangle$ is maximally twice as large as normal. **Red** lines show the effect of the symmetry breaking on the preferences between coherences, coherence to and from state $|S_1\rangle$ are eventually favoured over those to $|T_1\rangle$. **Green** area is the area which holds the time dependence of the analytical solution. In this case the ground states are oscillating whilst preserving the total population of the entire system.

$(58) \sim (\beta-1)^{\mathbf{1}}$ *and* $\sim (\beta-1)^0$ shows how it works.

The zeroth order term 1 in Eq. (58) is due to the blue dotted line $\sim 2\gamma_\Lambda$ as this is enhanced total decay, meaning the coupling to the wire in this case increases it. This also makes state $|S_0\rangle$ very lowly populated and coherences between this state and the three ground states in the green region of the second order. The first order terms in Eq. (58) are because of the driving out of the three ground-states in the green dotted region, and the loss of state $|S\rangle$ to state $|T_1\rangle$ and the free decay of states $|S_1\rangle$ and $|T_1\rangle$. The first order term with 1 that provides a loss to the fidelity independent of the driving out of state $|S\rangle$ is due to the steady state. At the steady state a recycling from population loss out of $|S\rangle$ into state $|T_1\rangle$ to the ground-states into state $|S_1\rangle$ and back into state $|S\rangle$ is stable and continues. There is always population stuck in this 'recycling-loop' due to the assumptions made. The first order term with 1 comes from the fact that some of these loop states can decay into other states.

This above described result is different from work in optical cavities[38;82] where the unwanted coherence between states $|S\rangle \longleftrightarrow |T_1\rangle$ are suppressed by detunings. Here the enhanced decay of this coherence and subsequent favouring to the coherence $|S_1\rangle \longleftrightarrow |T\rangle$, as seen in Fig. 20, take over the role of the detunings in the S1-scheme from earlier work.

As mentioned earlier, this strong wire decay also results in constructive coherence decay gains. These should be taken into account for all 3-level or more coupled emitters which have good coupling to a wire at half-integer distance. This regime is, from an analytical point of view complicated, but however poses a very real regime in practical applications of dissipative state preparation. It is these decay of high coherences into lower driven coherences and driven back into higher coherences that make the scheme lack a full analytical solution as a steady state. Alike the case of the wire decay mediating the process $|T_1\rangle \xrightarrow{|11\rangle} |S_1\rangle$, so also the process $|T_0\rangle\langle T_1| \xrightarrow{|T\rangle\langle 11|} |S_0\rangle\langle S_1|$ exists which occurs both wire-mediated and from spontaneous decay. This can complicate the analytical solution. For strong Ω_L the higher states will be more populated, and the decay dependence of $|T\rangle\langle 11|$ is increased dramatically. For strong Ω_{MW} the large coherence $|T\rangle\langle 11|$ has a minor effect too. These processes however disappear near $\beta = 1$. These effects can be illustrated by comparing the semi-analytical solution to a numerical solution. As done in Fig. 21.

Numerical analysis For the numerical analysis the eigenvalue method is applied. Unlike analytical solutions where a large symbolic matrix would increase calculation time exponentially with a larger amount of elements. The numerical method has a relative luxury that it simply consists out of just numbers.

An elaboration of the practical implementation of the method can be found in Appendix E

Comparison of Numerical and Analytical results From a comparison between the analytical approach with the numerical results it shows that for values where the assumption holds, the agreement is rather well. In Fig. (21) the striped curve represents the numerical result, and should be taken as the best reliable result for given parameters. The straight curve is for the analytical result.

The agreement is less well for more extreme differences between drives. For very low Ω_{MW} the numerical result will, as expected, result in an error of 1. The analytical solution does not do this as the main effect of Ω_{MW} is incorporated as an assumption and hence cannot be 0. Also for very high

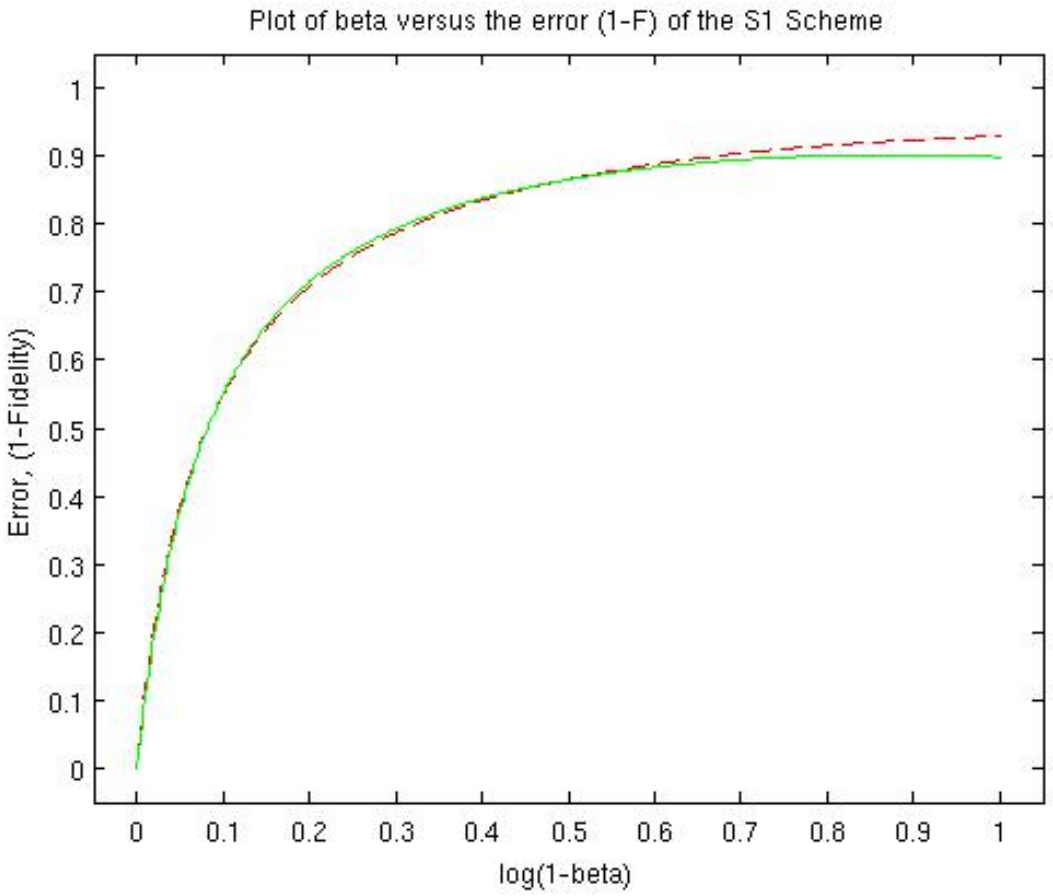

Figure 21: The error , all the population not in state $|S\rangle$, versus beta for the analytical (straight) and numerical (striped) solution. Values used here are $4\Omega_L = \Gamma$ & $20\Omega_{MW} = \Gamma$. Both methods show that a lower Ω_L gives better fidelities, and that the fidelity scales linearly near $\beta = 1$ . .

drive Ω_L it cannot really be assumed that only the ground states are populated, and hence the fidelity given by Eq. (58) will be higher then the numerical case, though the scaling will remain the same.

As can be seen from Fig. (21), the linear scaling of beta with the Fidelity with state $|S\rangle$ is found for both analytical and numerical results.

A point worth noting is that the driving strength scales with the total free decay, which for $\beta \to 1$ of course approaches zero. Hence as Fig. (21) approaches from right to left, the drives go to zero. Sustaining entanglement at high quality set-ups would hence ideally require only a *single* quantum of energy to compensate for noise.

Plasmonic Decay The wire to which the Λ-emitters couple supports plasmonic modes that can also decay. These decaying modes contribute to free decay as mentioned earlier. In that case $\beta \to \beta e^{-\frac{d}{L}}$. Then looking at the linear term in Eq. (58) it can be seen that as $\beta \to 1$ the drive term grows larger

and larger. Instead, if one were to substitute the decay into the first two terms the fidelity becomes in terms of total decay γ of the emitter

$$|S\rangle\langle S| = 1 - 8(1-Q)\left(\frac{3}{4} + \left(\frac{\Omega_L}{(1-Q)\gamma}\right)^2\right) + O((1-Q)^2) \tag{59}$$

where $Q = \beta e^{-\frac{d}{L}}$. This means that if the driving $\Omega_L \neq 0$ the best fidelity with state $|S\rangle$ is for an imperfect system where $Q \neq 1$. In other words, as can be seen from both Fig. (20) and the equation above, some free space decay is required to get the best fidelity, instead of just a perfect coupling to the wire. In essence the coupling to the wire (or the quality of the wire itself) need to be imperfect for the scheme to work most effectively.

4.5.2 Suggested schemes

As can be seen in the previous section, calculating schemes is a tedious and time consuming venture. However the same rules of symmetry apply in all cases and hence the following schemes, all based on the same principles as the S1-Scheme, are suspected to result the same scaling with the β-factor. Pending a few factors.

S0 - Scheme Alike the S1 scheme only now the coupling to the wire is with the L-transition ($|e\rangle \rightarrow |0\rangle$) , the reshuffling is the same as that of the S1 scheme. Now the driving is from $|11\rangle \leftrightarrow |S_1\rangle$, as can be seen in Fig. (22). This scheme is identical to the S1 scheme, with the symmetry breaking taking place between states $|T_0\rangle$ *and* $|S_0\rangle$.

The scheme prepares the state $|S\rangle$.

T1 - Scheme Alike the S1 scheme only now the symmetry of the whole system is inverted. So the coupling to the wire is with the L-transition ($|e\rangle \rightarrow |1\rangle$) but at half integer distance. The reshuffling is now anti-symmetric. And the driving is still anti-symmetric from $|00\rangle \leftrightarrow |S_0\rangle$, as can be seen in Fig. (23). This scheme is identical to the S1 scheme, with the symmetry breaking taking place between states $|T_1\rangle$ *and* $|S_1\rangle$ but this time in favour of the symmetric states.

The scheme prepares the state $|T\rangle$.

T0 - Scheme Alike the T1 scheme only now the coupling to the wire is with the L-transition ($|e\rangle \rightarrow |0\rangle$) , the reshuffling is the same as that of the T1 scheme. Now the driving is from $|11\rangle \leftrightarrow |T_1\rangle$, as can be seen in Fig. (24). This scheme is identical to the S1 scheme, with the symmetry breaking taking place between states $|T_0\rangle$ *and* $|S_0\rangle$.

The scheme prepares the state $|T\rangle$.

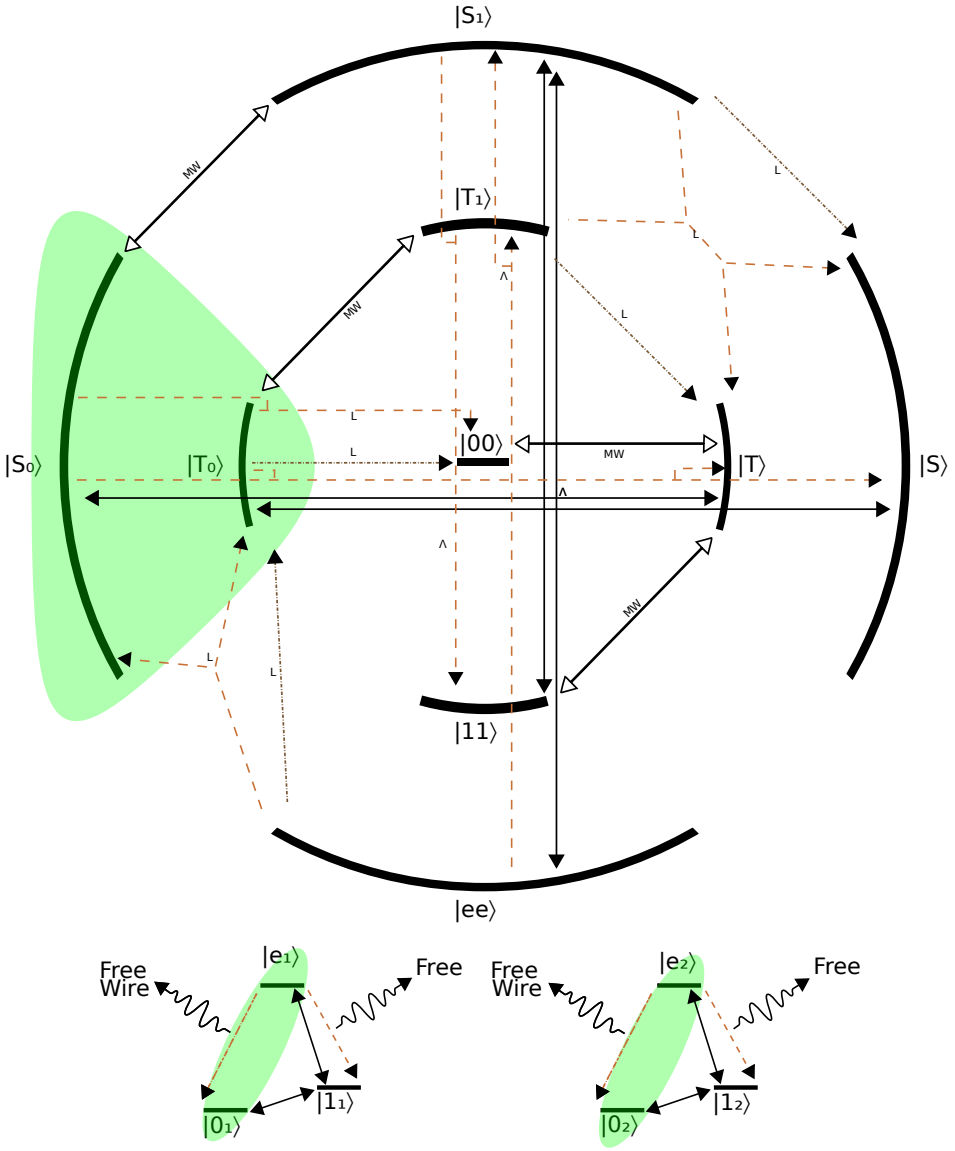

Figure 22: The S0-scheme. At integer distance decay is enhanced or subdued between various transitions favouring anti-symmetric states. A microwave field is applied to reshuffle the lower states with exception of the target state $|S\rangle$. A resonant driving of the Λ-transition is used which couples state $|T\rangle$ to state $|S_0\rangle$ and the target state $|S\rangle$ to state $|T_0\rangle$, where the latter has enhanced decay.

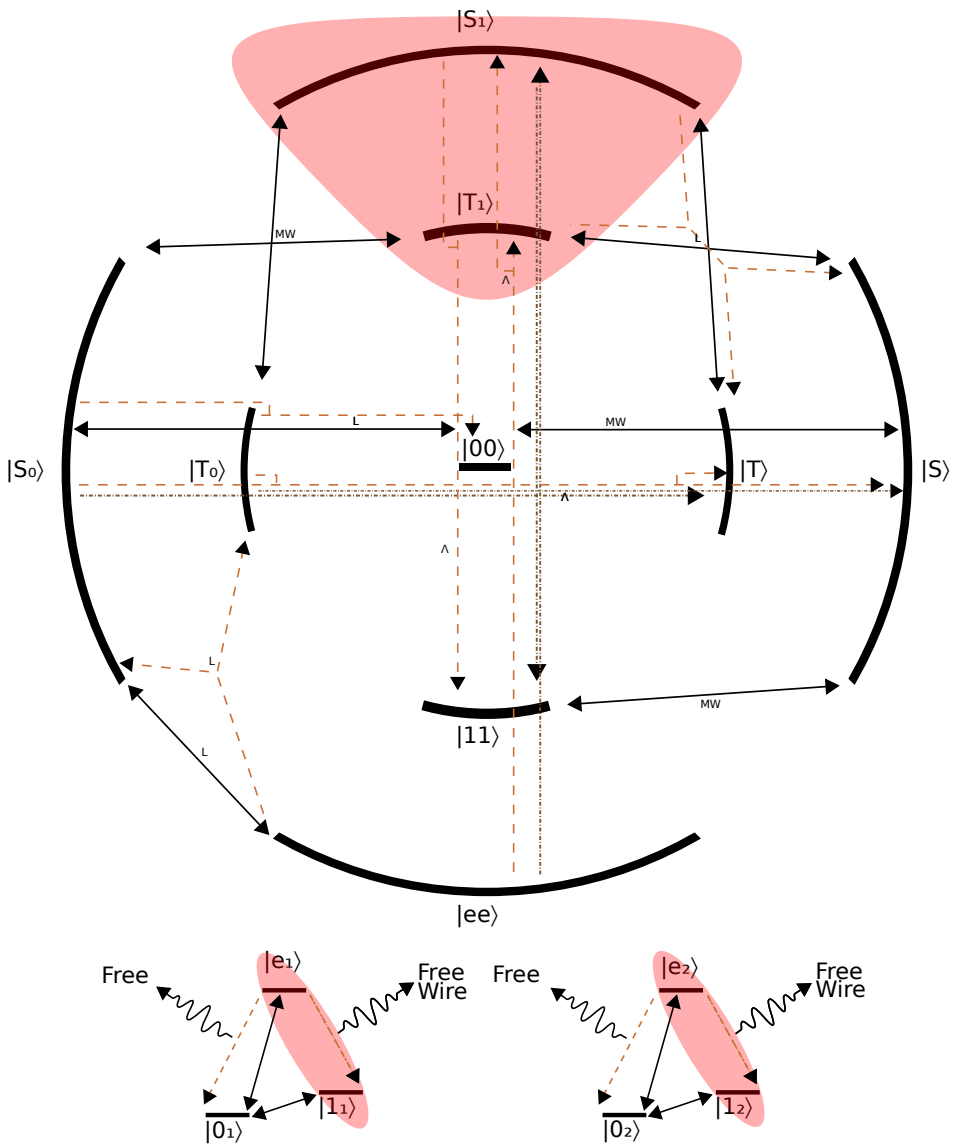

Figure 23: The T1-scheme. At half integer distance decay is enhanced or subdued between various transitions favouring symmetric states. A microwave field is applied to reshuffle the lower states with exception of the target state $|T\rangle$. A resonant driving of the L-transition is used which couples state $|T\rangle$ to state $|S_1\rangle$ and the target state $|S\rangle$ to state $|T_1\rangle$, where the former has enhanced decay.

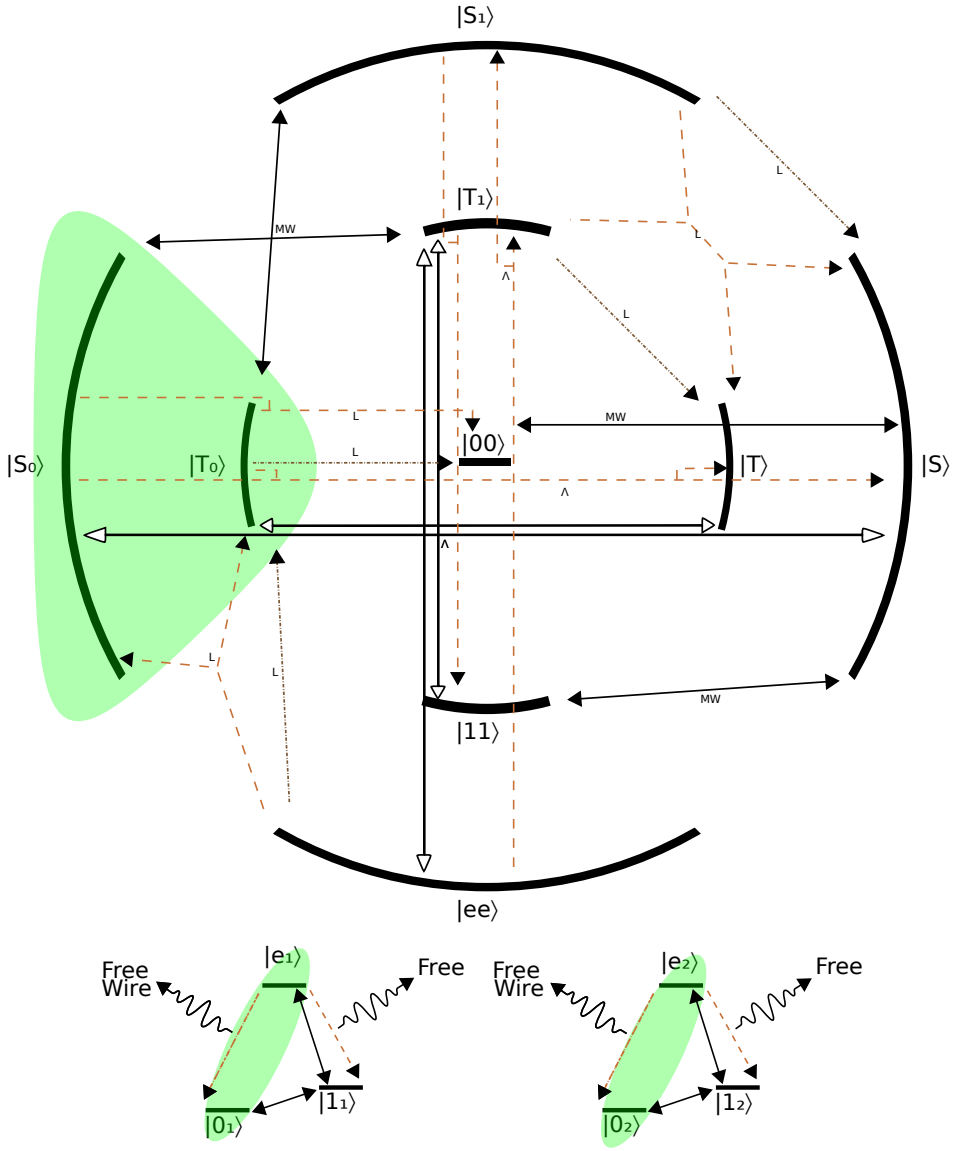

Figure 24: The T0-scheme. At half integer distance decay is enhanced or subdued between various transitions favouring symmetric states. A microwave field is applied to reshuffle the lower states with exception of the target state $|T\rangle$. A resonant driving of the Λ-transition is used which couples state $|T\rangle$ to state $|T_0\rangle$ and the target state $|S\rangle$ to state $|S_0\rangle$, where the former has enhanced decay.

Magnetic Schemes It is entirely seeming that the addition of a magnetic term is favourable for creation of entanglement schemes, as was the case in the two level section. It will however add a level of complexity which makes schemes, at least graphically, very hard to convey. As the strength of this interaction is based upon the Zeeman-effect, and the 3 different levels might react differently to the same applied magnetic field. Considering the relative complexity of this, it is this authors opinion that such attempts should only done numerically or experimentally. And an analytical method is strongly discouraged.

4.6 Results

It was shown that a linear scaling can be achieved via the S1 scheme. This scheme suffices with symmetry breaking taking only place via the wire. It was also shown that a weaker drive between ground and exited state results in better fidelity-error scaling. It is also shown that the most ideal scaling with the fidelity of the maximally entangled state $|S\rangle$, is achieved with wires that have a high but unequal to unity scaling with the β-factor.

The results of Λ-emitters are promising, as they predict better scaling with imperfect coupling and low driving, whilst pertaining long lived entangled states within the dissipative regime. Which would make it ideal for on-chip implementation.

4.7 Application in heterostructure qubit

Applying the top schemes into a functional qubit might seem difficult at first due to the strong dependence of the distance of the emitters. However the distance is only dependent on the plasmon wavelength. Hence production of a qubit is much simpler if one is able to modify the modal wavelength inside the wire. Hence the production of these qubits is not easily done with quantum wires that have a fixed modal plasmon wavelength. Instead having a wire with controllable width, and hence controllable quantization leading to controllable wavelength is preferred.[83] Here a suggestion of such a system that can tune the modal plasmon wavelength by dimensional control is made.

Emitters on a GaAs Quantum Wire One way of making quantum wires is by putting gates on top of a two dimensional electron gas (2DEG). It has already been shown that it is possible to make a single mode wire in this fashion.[84]. Though this showed single mode transmittance due to a single short confined blockage, it is reasonable to assume that an extended blockage will function with the same confinement characteristics normal to the plasmon propagation direction. The practical qubit allows for a large variety of, if not complete electronic control of the qubit. The qubit is shown in Fig. (25).

The difficulty of production is ensuring a good β-factor between the emitters and the 2DEG, and the right shape of the dots to be Λ-emitters. A good beta-factor is ensured by making sure that with exception of the driving laser fields, the dots only really couple to the wire just outside the barrier that confines them. This is controlled by the dot-gates and allows control of the levels of the emitter, and

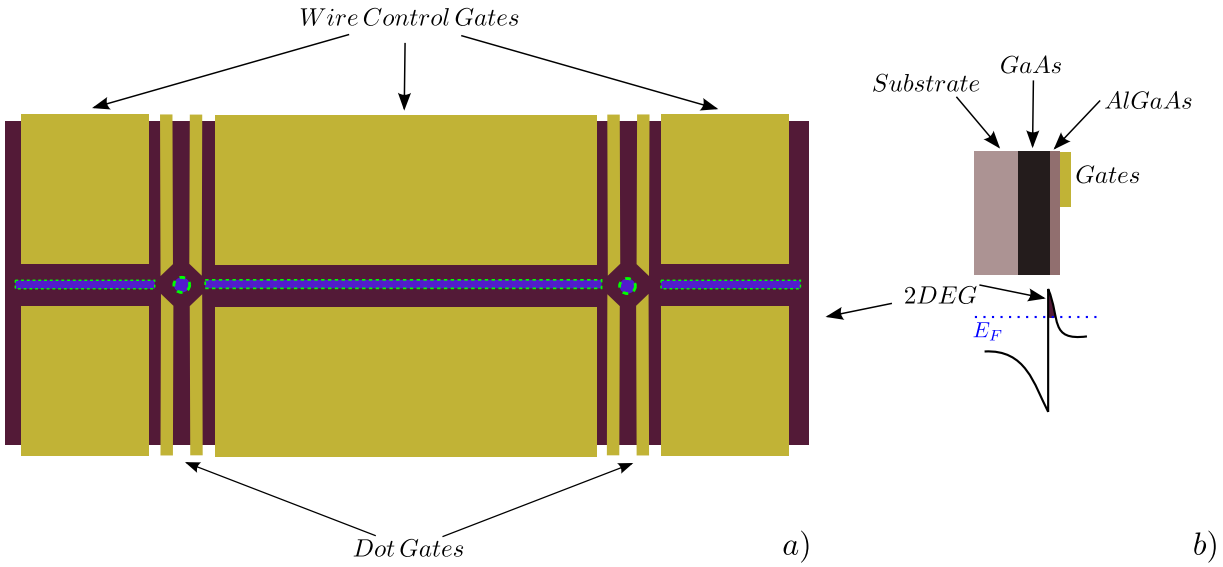

Figure 25: A 2DEG based qubit. **a)** Top view; Gates are applied to regulate the width of the Quantum wire, and with that the supported plasmon modal wavelength inside the wire. Also dot gates are applied to control the level structure and filling of the quantum +dots. The dotted region gives the non-depleted 2DEG giving two dots and a 1D wire between them **b)** A side-view showing the layers that make up the 2D electron gas and how gates locally deplete the electron gas.

hence the energy with which they decay into the wire. The distance between the dots can be a range of distances, but typically lies in between 50 and 400 nanometers. Large side gates in Fig. (25) can deplete the 2DEG in such a way that a single modal wavelength quantum wire is formed. These gates are on both sides of the emitters. The voltage of these gates modify the width of the quantum wires, the green dotted region in Fig. (25), and hence the wavelength of the plasmons. Externally only the geometry of the applied drives is dependent on the physics of the system.

The described set up allows to easily control all parameters of the qubit. Most importantly it allows electronic control of which transition in the Λ-emitters couples to the quantum wire and at what plasmonic wavelength. This means that in the same sample, different plasmonic distances can be made. A good tuning of the controllable parameters would make it possible to use some of the schemes as described in Sec. (4.5) within the same experimental set-up.

This means that, provided the qubit has a good β-factor and more or less the right distance between the emitters, one has electronic control over long lived quantum states. By varying the geometry of the drives, and the voltage and currents in the gates it is possible to make any combination of the 2 maximally entangled states by dissipative state preparation. This allows a large set of unitary transformations to be applied on the quantum bit.

More complicated structures could be developed in the future that allow for more complicated linear or surface quantum computation devices that are very long lived, based upon dissipative state preparation by quantum wires.

5 Conclusion, Discussion and Outlook

In this chapter a summary of the found conclusions with respect to the main focus of this thesis is given. For conclusions in the specific case of either two or either three level emitters one can look at Secs. (3.6) & (4.6). The focus of this work was the preparation of an entangled state in a solid state system of two emitters on a plasmonic one dimensional wave-guide by use of external optical drives and internal dissipative dynamics. The following can be concluded out of this work

5.1 Conclusions

This work has shown that within the master equation approach, it is possible for two emitters, of two or three levels each, on a single mode plasmonic waveguide, to be arbitrarily maximally entangled. The scaling of this entangling is generally linear with respect to the error, which is the amount of not-wire mediated decay. It was shown that for the two level emitter case the addition of a magnetic field gradient could improve this scaling to be scaling with a square root of the error.

It was also shown that the crucial step in entanglement preparation, the breaking of symmetry, can be done with decay dynamics in the wire alone. This process can be improved by another process of symmetry breaking alike the addition of a magnetic gradient between emitters. The resulting dissipative state preparation offer opportunities in symmetry breaking processes that are not seen similarly with optical cavities.

Finally it was shown that the use of higher level emitters, or emitters with more then two levels, seem to theoretically scale more favourable with 'natural' parameters. Due to the processes of the higher states these set-ups can benefit from scheme's that exploit an imperfect coupling to the wire.

For these reasons it is this author's opinion that from a theoretical point of view, the construction of dissipative state qubits on quantum wires offer a very real and good storage alternative to future qubit production. Also he is of opinion that solid state dissipative state preparation does not prove to be a regime of qubits that have a high noise, but instead a regime that offers long lived coherence suitable for entangled state preparation by spontaneous decay of states.

5.2 Discussions

In this work several assumptions and methods have been used which are not free of discussion. Therefore these discussion points have been split up between elementary theoretical discussion points, and between discussion points of the interpretation and predictions of the attained results.

Theoretical points The first point of discussion should be the master equation. Though rigorously derived by the cited authors, its application in three level-systems has seen very little publications. Other then perhaps practical reasons it does hold some problematic points in its formulation. The formulation of the decay part of equation (5) requires the use of raising and lowering operators. The choice of these operators automatically limit the possible physics in multi-level applications. Uncareful formulation might imply that it is not possible for a decay into the wire of transition A, to excite a different transition B inside another emitter. This problem does not arise in a two level system. And in this article it was circumvented by only considering half integer emitter distances for three level

systems. In this distance the locality of the emitters prevent an effective dipole-dipole coupling to form via the wire. In an experimental situation however this might happen and the current formulation of the used formalism does not support such possibilities, and would need to be expanded accordingly.

Another point of discussion is the use of decoherence. Here only first order coupling to the electromagnetic medium and vacuum have been used. This is generally a good approximation, however as in this case this first order coupling is used to create a strong coherence, there will come a point where the second order process of decoherence become of importance. These processes then will limit the arbitrarily good fidelity, yet these processes are generally much slower and should remain only a minor noise in the overall picture.

An important point of discussion is the methods applied in solving the two and three level cases. Though an unique analytical solution can often be found in the case of two level emitters, this is not the case for the three level emitters. Here the solution method itself is but a selection of formulas with respect to relevant and irrelevant interactions of the whole system. This is also discussed in the corresponding chapter. Even the usage of practical numerical methods have, as discussed, their respective drawbacks. It seems ironic but to fully comprehend even numerical solutions of this model, it would be best to have the simulations run on a universal quantum computer. However since the analytical results are generally very hard to come by, it is discussed that future research should employ numerical methods alone.

Interpretation points More practical points of discussion is whether or not it is feasible at all, to create a certain minimal coupling to a wire good enough for the proposed scheme's to function at all. Furthermore the distance between emitters, and the plasmon wavelengths of their decays are of crucial importance for the scheme's to work. Though, by use of gates and magnetic fields these can be tuned they also introduce in on their own multiple interactions which subsequently need to be incorporated within the model. However, once a good coupling of controllable emitters is achieved with a single controllable mode plasmon wire is achieved, such issue's should be easily resolved by experiment.

5.3 Outlook and future research

From this work it seems very interesting to take a better look at the application of magnetic gradients on three level emitters. Such research would however have to be conducted with numerical methods, or if possible, by experimental methods. A possible controllable set-up of this kind has been proposed. Since the distance between emitters is so crucial for scheme's to work the way they do. It is advised to couple quantum dots of some sort, to a two dimensional electron gas. Which can then be gated to control plasmon wavelength inside the wire. Hence both from a theoretical and experimental point of view, future research might provide interesting results and promising insights in the dissipative regime of entanglement preparation.

5.4 Word of the author

As a final piece, this author would like to elaborate more on the field and promises of quantum mechanics and their relation to society. There is a tendency to over-estimate the capacities of a quantum computer. They are sometimes hailed as the future science that will exponentially increase

our calculative power as a civilization. However paraphrasing Bennett; There are many ways to do quantum computing, and very few algorithms to do it efficiently.[59] The Quantum computer will always be limited by the effectiveness of its algorithms.

There lies a great responsibility with the physicist in the development and implementation of the quantum computer. It is already known that the broadly used RSA key can be broken swiftly by Shor's algorithm. And it is but a matter of time, until new algorithms occur that will run on the inevitably arriving universal quantum computer. Where the use of the word inevitable is due to the results from this very work, showing that on-chip implementation of qubits can be promising and not just a noisy qubit. It has the potential to be a greater threat to society then anything we have faced before. At the very least nuclear weapons were just big bombs, electricity but a commodity and Penicillin just a new medicine. Now, quantum engineering offers a field, that is difficult to comprehend from even a philosophical point of view. This puts it in a league of its own.

In the coming years it will be imperative that the layman gains greater understanding about the very philosophical basis of quantum theory. Whatever interpretation of quantum theory one might attain, one cannot do with the idea that it is 'weird' when its influences will dominate our every day lives a few decades from now. Society needs more, then just a handful of scientists, to comprehend the imminent arrival of technology that will undoubtedly transform the ways of banking, computing and communication as we know it. The quantum society will be our future, whether or not it is preferable over our status quo is however still open for debate.

5.5 Acknowledgments and thanks

This project would not have been completed if it was not for the generosity and help of the group of Anders S. Sørensen, and the invaluable support and patience of Florentin Reiter. Their support, guidance and placement at the Niels Bohr Institute were the most important benefactors of the completion of this project.

Also I would like to thank Steffen Wiedmann for his experimentalist point of view and inspiration of integration of the qubits. Also I would like to thank my family, friends and girlfriend for their support during my research-time abroad and in the Netherlands.

6 References

References

[1] A. Einstein, B. Podolsky, and N. Rosen, Physical review , 2 (1935).

[2] D. Bohm and Y. Aharonov, Physical Review **108**, 1070 (1957).

[3] M. Leslie, Science **305**, 1219 (2004).

[4] R. Feynman, Engineering and Science , 22 (1960).

[5] A. Einstein, Annalen der physik , 891 (1905).

[6] A. S. Holevo, Probl. Peredachi Inf. **9**, 3 (1973).

[7] R. S. Ingarden, Reports on Mathematical Physics **10**, 43 (1976).

[8] P. Benioff, Journal of Statistical Physics **29**, 515 (1982).

[9] A. Ekert, Physical review letters **67**, 661 (1991).

[10] P. Shor, ... of Computer Science, 1994 Proceedings., 35th ..., 124 (1994).

[11] M. S. Kim, J. Lee, D. Ahn, and P. L. Knight, Phys. Rev. A **65**, 40101 (2002).

[12] S. Schneider and G. Milburn, Phys. Rev. **65** (2002).

[13] A. M. Basharov, J. Exp. Theor. Phys. **94**, 1070 (2002).

[14] L. Jakobczyk, J. Phys. A: Math. Gen. **35**, 6383 (2002).

[15] D. Braun, p. 1 (2008), 0205019v2.

[16] F. Benatti, R. Floreanini, and M. Piani, Physical Review Letters **91**, 70402 (2003).

[17] F. Benatti, R. Floreanini, and U. Marzolino, Physical Review A **81**, 12105 (2010).

[18] F. Verstraete, M. Wolf, and J. I. Cirac, Nature Phys. **5**, 633 (2009).

[19] S. Diehl *et al.*, Nature Phys. **4**, 878 (2008).

[20] B. Kraus *et al.*, Phys. Rev. **78** (2008).

[21] K. G. H. Vollbrecht, C. A. Muschik, and J. I. Cirac, Phys. Rev. Lett. **107** (2011).

[22] J. T. Barreiro *et al.*, Nature **470**, 486 (2011).

[23] M. Müller, K. Hammerer, Y. L. Zhou, C. F. Roos, and P. Zoller, New J. Phys. **13** (2011).

[24] F. Pastawski, L. Clemente, and J. I. Cirac, Phys. Rev. **83** (2011).

[25] J. F. Poyatos, J. I. Cirac, and P. Zoller, Phys. Rev. Lett. **77**, 4728 (1996).

[26] M. B. Plenio, S. F. Huelga, A. Beige, and P. L. Knight, Phys. Rev. **59**, 2468 (1999).

[27] S. Clark, A. Peng, M. Gu, and S. Parkins, Phys. Rev. Lett. **91** (2003).

[28] A. S. Parkins, E. Solano, and J. I. Cirac, Phys. Rev. Lett. **96** (2006).

[29] G. Vacanti and A. Beige, New J. Phys. **11** (2009).

[30] X. Wang and S. Schirmer, arXiv preprint arXiv:1005.2114 , 1 (2010), arXiv:1005.2114v2.

[31] J. Cho, S. Bose, and M. Kim, Phys. Rev. Lett. **106** (2011).

[32] M. Kastoryano, F. Reiter, and A. Sø rensen, Phys. Rev. Lett. **106**, 1 (2011), arXiv:1011.1441v1.

[33] C. A. Muschik, E. S. Polzik, and J. I. Cirac, Phys. Rev. **83** (2011).

[34] H. Krauter *et al.*, Physical Review Letters , 1 (2011), arXiv:1006.4344v3.

[35] J. Busch *et al.*, Phys. Rev. **84** (2011).

[36] D. Martin-Cano *et al.*, Phys. Rev. **84** (2011).

[37] A. Gonzalez-Tudela and D. Martin-Cano, Phys. Rev. Lett. **106**, 1 (2011), arXiv:1010.5048v2.

[38] F. Reiter, M. M. J. Kastoryano, and A. S. A. Sø rensen, New Journal of Physics **14**, 53022 (2012), arXiv:1110.1024v2.

[39] S. Hughes, Physical review letters **227402**, 1 (2005).

[40] E. Gallardo, L. Martinez, and A. Nowak, Physical Review B , 2 (2010).

[41] T. Lund-Hansen, S. Stobbe, and B. Julsgaard, Physical review . . . , 1 (2008), arXiv:0805.3485v3.

[42] J. Bleuse *et al.*, Physical Review Letters **106**, 103601 (2011).

[43] Q. Quan, I. Bulu, and M. Lončar, Physical Review A **80**, 011810 (2009).

[44] H. Raether, *Surface plasmons* (Springer, Berlin, Germany, 1988).

[45] W. L. Barnes, A. Dereux, and T. W. Ebbesen, Nature **424**, 824 (2003).

[46] S. I. Bozhevolnyi, V. S. Volkov, E. Devaux, J.-Y. Laluet, and T. W. Ebbesen, Nature **440**, 508 (2006).

[47] P. Anger, P. Bharadwaj, and L. Novotny, Physical Review Letters **96**, 113002 (2006).

[48] P. Andrew and W. L. Barnes, Science (New York, N.Y.) **306**, 1002 (2004).

[49] A. G. Curto *et al.*, Science (New York, N.Y.) **329**, 930 (2010).

[50] D. Chang, a. Sø rensen, P. Hemmer, and M. Lukin, Physical Review Letters **97**, 053002 (2006).

[51] a. V. Akimov *et al.*, Nature **450**, 402 (2007).

[52] A. Falk, F. Koppens, and L. Chun, Nature Physics (2009).

[53] R. Heeres, S. Dorenbos, and B. Koene, Nano ... (2009).

[54] D. Chang, A. Sø rensen, E. Demler, and M. Lukin, arXiv preprint arXiv:0706.4335 , 1 (2008), arXiv:0706.4335v1.

[55] D. Dzsotjan, A. Sø rensen, and M. Fleischhauer, Physical Review B , 1 (2010), arXiv:1002.1419v2.

[56] D. Deutsch, Proceedings of the Royal Society of ... **117** (1985).

[57] W. van Dam, Nat Phys **3**, 220 (2007).

[58] A. Lenstra, Towards a quarter-century of public key cryptography **128**, 101 (2000).

[59] C. Bennett, E. Bernstein, G. Brassard, and U. Vazirani, ... Journal on Computing (1997).

[60] E. Schrödinger and M. Born, Mathematical Proceedings of the Cambridge Philosophical Society **31**, 555 (2008).

[61] J. Sakurai, *Modern quantum mechanics* (, 1994).

[62] H. Ditlbacher *et al.*, Physical Review Letters **95**, 257403 (2005).

[63] D. Arbel and M. Orenstein, Optics express **16**, 3114 (2008).

[64] A. Goni, A. Pinczuk, J. Weiner, and J. Calleja, Physical review ... **67**, 3298 (1991).

[65] T. Demel, D. Heitmann, P. Grambow, and K. Ploog, Physical review letters **66**, 2657 (1991).

[66] M. Andersen, S. Stobbe, A. Sø rensen, and P. Lodahl, Nature Physics **7**, 1 (2010), arXiv:1011.5669v1.

[67] T. Teperik, V. Popov, and F. García de Abajo, Physical Review B **69**, 155402 (2004).

[68] R. Lehmberg, Physical Review A **2** (1970).

[69] Z. Ficek and R. Tanaś, Physics Reports , 1 (2002), 0302082v1.

[70] G. Agarwal, Physical Review A **12**, 1475 (1975).

[71] C. Willis and R. Picard, Physical Review A **9** (1974).

[72] H. Dung, L. Knöll, and D.-G. Welsch, Physical Review A **66**, 063810 (2002).

[73] I. Bargatin, B. Grishanin, and V. Zadkov, Physical Review A **61**, 052305 (2000).

[74] G. Falci *et al.*, Physical Review B **87**, 214515 (2013).

[75] E. Brion, L. Pedersen, and K. Mø lmer, Journal of Physics A: Math. Theor. **40**, 1 (2007), 0610056v1.

[76] R. J. Schoelkopf and S. M. Girvin, Nature **451**, 664 (2008).

[77] T. Oosterkamp and T. Fujisawa, Nature **395**, 873 (1998).

[78] S. Tarucha, D. Austing, T. Honda, van der Hage RJ, and L. Kouwenhoven, Physical review letters **77**, 3613 (1996).

[79] T. Hayashi, T. Fujisawa, H. Cheong, Y. Jeong, and Y. Hirayama, Physical Review Letters **91**, 226804 (2003).

[80] T. Fujisawa, Science **282**, 932 (1998).

[81] E. Arimondo, V Coherent Population Trapping in Laser Spectroscopy, volume 35 of *Progress in Optics*, pp. 257–354, Elsevier, 1996.

[82] F. Reiter, L. Tornberg, G. Johansson, and A. S. Sø rensen, Physical Review A **88**, 032317 (2013).

[83] T. Ihn, *Semiconductor Nanostructures* (, 2010).

[84] van Wees BJ *et al.*, Physical review. B, Condensed matter **38**, 3625 (1988).

7 Appendices

A Full equations for the two 2-level scheme

In Sec. 3.2 solutions are found for a set of coupled equations. Here γ is the total decay, κ is the wire decay, Ω is the symmetric drive with phase difference $\phi = 0$, and Δ the level shift due to the dipole-dipole coupling. The matrix elements expressed as $\varrho_{ij} = |i\rangle\langle j|$ are part of the density matrix. It should be noted that these equations are the result from the master equation and non-zero elements in the off-diagonal coherences do not mean that such a coherence is externally applied. The relevant physics is in this case only in the diagonal elements.

Diagonal elements

$$\frac{\partial}{\partial t}\rho_{0000} = -\frac{i\Omega}{2}\left(\rho_{T00} - \rho_{00T}\right) + \left(\gamma + \kappa\right)\left(\rho_{TT} + \rho_{SS}\right)$$

$$\frac{\partial}{\partial t}\rho_{TT} = \frac{i\Omega}{2}\left(\rho_{T00} - \rho_{00T} - \rho_{11T} + \rho_{T11}\right) - \left(\gamma + \kappa\right)\rho_{TT} + \left(\gamma + \kappa\right)\rho_{1111} - 2ib\left(\rho_{TS} - \rho_{ST}\right)$$

$$\frac{\partial}{\partial t}\rho_{SS} = -\left(\gamma - \kappa\right)\rho_{SS} + \left(\gamma - \kappa\right)\rho_{1111} + 2ib\left(\rho_{TS} - \rho_{ST}\right)$$

$$\frac{\partial}{\partial t}\rho_{1111} = -\frac{i\Omega}{2}\left(\rho_{T11} - \rho_{11T}\right) - 2\gamma\rho_{1111}$$

Relevant coherences

$$\frac{\partial}{\partial t}\rho_{TS} = -\frac{i\Omega}{2}\left(\rho_{00S} + \rho_{11S}\right) - i\left(\Delta + \gamma\right) + 2ib\left(\rho_{SS} - \rho_{TT}\right)$$

$$\frac{\partial}{\partial t}\rho_{T00} = -i\frac{\Omega}{2}\left(-\rho_{0000} - \rho_{0011} + \rho_{TT}\right) + \frac{i}{2}\left(\delta + \Delta\right)\rho_{00T} - 2\,ib\rho_{00S} - \frac{1}{2}\left(g + \kappa\right)\rho_{00T} + \left(\gamma + \kappa\right)\rho_{T11}$$

$$\frac{\partial}{\partial t}\rho_{11T} = -i\frac{\Omega}{2}\left(\rho_{TT} - \rho_{1100} - \rho_{1111}\right) - \frac{i}{2}\left(3\,\delta - \Delta\right)\rho_{11T} - 2\,ib\rho_{11S} - \left(\frac{3}{2}\gamma + \frac{1}{2}\,\kappa\right)\rho_{11T}$$

$$\frac{\partial}{\partial t}\rho_{11S} = -\frac{i}{2}\left(3\,\delta + \Delta\right)\rho_{11S} - 2\,ib\rho_{11T} - i\frac{\Omega}{2}\rho_{TS} - \frac{1}{2}\left(3\,\gamma - \kappa\right)\rho_{11S}$$

$$\frac{\partial}{\partial t}\rho_{S00} = \frac{i}{2}\left(-\delta + \Delta\right)\rho_{S00} + 2\,ib\rho_{T000} + i\frac{\Omega}{2}\rho_{ST} - \frac{1}{2}\left(\gamma - \kappa\right)\rho_{S00} + \left(\gamma - \kappa\right)\rho_{11S}$$

$$\frac{\partial}{\partial t}\rho_{1100} = -i\frac{\Omega}{2}\left(-\rho_{o00T} + \rho_{T11}\right) + \left(2\,i\delta - \gamma\right)\rho_{0011}$$

B Full equations for the S1 scheme

In paragraph 4.5.1 there are some elements of the density matrix used. These are given here below. Here γ is the free decay of the desired transition, κ is the wire decay, the $\Omega's$ are the drives, Δ the level shift due to the dipole-dipole coupling. The matrix elements expressed as $\varrho_{ij} = f(\Pi) * |i\rangle \langle j|$ where Π is a set of parameters, are part of the density matrix.

Diagonal elements

$$\frac{\partial}{\partial t}\rho_{0000} = -\frac{i\Omega_L}{2}\left(\rho_{S000} - \rho_{00S0}\right) - \frac{i\Omega_{MW}}{2}\left(\rho_{T00} - \rho_{00T0}\right) + \gamma_L\left(\rho_{S0S0} + \rho_{T0T0}\right)$$

$$\frac{\partial}{\partial t}\rho_{1111} = -\frac{i\Omega_{MW}}{2}\left(\rho_{11T} - \rho_{T11}\right) + \gamma_\Lambda\left(\rho_{S1S1} + \rho_{T1T1}\right) + \kappa_\Lambda\rho_{T1T1}$$

$$\frac{\partial}{\partial t}\rho_{TT} = -\frac{i\Omega_{MW}}{2}\left(\rho_{00T0} - \rho_{T00}\right) - \frac{i\Omega_{MW}}{2}\left(\rho_{T11} - \rho_{11T}\right) + \frac{\gamma_L}{2}\left(\rho_{S1S1} + \rho_{T1T1}\right) + \frac{\gamma_\Lambda}{2}\left(\rho_{S0S0} + \rho_{T0T0}\right) + \kappa_\Lambda\rho_{T0T0} + \frac{i\Omega_L}{2}\left(\rho_{TS}\right.$$

$$\frac{\partial}{\partial t}\rho_{SS} = -\frac{i\Omega_L}{2}\left(\rho_{T1S} - \rho_{ST1}\right) + \frac{\gamma_L}{2}\left(\rho_{S1S1} + \rho_{T1T1}\right) + \frac{\gamma_\Lambda}{2}\left(\rho_{S0S0} + \rho_{T0T0}\right) + \kappa_\Lambda\rho_{S0S0}$$

$$\frac{\partial}{\partial t}\rho_{T0T0} = -\frac{i\Omega_{MW}}{2}\left(\rho_{T1T0} - \rho_{T0T1}\right) - \left(\gamma_L + \gamma_\Lambda + \kappa_\Lambda\right)\rho_{T0T0} + \frac{\gamma_L}{2}\rho_{EE}$$

$$\frac{\partial}{\partial t}\rho_{S0S0} = -\frac{i\Omega_L}{2}\left(\rho_{00S0} - \rho_{S000}\right) - \frac{i\Omega_{MW}}{2}\left(\rho_{S1S0} - \rho_{S0S1}\right) - \left(\gamma_L + \gamma_\Lambda + \kappa_\Lambda\right)\rho_{S0S0} + \frac{\gamma_L}{2}\rho_{EE} + \frac{i\Omega_L}{2}\left(\rho_{S0EE} - \rho_{EES0}\right)$$

$$\frac{\partial}{\partial t}\rho_{T1T1} = -\frac{i\Omega_L}{2}\left(\rho_{ST1} - \rho_{T1S}\right) - \left(\gamma_L + \gamma_\Lambda + \kappa_\Lambda\right)\rho_{T1T1} - \frac{i\Omega_{MW}}{2}\left(\rho_{T0T1} - \rho_{T1T0}\right) + \left(\frac{\gamma_\Lambda}{2} + \kappa_\Lambda\right)\rho_{EE}$$

$$\frac{\partial}{\partial t}\rho_{S1S1} = -\frac{i\Omega_L}{2}\left(\rho_{TS1} - \rho_{S1T}\right) - \left(\gamma_L + \gamma_\Lambda\right)\rho_{S1S1} - \frac{i\Omega_{MW}}{2}\left(\rho_{S0S1} - \rho_{S1S0}\right)$$

$$\frac{\partial}{\partial t}\rho_{EE} = -\frac{i\Omega_L}{2}\left(\rho_{S0EE} - \rho_{EES0}\right) - \left(\gamma_L + \gamma_\Lambda + \kappa_\Lambda\right)\rho_{EE}$$

Optical coherences

$$\frac{\partial}{\partial t}\rho_{TS1} = -\frac{i\Omega_L}{2}\left(\rho_{S1S1} - \rho_{TT}\right) - \frac{\left(\gamma_L + \gamma_\Lambda\right)}{2}\rho_{TS1} + \frac{\gamma_\Lambda}{4}\rho_{S0S1}$$

$$\frac{\partial}{\partial t}\rho_{S0S1} = -\frac{i\Omega_{MW}}{2}\left(\rho_{S1S1} - \rho_{S0S0}\right) - \left(\gamma_L + \gamma_\Lambda + \frac{\kappa_\Lambda}{2} + \frac{i\Delta}{2}\right)\rho_{S0S1}$$

$$\frac{\partial}{\partial t}\rho_{T1S} = -\frac{i\Omega_L}{2}\left(\rho_{SS} - \rho_{T1T1}\right) - \left(\frac{\gamma_\Lambda}{2} + \frac{\gamma_\Lambda}{2} + \frac{\kappa_\Lambda}{2} + i\Delta\right)\rho_{T1S} + \frac{\gamma_\Lambda}{4}\rho_{T1T0}$$

$$\frac{\partial}{\partial t}\rho_{11T} = -\frac{i\Omega_{MW}}{2}\left(\rho_{1111} - \rho_{TT}\right) + \frac{\gamma_\Lambda}{2}\rho_{S1T}$$

$$\frac{\partial}{\partial t}\rho_{T0T1} = -\frac{i\Omega_{MW}}{2}\left(\rho_{T1T1} - \rho_{T0T0}\right) - \left(\gamma_L + \gamma_\Lambda + \kappa_\Lambda - i\Delta\right)\rho_{T0T1}$$

$$\frac{\partial}{\partial t}\rho_{S000} = -\frac{i\Omega_L}{2}\left(\rho_{0000} - \rho_{S0S0}\right) - \left(\frac{\gamma_\Lambda}{2} + \frac{\kappa_\Lambda}{2} + \frac{i\Delta}{2}\right)\rho_{S000}$$

$$\frac{\partial}{\partial t}\rho_{S0EE} = -\frac{i\Omega_L}{2}\left(\rho_{EE} - \rho_{S0S0}\right) - \left(\gamma_L + \gamma_\Lambda + \kappa_\Lambda + \frac{i\Delta}{2}\right)\rho_{S0EE}$$

$$\frac{\partial}{\partial t}\rho_{T00} = -\frac{i\Omega_{MW}}{2}\left(\rho_{0000} - \rho_{TT}\right) + \frac{\gamma_\Lambda}{4}\rho_{S000} \tag{60}$$

All other elements of the density matrix are not required to find an analytical result.

C Off-diagonal total decay charts

In this table all the possible total decays terms on any of the 36 off diagonal elements of the density matrix is shown. These decays scale with parameter γ. Since the density matrix is Hermite, and decay is real this means that the contributions are the same for their respective Hermite conjugate. On the left side is the element of the density matrix under consideration with a different transition in each column. Entries are in blue for gain, entries in red are loses and black is for other. An element without a red entry does not decay by itself. And blue entries are generally a special case coinciding with a black entry at its symmetric opposite state. Unlike the diagonal case, these elements need not be conserved and are just an effect of computing all elements of the decay part of Eq. (5). All results were done by Maple.

It should be noted that not all entries seem as natural as one might expect. It is for this exact reason that these results were derived rigorously. They seem to indicate that the physics of the dissipative state is better explained in terms of symmetry preserving and symmetry breaking interactions, then jumps from states to states.

Each column has its own distinctive decay parameter noted in apostrophes.

	$'\gamma_{ii,oe}=\gamma_L'\ \|e\rangle\rightarrow\|0\rangle$	$'\gamma_{ii,1e}=\gamma_\Lambda'\|e\rangle\rightarrow\|1\rangle$	$'\gamma_{ii,o1}=\gamma_{MW}'\|1\rangle\rightarrow\|0\rangle$
$\rho_{0011}\,\dot{\|00\rangle}\langle 11\|$			$-1/4\rho_{0011}$
$\rho_{00T}\,\dot{\|00\rangle}\langle T\|$	$-\sqrt{2}/16\,(\rho_{S0S1}+\rho_{T0T1})$		$-1/8\rho_{00T}\ +1/4\rho_{T11}$
$\rho_{00S}\,\dot{\|00\rangle}\langle S\|$	$-\sqrt{2}/16\,(\rho_{S0T1}+\rho_{T0S1})$		$-1/8\rho_{00S}\ -1/4\rho_{S11}$
$\rho_{00T0}\,\dot{\|00\rangle}\langle T_0\|$	$-1/8\rho_{00T0}\ -1/4\rho_{T0ee}$	$-1/32\rho_{00T0}$	$+\sqrt{2}/16\,(\rho_{TT1}-\rho_{SS1})$
$\rho_{00S0}\,\dot{\|00\rangle}\langle S_0\|$	$-1/8\rho_{00S0}\ -1/4\rho_{S0ee}$	$-1/32\rho_{00S0}$	$+\sqrt{2}/16\,(\rho_{TS1}-\rho_{ST1})$
$\rho_{00T1}\,\dot{\|00\rangle}\langle T_1\|$	$-1/32\rho_{00T1}$	$-1/8\rho_{00T1}$	$-1/32\rho_{00T1}$
$\rho_{00S1}\,\dot{\|00\rangle}\langle S_1\|$	$-1/32\rho_{00S1}$	$-1/8\rho_{00S1}$	$-1/32\rho_{00S1}$
$\rho_{00ee}\,\dot{\|00\rangle}\langle ee\|$	$-1/4\rho_{00ee}$	$-1/4\rho_{00ee}$	
$\rho_{11T}\,\dot{\|11\rangle}\langle T\|$		$+\sqrt{2}/16\,(\rho_{S1S0}+\rho_{T1T0})$	$-3/8\rho_{11T}$
$\rho_{11S}\,\dot{\|11\rangle}\langle S\|$		$+\sqrt{2}/16\,(\rho_{S1T0}+\rho_{T1S0})$	$-3/8\rho_{11S}$
$\rho_{11T0}\,\dot{\|11\rangle}\langle T_0\|$	$-1/8\rho_{11T0}$	$-1/32\rho_{11T0}$	$-1/4\rho_{11T0}$
$\rho_{11S0}\,\dot{\|11\rangle}\langle S_0\|$	$-1/8\rho_{11S0}$	$-1/32\rho_{11S0}$	$-1/4\rho_{11S0}$
$\rho_{11T1}\,\dot{\|11\rangle}\langle T_1\|$	$-1/32\rho_{11T1}$	$-1/8\rho_{11T1}\ +1/4\rho_{T1ee}$	$-9/32\rho_{11T1}$
$\rho_{11S1}\,\dot{\|11\rangle}\langle S_1\|$	$-1/32\rho_{11S1}$	$-1/8\rho_{11S1}\ -1/4\rho_{S1ee}$	$-9/32\rho_{11S1}$
$\rho_{11ee}\,\dot{\|11\rangle}\langle ee\|$	$-1/4\rho_{11ee}$	$-1/4\rho_{11ee}$	$-1/4\rho_{11ee}$
$\rho_{TS}\,\dot{\|T\rangle}\langle S\|$	$-1/32\,(\rho_{T1S1}+\rho_{S1T1})$	$+1/32\,(\rho_{S0T0}+\rho_{T0S0})$	$-1/4\rho_{TS}$
$\rho_{TT0}\,\dot{\|T\rangle}\langle T_0\|$	$-1/8\rho_{TT0}\ +\sqrt{2}/16\rho_{T1ee}$	$-1/32\rho_{TT0}$	$-1/8\rho_{TST0}\ +\sqrt{2}/16\rho_{11T1}$
$\rho_{TS0}\,\dot{\|T\rangle}\langle S_0\|$	$-1/8\rho_{TS0}\ -\sqrt{2}/16\rho_{S1ee}$	$-1/32\rho_{TS0}$	$-1/8\rho_{TS0}\ +\sqrt{2}/16\rho_{11S1}$
$\rho_{TT1}\,\dot{\|T\rangle}\langle T_1\|$	$-1/32\rho_{TT1}$	$-1/8\rho_{TT1}\ +\sqrt{2}/16\rho_{T0ee}$	$-5/32\rho_{TT1}$
$\rho_{TS1}\,\dot{\|T\rangle}\langle S_1\|$	$-1/32\rho_{TS1}$	$-1/8\rho_{TS1}\ -\sqrt{2}/16\rho_{S0ee}$	$-5/32\rho_{TS1}$
$\rho_{Tee}\,\dot{\|T\rangle}\langle ee\|$	$-1/4\rho_{Tee}$	$-1/4\rho_{Tee}$	$-1/8\rho_{Tee}$
$\rho_{ST0}\,\dot{\|S\rangle}\langle T_0\|$	$-1/8\rho_{ST0}\ -\sqrt{2}/16\rho_{S1ee}$	$-1/32\rho_{ST0}$	$-1/8\rho_{ST0}+\sqrt{2}/16\rho_{11S1}$
$\rho_{SS0}\,\dot{\|S\rangle}\langle S_0\|$	$-1/8\rho_{SS0}\ +\sqrt{2}/16\rho_{T1ee}$	$-1/32\rho_{SS0}$	$-1/8\rho_{SS0}\ +\sqrt{2}/16\rho_{11T1}$
$\rho_{ST1}\,\dot{\|S\rangle}\langle T_1\|$	$-1/32\rho_{ST1}$	$-1/8\rho_{ST1}\ +\sqrt{2}/16\rho_{S0ee}$	$-5/32\rho_{ST1}$
$\rho_{SS1}\,\dot{\|S\rangle}\langle S_1\|$	$-1/32\rho_{SS1}$	$-1/8\rho_{SS1}\ -\sqrt{2}/16\rho_{T0ee}$	$-5/32\rho_{STS1}$
$\rho_{See}\,\dot{\|S\rangle}\langle ee\|$	$-1/4\rho_{See}$	$-1/4\rho_{See}$	$-1/9\rho_{See}$
$\rho_{T0S0}\,\dot{\|T_0\rangle}\langle S_0\|$	$-1/4\rho_{T0S0}$	$-1/16\rho_{T0S0}$	$+1/32\,(\rho_{S1T1}+\rho_{T1S1})$
$\rho_{T0T1}\,\dot{\|T_0\rangle}\langle T_1\|$	$-5/32\rho_{T0T1}$	$-5/32\rho_{T0T1}$	$-1/32\rho_{T0T1}$
$\rho_{T0S1}\,\dot{\|T_0\rangle}\langle S_1\|$	$-5/32\rho_{T0S1}$	$-5/32\rho_{T0S1}$	$-1/32\rho_{T0S1}$
$\rho_{T0ee}\,\dot{\|T_0\rangle}\langle ee\|$	$-3/8\rho_{T0ee}$	$-9/32\rho_{T0ee}$	
$\rho_{S0T1}\,\dot{\|S_0\rangle}\langle T_1\|$	$-5/32\rho_{S0T1}$	$-5/32\rho_{S0T1}$	$-1/32\rho_{S0T1}$
$\rho_{S0S1}\,\dot{\|S_0\rangle}\langle S_1\|$	$-5/32\rho_{S0S1}$	$-5/32\rho_{S0S1}$	$-1/32\rho_{S0S1}$
$\rho_{S0S1}\,\dot{\|S_0\rangle}\langle ee\|$	$-3/8\rho_{S0ee}$	$-9/32\rho_{S0ee}$	
$\rho_{T1S1}\,\dot{\|T_1\rangle}\langle S_1\|$	$-1/16\rho_{T1S1}$	$-1/4\rho_{T1S1}$	$-1/16\rho_{T1S1}$
$\rho_{T1ee}\,\dot{\|T_1\rangle}\langle ee\|$	$-9/32\rho_{T1ee}$	$-3/8\rho_{T1ee}$	$-1/32\rho_{T1ee}$
$\rho_{S1ee}\,\dot{\|S1\rangle}\langle ee\|$	$-1/32\rho_{S1ee}$	$-3/8\rho_{S1ee}$	$-1/32\rho_{S1ee}$

D Off-diagonal wire decay charts

In this table all the possible wire decays terms on any of the 36 off diagonal elements of the density matrix is shown. These decays scale with parameter $\beta\gamma$. Since the density matrix is Hermite, and decay is real this means that the contributions are the same for their respective Hermite conjugate. On the left side is the element of the density matrix under consideration with a different transition in each column. Each element can have a positive or negative contribution depending on emitter distance. Unlike the diagonal case, these elements need not be conserved and are just an effect of computing all elements of the decay part of Eq. (5). All results were done by Maple.

It should be noted that not all entries seem as natural as one might expect. It is for this exact reason that these results were derived rigorously.

Each column has its own distinctive decay parameter noted in apostrophes.

	$'\gamma_{ij,oe} = \beta_L \gamma_L' \ \|e\rangle \rightarrow \|0\rangle$	$'\gamma_{ij,1e} = \beta_\Lambda \gamma_\Lambda' \|e\rangle \rightarrow \|1\rangle$	$'\gamma_{ij,o1} = \beta_{MW} \gamma_{MW}' \|1\rangle \rightarrow \|0\rangle$
$\rho_{0011} \|\dot{0}0\rangle \langle 11\|$			
$\rho_{00T} \|\dot{0}0\rangle \langle T\|$	$-\sqrt{2}/16 (\rho_{S0S1} - \rho_{T0T1})$		$-1/8\rho_{00T} + 1/4\rho_{T11}$
$\rho_{00S} \|\dot{0}0\rangle \langle S\|$	$+\sqrt{2}/16 (\rho_{S0T1} - \rho_{T0S1})$		$+1/8\rho_{00T} + 1/4\rho_{S11}$
$\rho_{00T0} \|\dot{0}0\rangle \langle T_0\|$	$-1/8\rho_{00T0} + 1/4\rho_{T0ee}$		$+\sqrt{2}/16\rho_{TT1} + \sqrt{2}/16\rho_{SS1}$
$\rho_{00S0} \|\dot{0}0\rangle \langle S_0\|$	$+1/8\rho_{00S0} + 1/4\rho_{S0ee}$		$+\sqrt{2}/16\rho_{TS1} + \sqrt{2}/16\rho_{ST1}$
$\rho_{00T1} \|\dot{0}0\rangle \langle T_1\|$		$-1/8\rho_{00T1}$	
$\rho_{00S1} \|\dot{0}0\rangle \langle S_1\|$		$+1/8\rho_{00S1}$	
$\rho_{00ee} \|\dot{0}0\rangle \langle ee\|$			
$\rho_{11T} \|\dot{1}1\rangle \langle T\|$		$-\sqrt{2}/16 (\rho_{S1S0} - \rho_{T1T0})$	$-1/8\rho_{11T}$
$\rho_{11S} \|\dot{1}1\rangle \langle S\|$		$-\sqrt{2}/16 (\rho_{S1T0} - \rho_{T1S0})$	$-1/8\rho_{11S}$
$\rho_{11T0} \|\dot{1}1\rangle \langle T_0\|$	$-1/8\rho_{11T0}$		
$\rho_{11S0} \|\dot{1}1\rangle \langle S_0\|$	$+1/8\rho_{11S0}$		
$\rho_{11T1} \|\dot{1}1\rangle \langle T_1\|$		$+\sqrt{2}/16\rho_{T1ee} - 1/8\rho_{11T1}$	
$\rho_{11S1} \|\dot{1}1\rangle \langle S_1\|$		$+\sqrt{2}/16\rho_{S1ee} + 1/8\rho_{11S1}$	
$\rho_{11ee} \|\dot{1}1\rangle \langle ee\|$			
$\rho_{TS} \|\dot{T}\rangle \langle S\|$	$-1/32 (\rho_{T1S1} - \rho_{S1T1})$	$-1/32 (\rho_{S0T0} - \rho_{T0S0})$	
$\rho_{TT0} \|\dot{T}\rangle \langle T_0\|$	$+\sqrt{2}/16\rho_{T1ee} - 1/8\rho_{TT0}$		$+\sqrt{2}/16\rho_{11T1} - 1/8\rho_{TT0}$
$\rho_{TS0} \|\dot{T}\rangle \langle S_0\|$	$+\sqrt{2}/16\rho_{S1ee} + 1/8\rho_{TS0}$		$+\sqrt{2}/16\rho_{11S1} - 1/8\rho_{TS0}$
$\rho_{TT1} \|\dot{T}\rangle \langle T_1\|$		$+\sqrt{2}/16\rho_{T0ee} - 1/8\rho_{TT1}$	$-1/8\rho_{TT1}$
$\rho_{TS1} \|\dot{T}\rangle \langle S_1\|$		$+\sqrt{2}/16\rho_{S0ee} + 1/8\rho_{TS1}$	$-1/8\rho_{TS1}$
$\rho_{Tee} \|\dot{T}\rangle \langle ee\|$			$-1/8\rho_{Tee}$
$\rho_{ST0} \|\dot{S}\rangle \langle T_0\|$	$-1/8\rho_{ST0} - \sqrt{2}/16\rho_{S1ee}$		$+1/8\rho_{ST0} - \sqrt{2}/16\rho_{11S1}$
$\rho_{SS0} \|\dot{S}\rangle \langle S_0\|$	$+1/8\rho_{SS0} - \sqrt{2}/16\rho_{T1ee}$		$+1/8\rho_{SS0} - \sqrt{2}/16\rho_{11T1}$
$\rho_{ST1} \|\dot{S}\rangle \langle T_1\|$		$-1/8\rho_{ST1} + \sqrt{2}/16\rho_{S0ee}$	$+1/8\rho_{ST1}$
$\rho_{SS1} \|\dot{S}\rangle \langle S_1\|$		$+1/8\rho_{SS1} + \sqrt{2}/16\rho_{T0ee}$	$+1/8\rho_{SS1}$
$\rho_{See} \|\dot{S}\rangle \langle ee\|$			$+1/8\rho_{See}$
$\rho_{T0S0} \|\dot{T}_0\rangle \langle S_0\|$			$-1/32 (\rho_{S1T1} - \rho_{T1S1})$
$\rho_{T0T1} \|\dot{T}_0\rangle \langle T_1\|$	$-1/8\rho_{T0T1}$	$-1/8\rho_{T0T1}$	
$\rho_{T0S1} \|\dot{T}_0\rangle \langle S_1\|$	$-1/8\rho_{T0S1}$	$+1/8\rho_{T0S1}$	
$\rho_{T0ee} \|\dot{T}_0\rangle \langle ee\|$	$-1/8\rho_{T0ee}$		
$\rho_{S0T1} \|\dot{S}_0\rangle \langle T_1\|$	$+1/8\rho_{S0T1}$	$-1/8\rho_{S0T1}$	
$\rho_{S0S1} \|\dot{S}_0\rangle \langle S_1\|$	$+1/8\rho_{S0S1}$	$+1/8\rho_{S0S1}$	
$\rho_{S0S1} \|\dot{S}_0\rangle \langle ee\|$	$+1/8\rho_{S0ee}$		
$\rho_{T1S1} \|\dot{T}_1\rangle \langle S_1\|$			
$\rho_{T1ee} \|\dot{T}_1\rangle \langle ee\|$		$-1/8\rho_{T1ee}$	
$\rho_{S1ee} \|\dot{S}1\rangle \langle ee\|$		$+1/8\rho_{S1ee}$	

E Matlab template for effective matrix approach

The effective matrix approach is for complex time independent matrices for complicated quantum systems. Here the used approach is elaborated so that it can be reproduced.

Defining operators As a beginning single emitter states are defined in a complete basis, in this case the three unity vectors.

$$NUL = [1; 0; 0];$$
$$ONE = [0; 1; 0];$$
$$EXI = [0; 0; 1];$$

Then the raising and lowering operators of these single emitters are created via the use of the Kronecker product, in example the transition from state $|0\rangle \rightarrow |e\rangle$

$$\sigma_{e0} = kron(EXI, NUL');$$

Subsequently these are used to create raising and lowering operators per site

$$\sigma_{11} = kron(\sigma_{0e}, id);$$

Where the first subscript is the index, the second subscript the transition under consideration, and id the identity matrix. This results in a full set of possible operators without yet having a choice of basis. These operators can then be used to construct any Hamiltonian, as this is just a linear combination of these operators.

The effective matrix relies on the fact that a nine by nine density matrix has 81 elements. When such a matrix is multiplied by another matrix of the same dimensions, it creates a new matrix where each element is the sum of 9 multiplications between elements of the two starting matrices. Since this can then subsequently be multiplied with another matrix from the other side, this results in a total of $9 \times 9 \times 81$ elements. In other words, an 81×81 non Hermetian, non symmetric matrix can hold all possible terms regardless of they fact whether they were multiplied first left and then right or any combination of the two.

This means that the effective matrix consists out of a sum of 3 separate terms, $A, B\&C$

$$A\hat{\rho} \rightarrow Eff_A\hat{\rho}_{vector}$$
$$\hat{\rho}B \rightarrow Eff_B\hat{\rho}_{vector}$$
$$C_1\hat{\rho}C_2 \rightarrow Eff_C\hat{\rho}_{vector}$$

So that the sum of these matrices create the effective matrix, which is unique and upholding the rules of matrix multiplication and their non-commutativity. Matrices A and B are relatively easily found as they are again the superposition of the already known raising and lowering operators.

$$Eff_A = kron(IDEN, LEFT.');$$
$$Eff_B = kron(RIGHT, IDEN);$$

Where LEFT/RIGHT is the sum of all linear combinations of operators that multiply on the left/right from the density matrix, and IDEN the identity matrix. The effective matrix of the in between density matrix is more complex, and requires the a systematic subdivision of the effective matrix. An example of this is for instance for the transition from state $|0\rangle \rightarrow |e\rangle$

$$
\begin{aligned}
Eff_{C11} &= \gamma_{11}(kron(ONES, (\sigma_1{}_1').'). * kron(\sigma_{11}, ONES));\\
Eff_{C12} &= \gamma_{12}(kron(ONES, (\sigma_2{}_1').'). * kron(\sigma_{11}, ONES));\\
Eff_{C21} &= \gamma_{21}(kron(ONES, (\sigma_1{}_1').'). * kron(\sigma_{21}, ONES));\\
Eff_{C22} &= \gamma_{22}(kron(ONES, (\sigma_2{}_1').'). * kron(\sigma_{21}, ONES));
\end{aligned}
$$

Where ONES is a matrix with on its diagonal only ones and zero everywhere else. With exception of parameter names, all above formulas are in Matlab notation. The sum of the parts is the effective matrix. In other words,

$$(Eff_A + Eff_B + Eff_C)\,\hat{\rho} = Eff\hat{\rho} = \frac{\partial}{\partial t}\hat{\rho}$$

This is easily solvable in case of the steady state. In Matlab one has only to compute the null-vector of the effective matrix to find the steady state. If it exists. In all case encountered this exists, within the boundaries of computation. Since sufficiently small values become zero the state is found easily. It should be noted that Matlab has the possibility to distinguish between an analytical zero 0 and a numerical zero $'0.0'$. In all manually checked instances, other then trivial cases, no analytical null value was found, only numerical null values. This could indicate that the numerical approach is only the approximation of the steady state, whereas this analytically does not exist. The greatest benefit is though that the numerical approach is universal, and will always find the best approximation to the steady state.

Naturally more methods exist for finding a steady state. Programs were written for the solving of the time dependent differential equations as a whole. And intermediate steps with other matrix formulations were also developed. However none of these methods proved as practical in speed as the null-vector formalism. It is easily a factor of 10000 times faster then solving the differential equations, and hence it is the only used method when examining the β dependence.